EFFECT OF HIGH AVAILABILITY FUELS ON COMBUSTOR PROPERTIES

INTERIM REPORT
AFLRL No. 101

(12)

by

C. A. Moses and D. W. Naegeli

prepared by

U. S. Army Fuels and Lubricants Research Laboratory
Southwest Research Institute
San Antonio, Texas

for the

Navel Air Propulsion Center
Trenton, New Jersey

under contract to

U. S. Army Mobility Equipment Research
and Development Command
Energy and Water Resources Laboratory
Fort Belvoir, Virginia

Contract No. DAAK70-78-C-0001

January 1978

Disclaimers

The findings in this report are not to be construed as an official Department of the Army position unless so designated by other authorized documents.

Trade names cited in this report do not constitute an official endorsement or approval of the use of such commercial hardware or software.

DDC Availability Notice

Qualified requestors may obtain copies of this report from Defense Documentation Center, Cameron Station, Alexandria, Virginia 22314.

Disposition Instructions

Destroy this report when no longer needed. Do not return it to the originator.

Unclassified

SECURITY CLASSIFICATION OF THIS PAGE *(When Data Entered)*

REPORT DOCUMENTATION PAGE		READ INSTRUCTIONS BEFORE COMPLETING FORM
1. REPORT NUMBER (14) AFLRL-No. 101	2. GOVT ACCESSION NO.	3. RECIPIENT'S CATALOG NUMBER
4. TITLE (and Subtitle) (6) Effects of High Availability Fuels on Combustor Properties.		5. TYPE OF REPORT & PERIOD COVERED (4) Interim rept.
		6. PERFORMING ORG. REPORT NUMBER AFLRL No. 101
7. AUTHOR(s) (10) C.A. Moses, D.W. Naegeli		8. CONTRACT OR GRANT NUMBER(s) (15) DAAG53-76-C-0003, DAAK70-78-C-0001
9. PERFORMING ORGANIZATION NAME AND ADDRESSES U.S. Army Fuels & Lubricants Research Laboratory, Southwest Research Institute San Antonio, Texas 78284		10. PROGRAM ELEMENT, PROJECT, TASK AREA & WORK UNIT NUMBERS (12) 101p.
11. CONTROLLING OFFICE NAME AND ADDRESS U.S. Army Mobility Equipment Research & Development Command, Energy & Water Resources Lab., Ft. Belvoir, VA 22060		12. REPORT DATE (11) Jan 1978 13. NUMBER OF PAGES
14. MONITORING AGENCY NAME & ADDRESS *(if different from Controlling Office)* U.S. Naval Air Propulsion Center Trenton, New Jersey		15. SECURITY CLASS. *(of this report)* Unclassified 15a. DECLASSIFICATION/DOWNGRADING SCHEDULE

16. DISTRIBUTION STATEMENT *(of this Report)*

Approved for public release; distribution unlimited.

17. DISTRIBUTION STATEMENT *(of the abstract entered in Block 20, if different from Report)*

18. SUPPLEMENTARY NOTES

19. KEY WORDS *(Continue on reverse side if necessary and identify by block number)*

Turbine - Fuels Research
Fuel Properties
Turbine - Fuel Tolerance
Aromatic Turbine Fuels

20. ABSTRACT *(Continue on reverse side if necessary and identify by block number)*

Engines now in production or under development were designed for satisfactory performance and life on current specification fuels; many of these engines may not be able to handle the stress implied by a broadened fuel specification. Among the fuel properties of greatest concern to turbine engine combustion are the aromatic content, the distillation curve,

(over)

DD FORM 1 JAN 73 1473 EDITION OF 1 NOV 65 IS OBSOLETE

Unclassified

SECURITY CLASSIFICATION OF THIS PAGE *(When Data Entered)*

387 339

20. ABSTRACT (cont.)

and the viscosity. Fuel bound nitrogen is one new property which has emerged from the use of syncrude fuels because of additional NO_x found in the exhaust.

A high pressure and temperature research combustor was operated over a matrix of conditions involving

(a) burner inlet pressure, BIP = 2, 5, 10 and 15 atm,

(b) burner inlet temperature, BIT = 532, 812 and 1034°K,

(c) fuel/air ratio (heat input rate), H = 212, 424 and 848 KJ/Kg of air, and

(d) reference velocity (turbulence and residence time), V = 22, 44 and 66 M/sec.

Six petroleum base JP-5 fuels (principally aromatic blends) and three JP-5 syncrudes (from oil shale, coal and tar sands) were examined.

Flame radiation and exhaust smoke from petroleum based fuels correlated equally well with fuel hydrogen, aromatics and ring carbon. The radiation and smoke from the syncrude fuels correlated best with hydrogen content. The oil shale and tar sand derived fuels behaved similar to petroleum base fuels while the syncrude from coal gave relatively higher radiation and smoke based on its hydrogen content. Flame radiation and exhaust smoke were relatively insensitive to fuel at low levels of radiation and smoke, but at higher levels, the fuel sensitivity increased significantly. NO_x and CO emissions were essentially the same for all fuels; the syncrude from oil shale containing fuel bound nitrogen gave higher NO_x. Combustion efficiency was very high, above 99%.

FOREWORD

This program on the Effect of High Availability Fuels on Combustor Properties was authorized by the Naval Air Propulsion Center, Trenton, New Jersey, under contract to U. S. Army Mobility Equipment Research and Development Command, Energy and Water Resources Laboratory, Fort Belvoir, Virginia, contract Nos. DAAG53-76-C-0003 and DAAK70-78-C-0001.

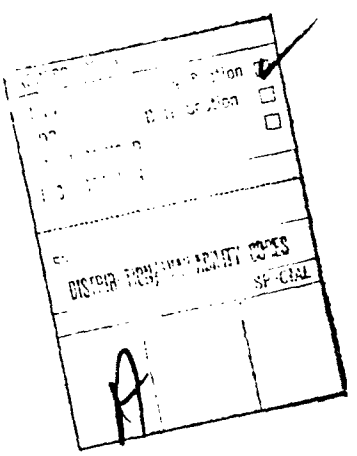

TABLE OF CONTENTS

LIST OF ILLUSTRATIONS

LIST OF TABLES

INTRODUCTION

Changing patterns in the production and supply of petroleum products have caused the U.S. Navy to consider two problems in obtaining adequate supplies of jet fuels:

a. Shortages of acceptable products which may exist either worldwide or in specific areas, and

b. The necessity or expediency, in certain cases, to use nonaviation fuels for aircraft.

One method of alleviating the problem is to broaden the fuel specifications thus increasing the availability of fuels which are acceptable. Another method is to use non-petroleum crudes as refinery feed stock. There are difficulties, however, with both of these approaches. Fuel specifications are established to eliminate combustion and handling problems and assure an adequate supply of fuel. Engines now in production or under development were designed for satisfactory performance and life on the current specification fuels; many of these engines may not be able to handle the stress implied by a broadened fuel specification, for example, higher liner temperatures or reduced atomization. Furthermore, the current specifications were designed for petroleum derived fuels. In many cases, the specific details of relating these problems to fuel chemistry have not been conducted; thus, the current specifications may not be adequate to eliminate these same problems from syncrude fuels because of differing fuel composition.

Among the fuel properties of greatest concern to turbine engine combustion are the aromatic content, the distillation curve, and the viscosity. The first property is generally associated with flame radiation and exhaust smoke; the latter two affect atomization and vaporization and, therefore, combustion efficiency. The distillation curve also controls the ignition requirements. Fuel-bound nitrogen is one new fuel property which has emerged from the use of syncrude fuels because of the additional NO_x found in the exhaust.

This report describes work performed for the Naval Air Propulsion Center under Contract No. DAAG53-76-C-0003 to investigate relationships between fuel properties and combustion performance in turbine engines. A high pressure and temperature research combustor was operated over a matrix of operating conditions involving:

a. burner inlet pressure, BIP
b. burner inlet temperature, BIT
c. fuel-air ratio (heat input rate), H
d. reference velocity (turbulence and residence time), $V_{ref.}$

Ten JP-5 type test fuels were used to address the following specific questions:

1. How will flame radiation and smoke be affected by increasing the allowable aromatic content?

2. How are flame radiation and smoke affected by the types of aromatics that are present, i.e., single, double, or triple ring?

3. How will combustion be affected by raising the end point of the distillation curve?

4. How are gaseous emissions affected by these changes in fuel properties?

5. How do the combustor performance/fuel property correlations for syncrude fuels compare with the correlations for conventional petroleum-based fuels?

SUMMARY

Flame Radiation

The flame radiation measurements were generally quite good and followed anticipated trends. In a few cases the measurements were anomalous but these were attributed to changes in the flame length as flow conditions were changed so that the same part of the flame was not measured. Fuel dependence was not affected by this.

Flame Radiation vs. Combustor Operating Conditions: Two factors go into the luminosity of a flame: the temperature and the soot concentration; the temperature affects both the spectral radiation from the gas and the black body radiation from the soot. The black body radiation is generally the dominant source. The results are as expected in that factors which contribute to increased soot formation yield higher flame radiation, i.e., increased pressure, higher heat input (fuel/air ratio) and reduced reference velocity (poor turbulent mixing). Temperature probably doesn't have a strong effect on the formation of soot but may affect the rate of oxidation of soot in various parts of the primary zone, thus effectively reducing the normal fourth power dependence of temperature on radiation.

Flame Radiation vs. Fuel Properties: The flame radiation from the petroleum-based fuels correlated equally well with the following fuel properties:

1. hydrogen content (percent wt)
2. aromatic content (percent vol.)
3. ring carbon (percent wt)

The flame radiation from the syncrude fuels correlated best with hydrogen content. Different aromatics did not affect the correlation. The flame radiation from the fuels processed from oil shale and tar sands correlated with hydrogen content in the same manner as the petroleum-based fuels; however, the radiation from the coal-derived fuel averaged about 8 percent higher than this correlation.

When correlated with aromatics or ring carbon, the coal and tar sand-derived fuels produced higher radiation than the petroleum fuels, while the shale oil-derived fuel produced lower radiation. These differences relate to the correlations of hydrogen content with aromatics and ring carbon for the fuels.

It was found that the flame radiation intensity was relatively insensitive to fuel at low radiation levels (generally less than 40 KW/M^2). However, as the radiation level was increased, the fuel sensitivity initially increased to a maximum value and then began to decrease as the flame emissivity approached unity.

From this program, it is concluded that engines with combustors of low luminosity (clean combustors?) may not be as strongly affected by changes in aromatics as those which have inherently higher flame radiation. Hydrogen content was the most effective parameter for correlating flame radiation to fuel properties; some further sensitivities to hydrocarbon structure were apparent but the data base was too small to draw conclusions.

Smoke

The smoke measurements had more scatter than the radiation measurements. The reason for this is not understood, since the combustor air and fuel flow parameters were quite stable and consistent from fuel to fuel at a prescribed combustor operating condition. It is also surprising since the flame radiation was generally consistent, with some exceptions, and soot which is the main radiation source is also the source of the smoke.

Smoke vs. Combustor Operating Conditions: Temperature was by far the controlling factor for exhaust smoke. At the higher burner inlet air temperature of 833 deg K, smoke was significantly lower than at the lower temperature used in the experiments. This is in agreement with the understanding that a higher air temperature means higher temperatures in the secondary and quench zones, thus increasing the oxidation rates of the free carbon coming from the primary zone. Increasing combustor pressure and heat input rate (fuel/air ratio) increased the smoke levels as is typical with real combustors. Reference velocity can have two effects on smoke; one, in terms of the turbulent mixing in the primary zone which reduces the production of soot and, two, the residence time in the secondary and quench zones for the oxidation of the free carbon. In this work, it was found that smoke levels were inversely proportional to reference velocity indicating that the effect on primary zone mixing was the stronger effect.

Smoke vs. Fuel Properties: As with the radiation, petroleum-based fuels correlated equally well with hydrogen content, aromatics and ring carbon. Aromatic structure did not affect these correlations. The syncrude fuels again correlated best with hydrogen content. On the average, the shale oil-derived fuel produced less smoke for its aromatic content or ring carbon than the correlation for the other fuels.

The fuel sensitivity of the smoke was similar to that of the radiation: smoke number was found to be inversely proportional to the hydrogen content; at conditions of low smoke the smoke number was almost independent of the fuel property while at high smoke the fuel sensitivity was significant.

Again, it appears that clean-burning engines may have less sensitivity to fuel aromatics than engines which produce more smoke.

Gaseous Emissions

Only CO and NO_x were found to be of significance as the unburned hydrocarbon levels were generally less than 1 ppm. NO_x is discussed rather than both NO and NO_x because that is what the emissions index is based upon.

Gaseous Emissions vs. Combustor Operating Conditions: The measured values of CO and NO_x followed the expected trends with the air and fuel flow parameters. Temperature, of course, is the greatest factor in NO_x production, which is produced very rapidly in the primary zone and decays only slightly in the rest of the combustor. Average primary zone temperature is the result of inlet air temperature plus the heat release from the fuel, so increases in these is expected to produce increases in NO_x. Poor mixing can cause local zones that burn closer to stoichiometric and, therefore, at higher temperatures. Thus, increases in reference velocity improve mixing and reduce the ratio of NO_x production.

CO on the other hand is reduced by higher temperatures, both in the primary and secondary zones. Reference velocity in this case appears to affect CO thru the residence time available for oxidation to CO_2 rather than mixing.

Both CO and NO_x were found to correlate very well with the following model:

$$\text{E.I. (CO or } NO_x) = K\, P^a\, T^b\, V^c\, H^d$$

where P = burner inlet pressure

T = burner inlet temperature

V = reference velocity

H = heat input rate (fuel/air ratio)

Typical values were:

$$\text{E.I. } (NO_x) \propto \cdot\ P^{0.3}\ T^{3.2}\ V^{-0.5}\ H^{0.5}$$

$$\text{E.I. (CO)} \propto \cdot\ P^{0.8}\ T^{-2.3}\ V^{0.6}\ H^{0.8}$$

Correlations are indicated by r^2 values of 0.95 for NO_x and 0.8 for CO.

Gaseous Emissions vs. Fuel Properties: There were only three fuels which were expected to show any significant differences in the NO_x levels: the shale oil derived fuel contained 0.10 percent fuel bound nitrogen as compared to < 0.01 percent for all the other fuels. As a result, the NO_x found in the exhaust was higher. The average value for the conversion of fuel bound nitrogen to NO_x was about 46 percent.

Two of the fuels had significantly higher end points than the other fuels; the end points for the tar sand-derived fuel and the fuel blended for high end point were about 360 deg C compared to 302-307 deg C for the other fuels. NO_x measurements in ppm were slightly lower for these fuels, but based on fuel flow, the NO_x emission indices were essentially identical with the other fuels.

Carbon monoxide was relatively insensitive to fuel properties. The important fuel parameters are viscosity and end point as they control droplet size and vaporization rate and hence droplet lifetime. It appears that the rate of combustion in the Phillips 2" combustor is not limited by droplet vaporization.

It is concluded that gaseous emissions are not sensitive to the fuel properties examined in this program with the exception of fuel-bound nitrogen.

Combustion Efficiency

The geometry of this combustor is such that if the flame can be stabilized in the primary zone, then combustion is very efficient, >99 percent. This can be seen from the very low levels of CO and UBH. As a result, it is very difficult to draw significant conclusions about the effects of fuel properties on combustion efficiency. Even the two fuels with the highest end points and viscosities were not significantly different.

RECOMMENDATIONS

It is recommended that further studies of "high availability fuels" be conducted in a more conventional burner that may be more limited in operating pressures and temperatures, but will nevertheless permit experiments at conditions of low efficiency and/or marginal combustion, e.g., the T-63 combustor.

As the end point and viscosity of jet fuels are raised, either by specification to increase availability or by emergency blending with heavier fuels to stretch shipboard stocks, problems associated with fuel atomization and vaporization will also become important. Examples of such problem areas are:

- ignition
- flame stability
- combustion efficiency
- gaseous emissions - CO and UBH.

The Phillips 2" combustor operates only at very high efficiencies, upwards of 99%. It has been shown to be an excellent burner for studying such fuel-related problems in gas-turbine combustors as flame radiation and smoke because these are most severe at conditions of high power and efficiency. It is not adequate for testing fuels under off-design or marginal combustion conditions where atomization and vaporization are controlling parameters. The combustor from the T-63 engine is suggested as a small combustor with wide stability characteristics but with low fuel flow requirements to minimize fuel costs.

BACKGROUND

In previous studies[1-6], the effects of fuel properties and composition on several aspects of combustion performance have been examined. The fuel-related combustion-performance characteristics include flame stability, ignition, flame radiation, exhaust smoke, gaseous emissions (CO, NO_x and unburned hydrocarbons) and combustion efficiency. Combustion efficiency, stability, and ignition are related to fuel properties such as viscosity and boiling point distribution, while flame radiation and exhaust smoke correlate better with composition, i.e., aromatic content. Gaseous emissions generally show a weak correlation with fuel composition and are more dependent on fuel properties such as viscosity and end point. For example, reduced combustion efficiency is indicated by increased emissions of CO and unburned hydrocarbons which may result from poor atomization and slow rates of vaporization. The burning time of a droplet is given by d_o^2/B where B is the burning constant and d_o is the initial droplet diameter. The burning constant for hydrocarbon fuels is partly related to end point but changes very slightly over the boiling range of common distillate fuels. Droplet diameter is therefore the most significant rate-determining factor in droplet combustion. The droplet size, characterized by the sauter mean diameter (SMD) of a typical spray nozzle, may be expressed as

$$SMD = \frac{90.5\ \nu^{0.3}\ p^{0.2}\ Q^{0.2}}{\Delta P^{0.354}}$$

where viscosity (ν), density (P), volumetric flow rate (Q) and nozzle differential pressure (ΔP) are the important variables. Because of the d^2 dependence on burning rate and the $\nu^{0.3}$ dependence on sauter mean diameter, the burning rate of a given fuel is dependent on $\nu^{0.6}$ in cases where the rate of combustion is vaporization and mixing limited. This is observed in situations where the pressure drops and flow velocities into the combustor are too low to produce the turbulence required for adequate mixing.

NO_x EMISSIONS

The emissions of NO_x have been observed to be almost totally dependent on temperature and to some extent on the residence times of the gas in various environments. NO_x is produced in oxidizing environments by the Zeldovich reactions:

$$O + N_2 = NO + N$$

$$N + O_2 = NO + O$$

The first reaction is very slow, but its rate increases very rapidly with increasing temperature. The second reaction is very fast and is almost temperature independent. Hence, the first step, the slow reaction of oxygen atoms with nitrogen, controls the rate of formation of NO_x and explains the importance of residence time. Note, equilibrium quantities of NO are seldom ever formed in combustion systems simply because of insufficient residence time. However, the formation of NO_x in combustors is not a trivial matter. For example, one might expect NO_x formation to be reduced by increased flow velocity (decreased residence time), but the contrary is possible if the increased velocity generates better mixing and high combustion intensity resulting in higher temperatures in the primary zone. The effect of fuel type on NO_x formation is significant if the combustion efficiency is seriously affected by fuel properties. Slow vaporization resulting from unusually high viscosity and end point will cause the flame length to increase (slow heat release) by increasing the burning time. Although this will increase the residence time of gases in the flame zone, the NO_x formation may be reduced because of a significantly lower peak flame temperature.

NO_x formation may be influenced substantially by composition when fuel-bound nitrogen is present but the combustion characteristics of the burner appear to be important. In flat-flame studies of CH_4/O_2 and C_2H_4/O_2 flames doped with low-molecular-weight nitrogen-containing compounds, it was found by de Soete[8] that lean and stoichiometric flames exhibited nearly total conversion of the fuel-nitrogen to NO while rich flames resulted in significantly less conversion. It was suggested that HCN is an important precursor to NO formation from fuel-bound nitrogen and also the prompt NO formed in the preflame zone. Pyrolysis studies by Axworthy and Schuman[9] have shown that hetrocyclic-N aromatics such as pyridine decompose readily at temperatures above 1176°K and give an almost complete conversion of bound nitrogen into HCN. These results suggest that high burner inlet temperatures (>1000K) would favor the formation of HCN from fuel-nitrogen species and thereby could conceivably give high yields of NO_x. Recent gas turbine combustor studies by Blazowski have shown that the percent conversion of fuel-bound nitrogen to NO_x is reduced by (1) increased burner inlet temperatures up to 838°K and (2) increased fuel-bound

nitrogen content. While these results may seem contrary to the aforementioned fundamental studies, it is possible that fuel vaporization and mixing (variations in stoichiometry) in a combustor could have a strong influence on fuel-nitrogen conversion to NO_x.

FLAME RADIATION

In modern combustors the combustion chamber walls are often protected from hot flame gases by techniques of film cooling. However, this protective air film is incapable of resisting heat transferred via flame radiation. Radiation from flame particulates account for a significant part of the total heat transfer to the combustion chamber wall. In fact, flame radiation can be the predominant mode of heat transfer at high load conditions.

Flame radiation (W) may be expressed by the Stefan-Boltzman law as

$$W = \varepsilon\sigma AT^4$$

where ε is the emissivity, σ (is the accepted symbol) is the Stefan-Boltzman constant, A is the radiant area and T is the absolute temperature. The factor of main concern is the emissivity (ε) of a flame which is dependent on the particle density. At a constant flame temperature, the radiation from a flame is controlled by the particle density or ε. It has been recognized by Lefebvre[10] that the particle density is dependent on several variables including combustion chamber design, inlet conditions of pressure, temperature, velocity and heat input, fuel atomization and various fuel factors, namely, chemical composition. For hydrocarbon fuels, radiation correlates quite predictably with hydrogen content. Aromatic content also appears to be a good indicator, but it is generally overruled by hydrogen content. It is important to note that when comparing the radiation from one fuel with that of another, it is necessary that the observation be made at conditions where $\varepsilon < 1$. Basically, the relative emissivity is the parameter that changes when various fuel types are examined at equivalent conditions.

Both smoke point and luminometer number traditionally have been used as indicators to control radiation and the smoking tendency of aviation turbine fuels. In light of the fact that these measurements are made on diffusion flames, it has been recommended by Schirmer[2] that hydrogen content of the fuel is a better indicator of flame radiation in turbine engines, because of observations that support the concept that there are differences in the mechanism of oxidative decomposition of hydrocarbons in diffusion and premixed flames. It is reasonable to believe that the pyrolytic decomposition of hydrocarbons involves a somewhat different reaction mechanism than that of hydrocarbon oxidation, but nevertheless, it is understood that radiation in combustors is caused by such factors as poor atomization and

mixing. Basically the statement "poor quality mixing" may be interpreted as diffusion flames around fuel rich eddies. Thus, although hydrogen content may in most cases be the best indicator of how severe the radiation might be for one fuel as compared with another, it does not appear to be clearly understood why this is the case.

EXHAUST SMOKE

Turbine engines with excessive smoke offer a military tactical problem in the form of smoke trails as visual aids to the enemy as well as a concern to environmentalists. Smoke does not amount to a measurable loss in combustion efficiency. Of main concern to combustor designers is the problem of meeting the stringent environmental standards which may become even more severe in the future. The basic problem in establishing reasonable standards for smoke emissions from turbine engines is to define what constitutes particulates. Generally, particulates have been defined in terms of specific test methods (e.g., particulate weight, smoke number and opacity), which each measure something different and are difficult to compare. Higher aromatics in future fuels will make these standards more difficult to achieve and because of increased varieties of aromatic structures from syncrudes, the specific test methods may show considerable variation in response.

It is well known that there is little difference in the basic combustion characteristics of hydrocarbon fuels of a single specification, e.g., fundamental flame velocity, minimum ignition energy, and flammability limits; however, considerable differences may be observed in the coking and smoking tendency of jet fuels. The soot producing tendency of hydrocarbon fuels in diffusion flames decreases as follows, aromatics > alkynes > olefins > *n*-paraffins.[11] The smoking tendency for all aromatics is fairly uniform and extremely high. It has been shown in several investigations that aromatics are about 12 times as smoky as olefins and about 24 times as smoky as *n*-paraffins. The smoking tendency for alkynes and olefins, except for ethene through butene, decreases with increasing chain length, i.e., they approach paraffinic behavior. Paraffins tend to smoke more with increasing chain length, branching and ring formation. Similarly, polycyclic aromatics, including naphthalenes, have a greater tendency to smoke than monocyclic aromatics.

It has been found that the smoking tendency in diffusion flames and Bunsen flames is essentially independent of the ambient temperature and premixed gas temperature respectively. Contrarily, pressure was found to substantially increase smoke formation in diffusion flames, while having very little effect on smoke formation in premixed Bunsen flames. These results suggest that the rate of diffusion and, consequently, the rate of mixing fuel and air may account for the variation in smoke formation since diffusion coefficients are inversely proportional to pressure.

Previous studies[3] in the Philips 2-inch high pressure combustor have demonstrated that exhaust smoke is increased by boosting pressure and heat input (fuel/air ratio) and is reduced with increasing burner inlet temperature. Increased gas velocity was observed to moderately reduce exhaust smoke density. In agreement with Lefebvre's observations[10], it was consistently found that reductions in exhaust smoke density resulted from the use of fuels with higher hydrogen content.

EXPERIMENTAL TEST EQUIPMENT AND METHODS

General Description

The AFLRL combustor facility was especially designed for the study of fuel-related problems in the operation of turbine engines. As illustrated by the operating envelope in Figure 1, the air supply system provides a clean smooth flow of air to the combustion test cell at rates up to 2.5 lbs/sec with pressures to 16 atm and temperatures to 1500°F at all flow rates. The fuel delivery system is capable of pumping fuels ranging in properties from gasoline to No. 5 fuel at flow rates of over 1 gpm and pressures up to 1000 psi. The data reduction is performed on-line with test results available immediately; up to 50 channels of thermocouple and transducer signals can be samples. The system has been designed for maximum flexibility and growth. Conceivably, any combustion chamber and associated rig can be "plugged-in", instrumented, and operated within the air flow capabilities of the laboratory.

In this particular examination of fuel properties and combustion performance, the Phillips high-pressure 2-inch combustor was employed (see Figure 2).

The Phillips 2-Inch Combustor

Basically, the Phillips 2-inch combustor[2] is a straight-through cylindrical type, with fuel atomization by a single-orifice, oil-burner-type pressure atomizer. The combustor liner is constructed from 2-inch, Schedule 40, Inconel pipe. Film cooling of surfaces exposed to the flame is accomplished by internal deflector rings. The combustor rig shown in Figure 3 is a more rugged version of the original Phillips rig: Some major design changes were incorporated for the purpose of reaching higher inlet temperatures (1500°F), namely, the uprating of the flanges to the 1500# class and fabricating them and the combustor housing from 316 stainless steel. No changes were made in the flow dimensions.

The Combustor Facility

A detailed layout of the AFLRL combustor laboratory is shown in Figure 4. The facility consists of a variable pressure-temperature air supply, a control room for operating the air

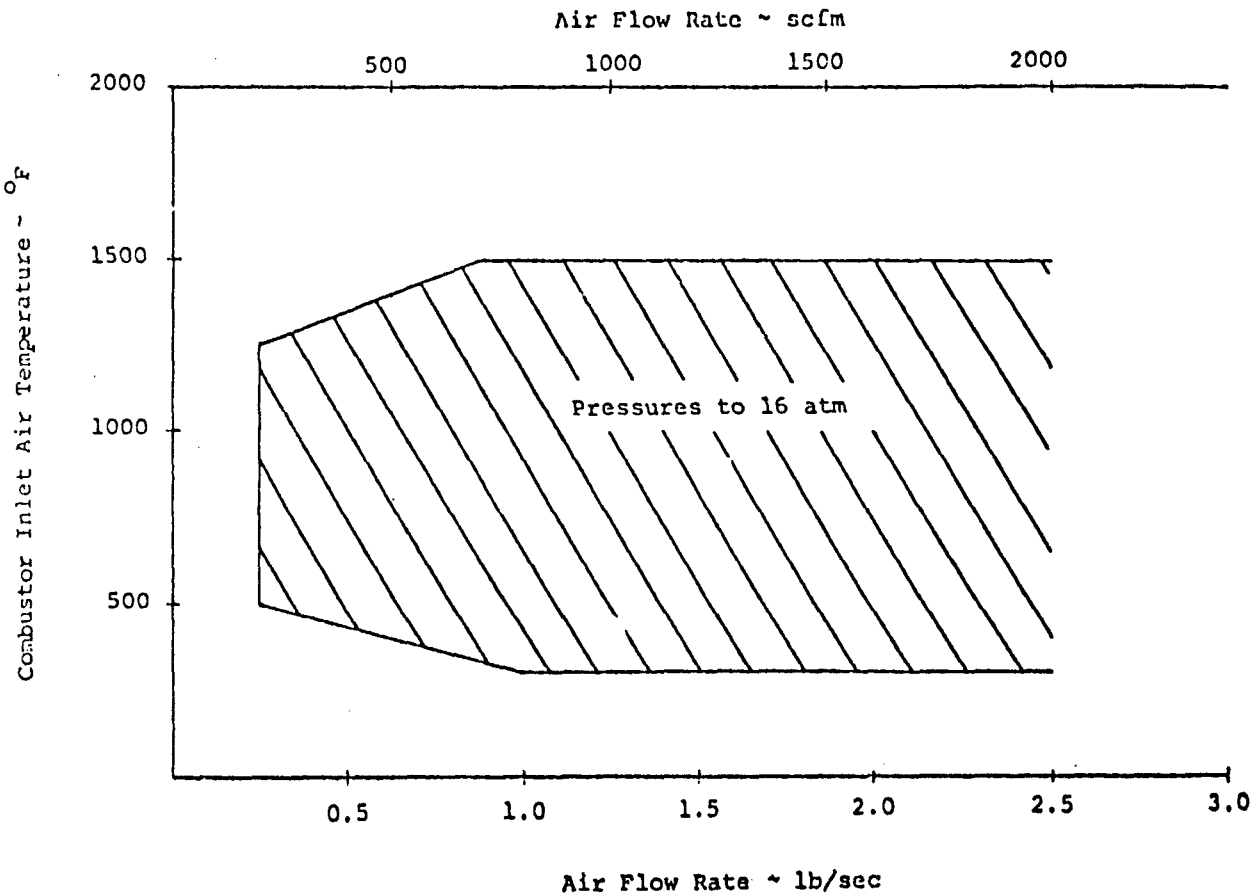

FIGURE 1. ENVELOPE OF OPERATING CONDITIONS FOR AFLRL TURBINE COMBUSTOR LABORATORY

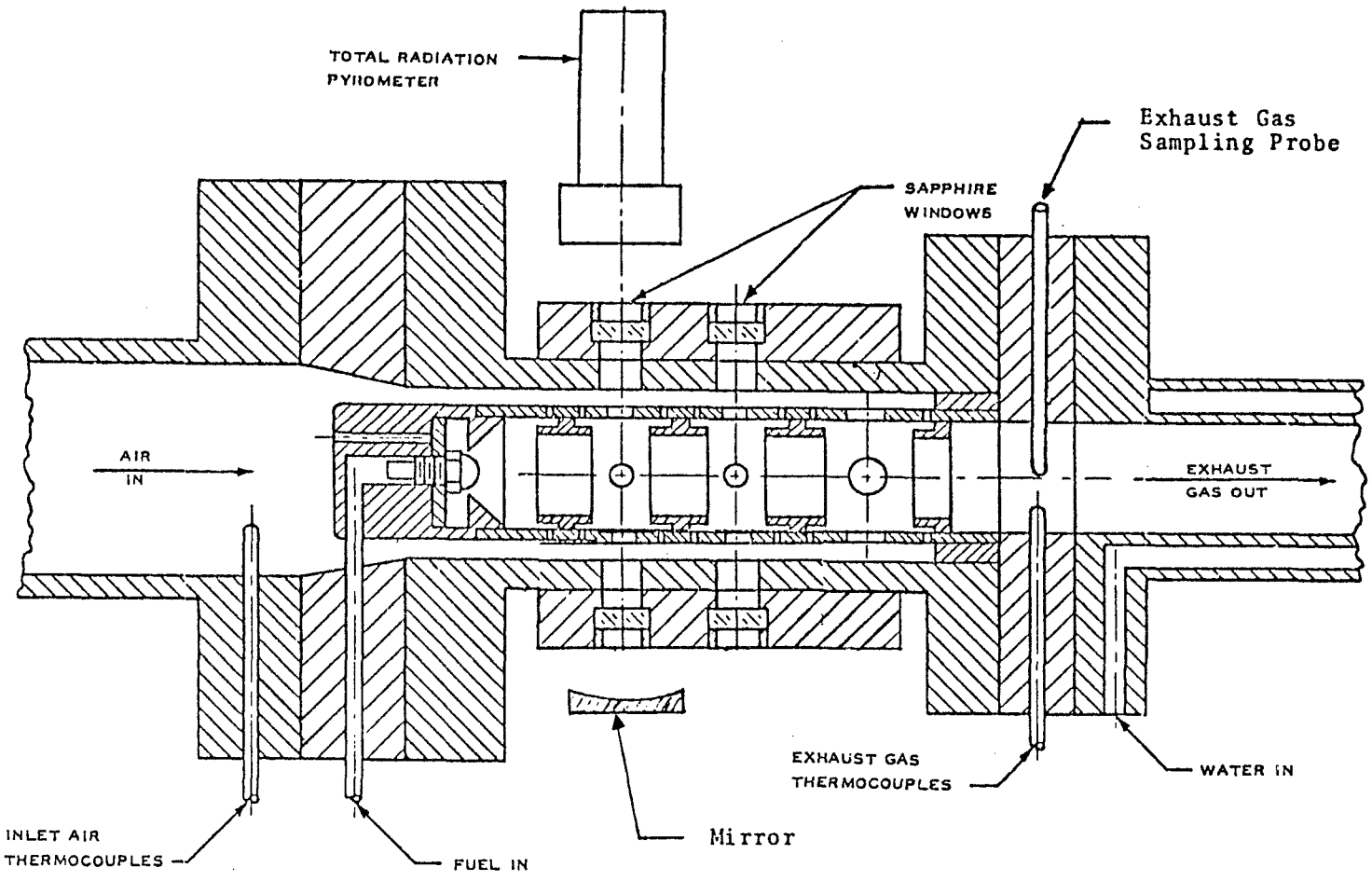

FIGURE 2

PHILLIPS 2 – INCH COMBUSTOR

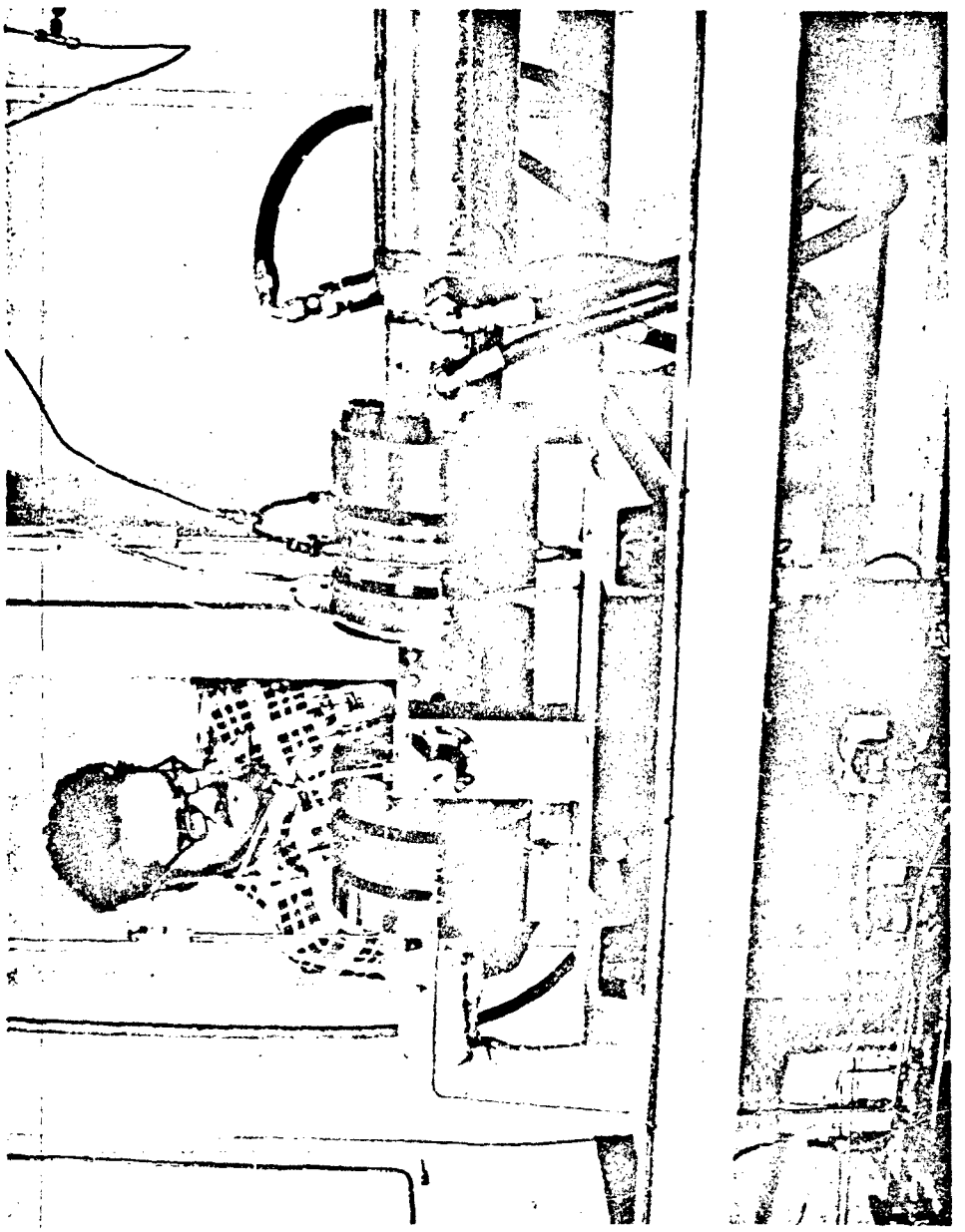

FIGURE 3. VIEW OF COMBUSTOR RIG

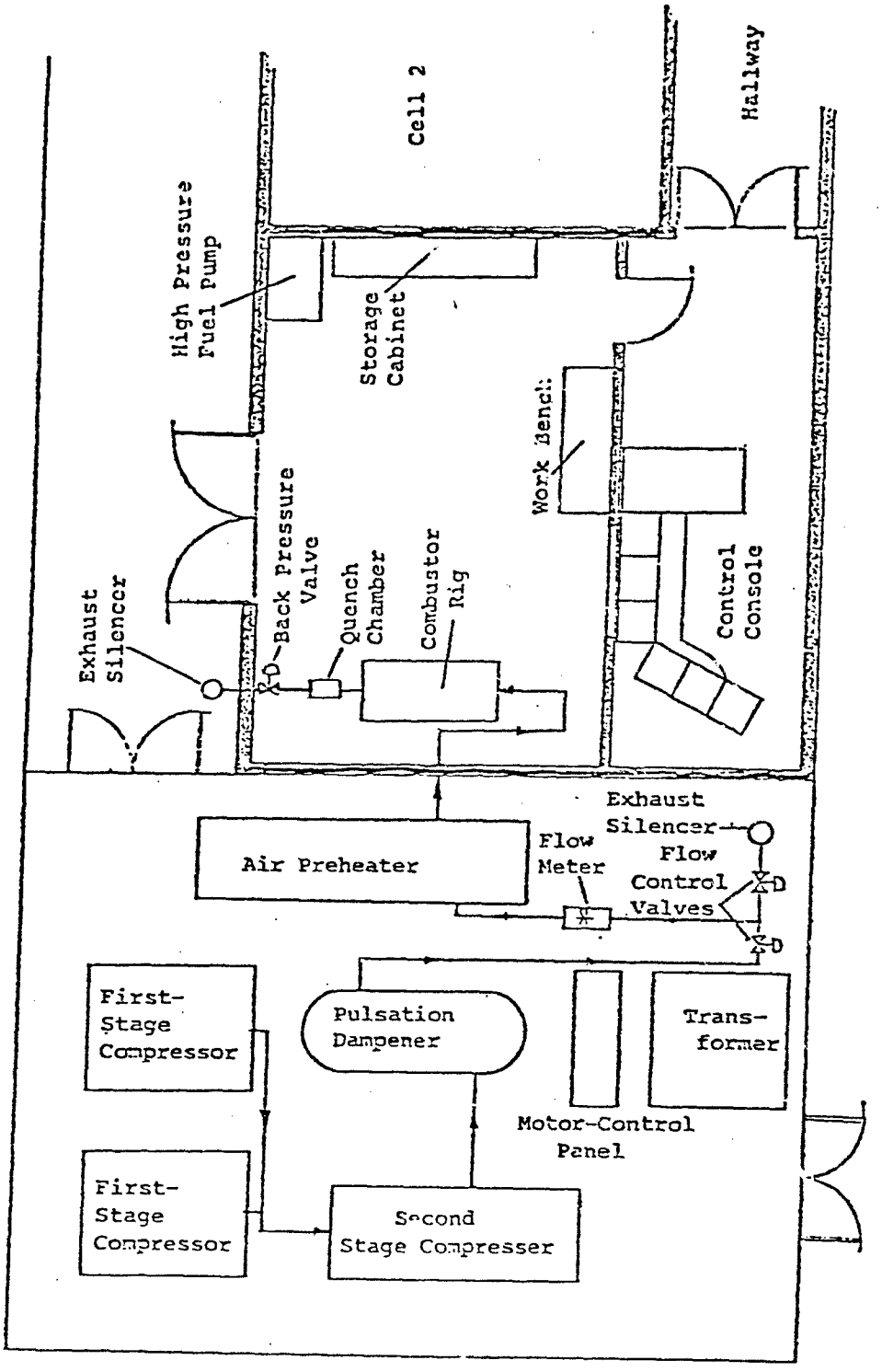

FIGURE 4. LAYOUT OF TURBINE FUEL RESEARCH COMBUSTOR LABORATORY

flow system, the fuel flow system, the combustor and its exhaust system; also there are the components of the data acquisition system (see Figures 5 and 6 for views of the control panel).

The Air Flow System

A flow diagram of the "air factory" is shown in Figure 7. The compressed air for the lab is generated in two stages: two Ingersoll-Rand "Pac-Air" rotary-screw compressors are connected in parallel, each deliverying 1000 SCFM at 100 psig. This air goes through an intercooler and then to a single-cylinder reciprocating compressor where it is compressed to 250 psia. From there the air passes through an aftercooler, a receiver, and an oil filter before going to the flow controls. The oil carryover after the oil filter has been measured and is less than 5 ppm. There are suction and discharge bottles on the booster compressor which, in conjunction with the receiver, were designed on an analog computer by Ingersoll-Rand to eliminate pulsations from the air flow. Pressure fluctuations on the downstream side of the receiver have been measured at less than 0.1 psi peak to peak on a 235 psia flow at a frequency of about 45 hz.

The flow control system operates in two parts: one valve is used to provide a pressure drop to the system while a second valve bypasses any excess air flow through an exhaust silencer. The compressors are always operating at full capacity--a method which uses more total energy but eliminates any surging caused by the compressors unloading.

A 3 in. turbine flow meter is used to measure the air flow rate. Because a turbine meter measures volume flow, the pressure and temperature are also sensed at the meter so the flow measurement can be converted to mass flow rate.

The air flow then enters a preheater which is capable of heating the flow from roughly 100°F to 1550°F. Designed by Fabricating Engineering Corporation, this heater is an indirect, gas-fired system with a counterflow heat exchanger; the air remains unvitiated. The combustion control system was designed in accordance with FIA safety standards to automatically shut down the preheater in the event of a malfunction in the fuel supply or temperatures exceeding established limits. The final air temperature is automatically controlled by a Honeywell recorder-controller system which regulates the air/fuel ratio in the combustion chamber and dilutes the hot-exhaust gases going to the tube bundle.

At this point the air no longer has the same moisture content as the atmospheric air because of the water removed at the intercooler and aftercooler. This does not happen in the compressor section of a real turbine engine as the air is not cooled between the compressor and burner. Since several aspects of the combustion process are affected by the presence

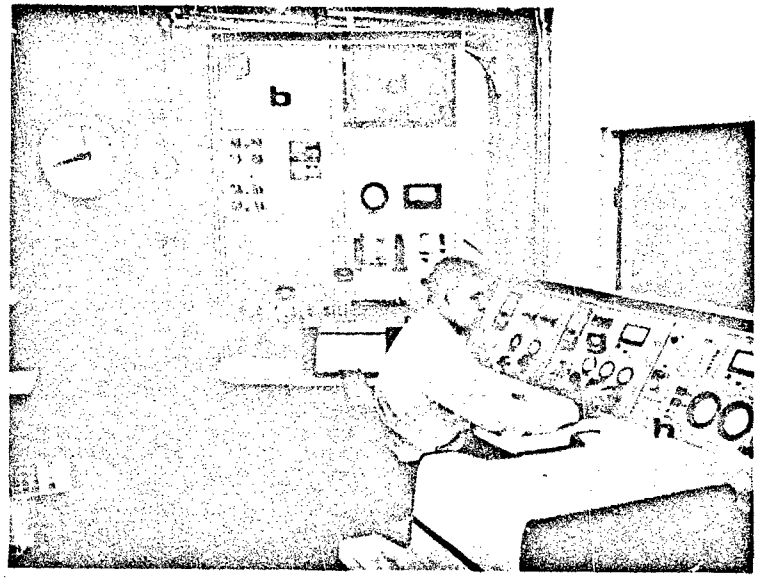

a. Air Heater Control System

b. Compressor Motor Controls

c. Pressure Transducer Reference System

d. Thermocouple Reference Oven

e. Moisture Readout

f. Quench Water Control

g. Air Flow Control

h. Ignition and Fuel Flow Control

i. Window Looks Into Combustion Room

FIGURE 5. VIEW OF CONTROL CONSOLE

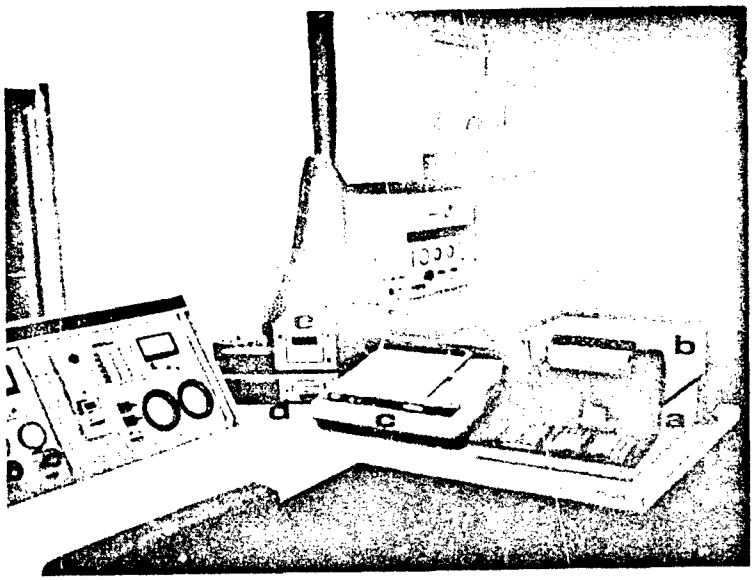

a. Programmable Calculator

b. Printer

c. X-Y Plotter

d. Scanner and Digital Voltmeter

e. Magnetic Tape Cassette

FIGURE 6. VIEW OF CONTROL CONSOLE SHOWING DATA AQUISITION SYSTEM

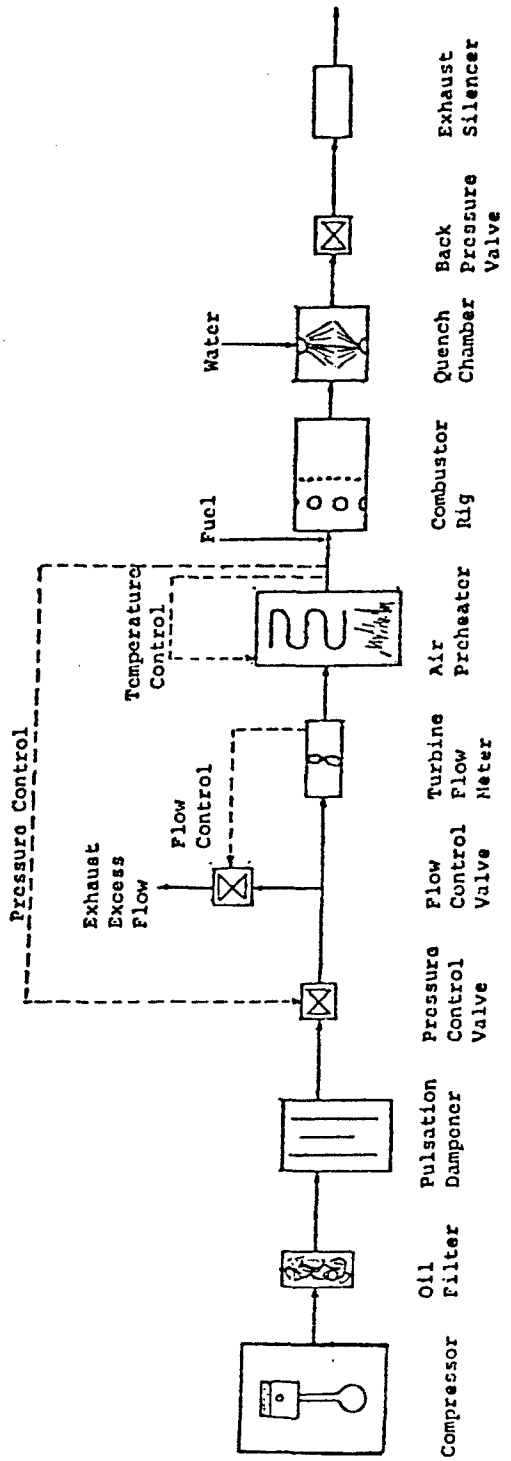

FIGURE 7. FLOW DIAGRAM OF TURBINE COMBUSTOR SYSTEM

of water, e.g., exhaust temperature and NO_x concentration, a method for making up this water loss has been included. De-ionized water can be sprayed into the air flow in the inlet manifold of the air heater so it is vaporized in the heater. Downstream of the heater, a sample of the air is bled off and the moisture control monitored. The moisture content can then be controlled to any reasonable level.

The air flow is piped into the test cell and for all practical purposes is the same as the air from any turbine compressor. It is essentially pulsation free and oil free, and its moisture content is controlled. The air flow rate, pressure, and temperature are independently adjustable to any values within the operating envelope.

The Fuel Supply System

The fuel supply system is capable of pumping fluids ranging in properties from gasoline to No. 5 diesel at flow rates of over 1 gpm and pressures up to 1000 psi. For this program, the fuels were forced from drums to the fuel selection manifold system (see Figure 8) with pressurized inert gas. The manifold employs twelve solenoid valves (for 12 fuels) from Automatic Switch Co. After the manifold, a high pressure pump delivers fuel to the combustor. The plumbing from the pump to the combustor is stainless steel to facilitate cleaning when special fuels or fuel additives are used.

A turbine flow meter is used to measure the flow rate of the fuel. On starting, a system of valves and bypasses are used to bring the flow rate up to the desired level before introducing it to the combustion chamber. On shutdown, the lines can be drained and purged with an inert gas.

Exhaust System

Exhaust temperatures from turbine-engine combustion chambers typically approach 2000°F and advanced designs even higher. The exhaust gases must be cooled to more reasonable temperatures to be able to handle them. Eight spray nozzles are located just downstream of the combustor and are capable of spraying over 16 gpm of water into the exhaust; this is sufficient to cool the flow from 3000°F to 400°F. The water flow rate is automatically controlled by sensing the temperature at the back pressure valve. The nozzles are fed by a centrifugal pump at pressures up to 350 psia. The water is pumped from a holding tank; should the water supply be interrupted, an alarm sounds and the operator has three minutes to shut down before running out of quench water.

A pneumatically-controlled valve is located downstream of the quench section to maintain the pressure in the combustor system. A silencer is used to attenuate the flow noise from the valve.

FIGURE 8. FUEL SELECTION MANIFOLDING SYSTEM

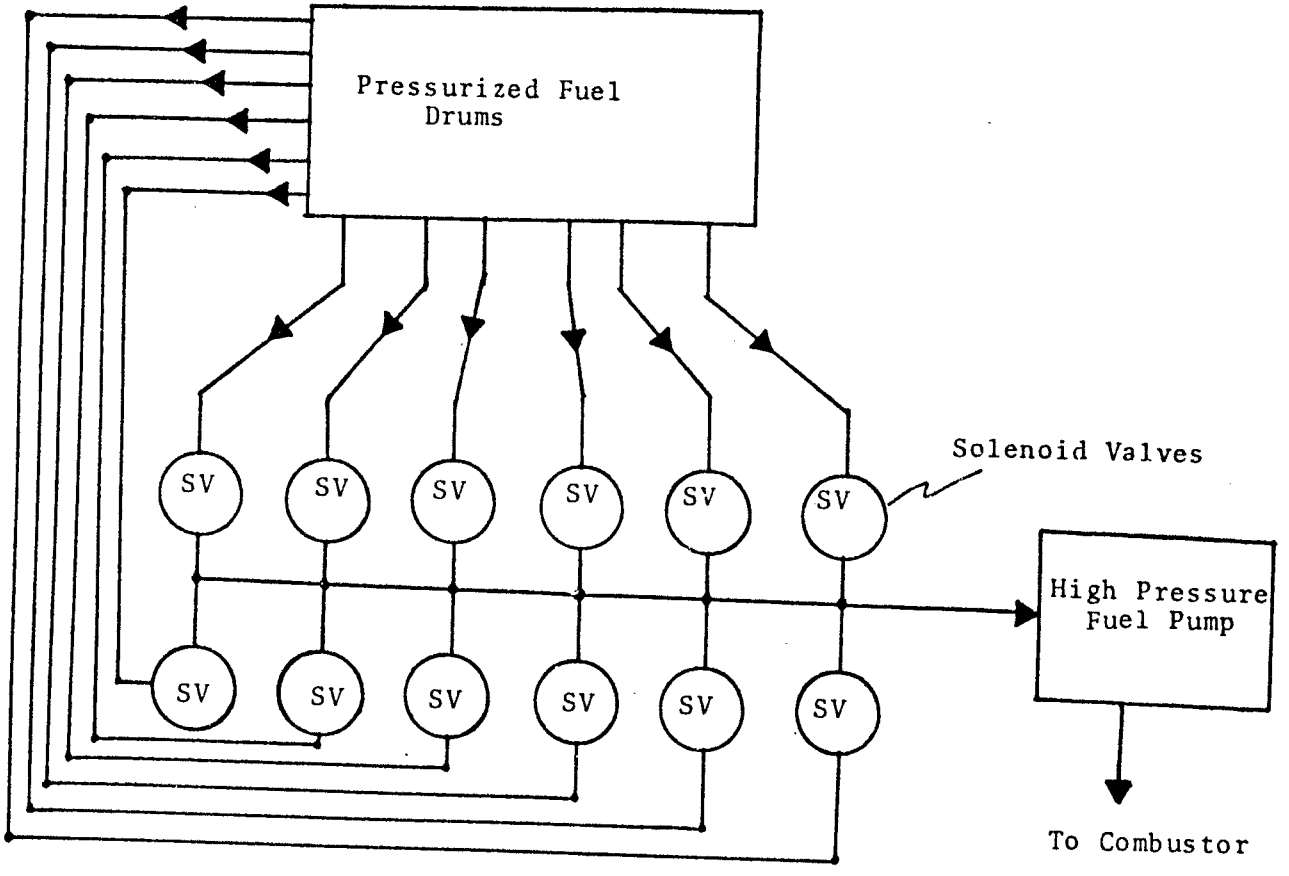

Data Acquisition System

The heart of the data acquisition system is a Hewlett-Packard 9820 programmable calculator with associated software. Figure 9 shows a flow chart of the system. A digital voltmeter is coupled to a 50-channel scanner which samples the voltage outputs from the various sensor systems and then feeds the corresponding digital values into the calculator. The calculator handles all of the data reduction and any necessary calculations, e.g., combustion efficiency, flow factor, and exhaust emissions coefficients. The resulting data is then output in one of three ways:

1. It can be stored on magnetic tape for further reduction at a later time;

2. It can be output graphically on an X-Y plotter; or

3. It can be put on a printer along with any appropriate alphanumeric titles or column headings.

Figure 10 shows an example of a graphical output. Table 1 illustrates the use of the printer for the continuous monitoring of several channels of data while Table 2 is an example of a complete test report available immediately after the data was measured. The fifty channels can be scanned, the data reduced, and a report such as Table 2 printed out in less than two minutes.

The sensing systems consist of strain-gauge pressure transducers, thermocouples, and turbine flowmeters. Regulated power supplies are used with the pressure transducers. A vacuum/pressure reference system is used to calibrate the transducers against a Wallace and Tiernan gauge; use of three-way valves allows this to be done during a test and without disconnecting the transducers. The thermocouples are referenced to a 150°F oven; the unit will handle up to 50 thermocouples of any type including platinum.

Exhaust Analysis Instrumentation

Exhaust emissions were measured on-line using the following instruments:

Sample	Instrument	Sensitivity
Carbon Monoxide	Beckman Model 315B NDIR	50 ppm to 16%
Carbon Dioxide	Beckman Model 315B NDIR	300 ppm to 16%
Unburned Hydrocarbons	Beckman Model 402 FID Hydrocarbon Analyzer	0.5 ppm to 10% (CH_4)
Nitric Oxide	Thermo-Electron 10A Chemiluminescence Analyzer	3 ppm to 10,000 ppm
Total Oxides of Nitrogen	Thermo-Electron 10A Chemiluminescence Analyzer with NO_x Converter	3 ppm to 10,000 ppm
Oxygen	Beckman Fieldlab Oxygen Analyzer	0.1 ppm to 100%

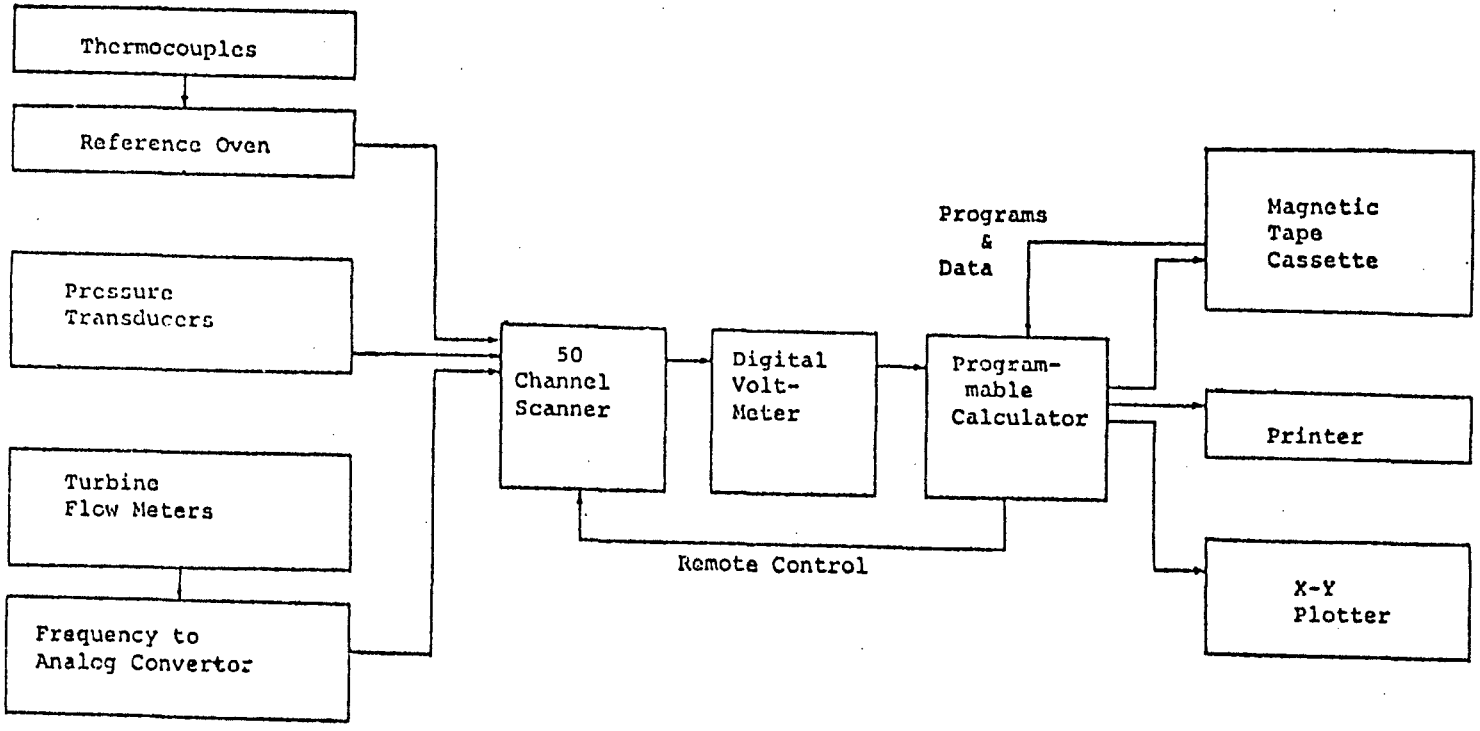

FIGURE 9. DATA ACQUISITION SYSTEM

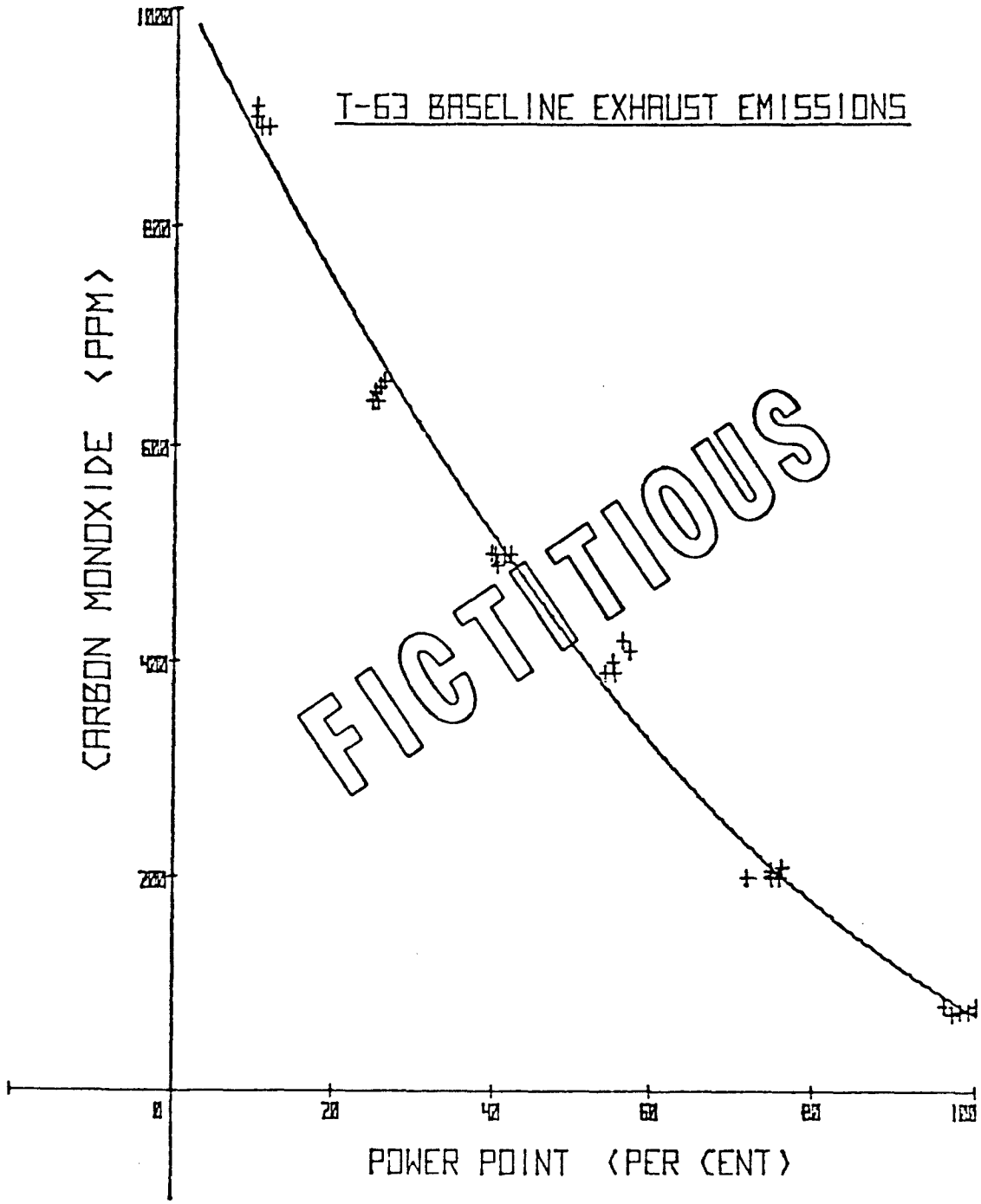

FIGURE 10. EXAMPLE OF GRAPHIC OUTPUT

TABLE 1. EXAMPLE OF CONTINUOUS
MONITORING OF SEVERAL DATA CHANNELS

U.S. ARMY FUELS & LUBRICANTS RESEARCH LABORATORY
TURBINE-FUELS RESEARCH COMBUSTOR LAB

2-INCH, 16-ATM COMBUSTOR
GENERAL COMBUSTOR OPERATING CONDITIONS 2: 2 6/ 1/77

BIP....BURNER INLET PRESSURE,PSIA
BIT....BURNER INLET TEMPERATURE,F
WA.....AIR FLOW RATE,LBM/SEC
WF.....FUEL FLOW RATE,LBM/MIN
F/A....FUEL/AIR RATIO
VREF...COLD FLOW REFERENCE VELOCITY, FT/SEC
H I....HEAT INPUT, BTU/LBM AIR
ET.....EXHAUST TEMPERATURES, DEG F

BIP	BIT	WA	WF	F/A	VREF	H	ET-1	ET-2	ET-3	ET-4
147.00	1400.0	.888	.522	.010	225.0	180.0				
DESIRED SET POINT...TIME 2: 3										
146.40	1397.3	.915	.521	.009	232.2	174.4	1946	1890	1883	935
146.50	1398.1	.887	.524	.010	225.0	180.9	1945	1895	1888	948
146.40	1397.7	.898	.527	.010	227.9	179.6	1944	1889	1882	991
146.30	1398.1	.899	.529	.010	228.4	180.3	1945	1908	1880	1019
146.80	1397.3	.887	.529	.010	224.5	182.7	1942	1880	1884	973
146.70	1399.0	.897	.529	.010	227.4	180.7	1941	1923	1883	1152
146.40	1399.0	.896	.516	.010	227.6	176.2	1940	1911	1883	1103
146.60	1399.0	.906	.524	.010	230.0	176.9	1943	1880	1884	965
146.60	1399.9	.911	.516	.009	231.2	173.3	1940	1915	1880	1111
146.90	1399.4	.905	.521	.010	229.1	176.3	1937	1893	1883	1059
146.60	1400.3	.909	.508	.009	230.7	171.1	1939	1924	1877	1106
146.60	1399.9	.898	.510	.009	227.9	174.0	1937	1887	1876	987
146.70	1400.3	.902	.513	.009	228.8	174.1	1937	1881	1880	997
147.00	1400.7	.899	.516	.010	227.8	175.5	1936	1875	1880	973
146.70	1400.7	.909	.524	.010	230.6	176.5	1949	1914	1884	1094
146.80	1401.2	.880	.535	.010	223.3	185.9	1954	1923	1884	1103
147.00	1400.7	.895	.535	.010	226.6	182.9	1955	1940	1884	1146
147.10	1400.3	.896	.524	.010	226.6	179.0	1952	1897	1893	1060
147.00	1400.3	.883	.532	.010	223.6	184.4	1949	1922	1889	1155
147.20	1399.4	.905	.524	.010	228.9	177.1	1949	1923	1890	1121
147.00	1399.0	.908	.527	.010	229.8	177.5	1949	1927	1889	1077
147.60	1398.6	.882	.527	.010	223.0	182.9	1950	1906	1894	1017
147.10	1399.0	.898	.529	.010	227.0	180.5	1949	1936	1892	1137
147.20	1397.7	.904	.532	.010	228.3	180.1	1951	1901	1895	978
147.10	1398.6	.919	.529	.010	232.2	176.4	1954	1900	1889	935
147.00	1399.0	.892	.529	.010	225.8	181.6	1952	1918	1893	1086
147.20	1399.0	.900	.529	.010	227.4	180.0	1949	1896	1893	977
147.40	1399.0	.884	.535	.010	223.2	185.1	1954	1919	1889	1034
147.10	1400.3	.895	.532	.010	226.5	181.9	1954	1936	1891	1120
147.20	1399.4	.888	.529	.010	224.5	180.4	1953	1903	1890	982
147.00	1400.7	.891	.529	.010	225.7	181.8	1954	1944	1894	1169
AVERAGING										

TABLE 2. EXAMPLE OF A TEST REPORT

U.S. ARMY FUELS & LUBRICANTS RESEARCH LABORATORY
TURBINE COMBUSTOR FACILITY

*** EFFECT OF HIGH AVAILABILITY FUEL ON COMBUSTOR PROPERTIES ***
U.S. NAVAL AIR PROPULSION TEST CENTER

DATE: 11/15/76 TIME: 1: 3
COMBUSTION SYSTEM: 2-INCH COMBUSTOR
TEST FUEL: JP5-DERIVED FROM TAR SANDS

***** EXPERIMENTAL CONDITIONS *****

	AVERAGE	STD.DEV.	DESIRED	LAST SCAN
INLET AIR PRESSURE, ATM	9.96	.02	10.00	9.96
INLET AIR TEMPERATURE, DEG K	814.25	.76	810.89	814.05
AIR FLOW RATE, KG/SEC	.516	.006	.513	.524
FUEL FLOW RATE, KG/MIN	.480	.005	.598	.483
FUEL/AIR RATIO	.01550	.00026	.01941	.01537
REFERENCE VELOCITY, M/SEC	69.4	.9	68.6	70.5
HEAT INPUT, KJ/KG AIR	668.7	11.2	837.4	662.9

FUEL PRESSURE= 855KPA (124 PSIA)
FUEL TEMPERATURE=300.0 DEG K
MOISTURE CONTENT OF INLET AIR= 3.5 GMS/KG AIR (309K DEW PNT @ 9.7 ATM)

***** PERFORMANCE SUMMARY *****

FLAME RADIATION	...SIGNAL (MV)...	..RADIATION (KW/SQ M).
TOTAL RADIATION	1.310	84.915
4-5 MICRON BAND	0.000	
BLACK BODY ABSORBTION	1.450	
4-5 MICRON ABSORBTION	0.000	

EXHAUST TEMPERATURES

TC#	AVERAGE	STD.DEV
1	1263 K	3
2	1334	3
3	1367	3
4	1259	3

AVERAGE EXHAUST TEMPERATURE 1306 K
COMBUSTOR TEMPERATURE RISE 491 K

EXHAUST EMMISSIONS

CONCENTRATIONS						EMISSION INDEX			
<---PPM BY VOL--->			<------VOL %------>			<-------GMS/KG FUEL------->			
NO	NOX	HC *	CO	CO2	O2	NO	NOX	HC *	CO
153.0	170.0	0	.002	3.2	16.8	10.4	17.7	0.00	1.27

SMOKE NUMBER: 4.29

COMBUSTION EFFICIENCY, CALCULATED FROM EXHAUST CHEMISTRY: 99.8670 %
FUEL/AIR RATIO, CALCULATED FROM EXHAUST CHEMISTRY: .014934
REMARKS:

The exhaust sample was brought to the instruments through a 350°F heated teflon line and then appropriately distributed.

Smoke Analysis System

The system used for measuring exhaust smoke level was designed according to the requirements of SAE-ARP1179. Briefly, a sample of the exhaust is passed through a strip of filter paper. Particulates from the exhaust are trapped on the surface, leaving a spot ranging in "grayness" from white to black, depending on the sample size and particulate content of the exhaust. The "grayness" of the spot is evaluated with a reflectometer. The smoke number, SN, of each spot is then calculated by:

$$SN = 100 \quad 1 - \frac{R_s}{R_w}$$

where R_s and R_w are the diffuse reflectance of the sample spot and the clean filter paper. Exhaust samples are taken over a range of sample sizes around W/A = 0.023 pound of sample per square inch of filter area. The resulting smoke numbers are plotted against log (W/A). These are least-squares fitted with a straight line; the interpolated value of SN at W/A = 0.023 is the reported smoke number for the engine operation condition. Champagne[12] gives a complete description of the procedure and relates the results to particulate concentration and exhaust plume visibility. Troth et al[13] provide a numerical relationship for that correlation:

$$d_s = a_1 \exp (a_2 SN) [1-\exp (-a_3 SN)] + a_4 \exp [-a_5 (SN-a_6)^2]$$

where d_s = true smoke density, mg/m^3
SN = EPA Smoke Number
$a_1 = 0.8$
$a_2 = 0.057565$
$a_3 = 0.1335$
$a_4 = 0.0942$
$a_5 = 0.005$
$a_6 = 27.5$

Radiation Measurement

Flame radiation is measured with a Rayotube, Model 8890-S, detector, a transverse observation of flame radiation is made via sapphire windows mounted in the sides of the combustor housing (see Figure 2). To determine the flame emissivity, a mirror opposing the radiation detector on the opposite side of the combustor housing is used to reflect radiant energy back through the flame to the detector. For this optical configuration, the emissivity (ε) may be expressed as

$$\varepsilon = 1 - \frac{R_2 - R_1}{r\pi^2 R_1}$$

where r is the reflectivity of the mirror, τ is the transmission coefficient of the window and, R_1 and R_2 are the measured values of flame radiation without and with the mirror respectively. Note, the flame emissivity is unity when the presence of the mirror has no effect on the magnitude of the detected radiation, i.e., all of the reflected radiation is absorbed by the flame.

Combustion Efficiency

Combustion efficiencies are calculated from the exhaust gas analysis according to a relationship developed by Hardin[14]:

$$n_b = 1 - \frac{A \cdot f(UBH) - 121{,}745 \cdot f(CO - 38{,}880 \cdot f(NO) - 14{,}654 \cdot f(NO_2)}{A \cdot [f(CO_2) + f(CO) = f(UBH)]}$$

where f(i) is the concentration of "i" in the exhaust and A is a constant based on the heat of combustion and hydrogen/carbon ratio of the fuel.

TEST FUELS

Ten kerosene-type fuels were used in this program. Nine fuels were specified by NAPTC and were JP-5 fuels or modifications thereof. The tenth was a Jet-A fuel used primarily to stabilize the combustor operating conditions before burning the other nine fuels which were available only in limited quantity; test data was also taken with the Jet-A because, although it is a similar fuel in boiling range, it had a low aromatic and high hydrogen content.

The test fuels were specifically chosen to address the questions stated earlier, namely how extending the fuel specification for aromatics and end point affect combustor operation and if syncrude fuels will correlate in the same manner as petroleum fuels. The requirements for the properties of the six petroleum-derived fuels, which were supplied by AFLRL, are given in Table 3; the three syncrude fuels were supplied by NAPTC and were JP-5 fuels derived from oil shale, coal, and tar sands respectively. It should be noted that the modified JP-5 fuels Nos. 1 through 5 were derived from the base fuel by blending it with stocks of mixed composition within the JP-5 boiling range instead of using pure compounds to get more realistic fuels.

FUEL PROPERTIES

Test fuels were blended as close as possible to the above specification in terms of meeting the allowable variations in viscosity, freeze point, flash point, boiling point range, etc. for JP-5 distillates. Fuel properties such as smoke point, viscosity, flash point, etc. shown in Table 4 were measured by standard ASTM methods. The boiling point distributions (ASTM D2887) are shown in Table 5. Figures 11 to 19 are the gas

TABLE 3. FUEL BLEND CHARACTERISTICS

Fuel No.	
B	Base Fuel - JP-5 with 1 to 2% olefins, 2 to 3% napthalenes and 10-15 percent aromatics. Fuels 1 to 5 are derived by adding materials to this fuel.
1	16 mm smoke point obtained by adding dicyclic polynuclear aromatics to base fuel.
2	16 mm smoke point obtained by increasing naphthalene to 4% and adding monocyclic aromatics as necessary to JP-5 base fuel.
3	Addition of 40% aromatics typical of petroleum distillates in JP-5 distillation range (smoke point must be <19 mm).
4	Specification maximum for aromatics (25%) and olefins (5%) typical of petroleum distillates in the JP-5 distillation range (smoke point variation below 19 mm permissible).
5	Distillation end point of 580°F, achieved by adding compounds typical of petroleum distillates in the required range (variations in other specification limits permissible--except aromatic content).
6	Synthetic JP-5 from Oil Shale. } Supplied by NAPTC
7	Synthetic JP-5 from Coal. } Supplied by NAPTC
8	Synthetic JP-5 from Tar Sands. } Supplied by NAPTC
	Jet-A - Used for adjusting combustor operating conditions.

TABLE 4. SUMMARY OF FUEL PROPERTIES

AFLRL CODE STATEMENT OF WORK, PARAGRAPH	B 6400 4.1.6	1 6401 4.1.2	2 6402 4.1.1	3 6403 4.1.4	4 6537 4.1.3	5 6505 4.1.5	6 6526 Oil Shale	7 6355 Coal	8 6354 Tar Sand
Heat of Combustion, Net (BTU/lb)*	18484	18192	18389	18147	18537	18597	18405	18258	18543
Carbon, % by weight	85.94	86.74	86.60	87.26	86.53	86.38	86.20	86.69	86.61
Hydrogen, % by weight	13.68	13.06	12.86	11.99	12.91	13.60	13.32	13.24	13.32
Nitrogen, % by weight	0.006	0.006	0.010	0.005	0.02	0.007	0.10	0.004	0.004
Oxygen, % by weight	0.42	< 0.03	0.36	0.28	0.35	None	0.28	None	None
Sulfur	0.022	0.024	0.023	0.026	0.026	0.025			
Aromatics by U.V.*									
Single Ring, % by weight	5.7	7.65	10.5	16.6	11.3	5.7	15.1	7.5	7.0
Double Ring, % by weight	1.2	7.81	4.9	9.4	4.5	1.6	1.7	0.3	0.1
Triple Ring, % by weight	0.01	0.03	0.01	0.03	0.05	0.06	0.02	0.02	0.01
Total, % by weight	6.91	15.49	15.5	26.03	15.85	7.36	16.82	7.82	7.11
HPLC Analysis*									
Saturates, % by weight	89.1	76.4	73.2	62.2	74.6*	88.1	74.0	82.7	84.5
Aromatics, % by weight	10.9	23.6	26.7	37.8	21.9*	11.9	23.0	17.3	15.5
Olefins, % by weight	0.0	0.0	0.0	0.0	3.5*	0.0	3.0	0.0	0.0
Viscosity at -30°F, cSt*	8.25	3.45	8.53	11.20	9.04	13.35	7.76	8.90	12.77
Freeze Point, °F*	-70.6	-68.8	-76.0	-68.8	-57	-23.8	-27.4	-90.4	-70.6
Flash Point, °F*	141	147	141	130	144	143	131	138	149
Specific Gravity at 60°F*	0.8108	0.8270	0.8216	0.8541	0.8285	0.8071	.8056	0.8485	0.8285
Smoke No.	26	16	16	12	16.5	23	17	17	18
Aniline Point, °F	128.5	127.4	129.5	101.8	145.4	149.7	--	--	--
Aniline Gravity Const.	5114	4981	5050	3422	6194	6692	--	--	--
B.P. @ 98%, °C	271	279	277	284	281	321	295	278	288

*by FIA.

TABLE 5. SUMMARY OF

BOILING POINT DISTRIBUTION

BY ASTM D2887, METHOD: SD/SE3

% Off	A (°C)	Base (°C)	1 (°C)	2 (°C)	3 (°C)	4 (°C)	5 (°C)	6 (°C)	7 (°C)	8 (°C)
IBP	120	148	144	147	145	135	146	114	155	140
5	145	182	181	181	185	186	182	160	167	168
10	157	187	187	187	192	191	187	171	172	183
15	166	191	190	191	195	195	191	180	177	192
20	171	193	194	194	197	197	193	190	182	197
25	178	196	196	196	201	198	196	196	186	203
30	186	198	198	198	205	200	197	198	188	207
35	192	198	199	200	210	202	198	206	193	212
40	198	200	202	201	213	205	200	213	197	216
45	205	201	205	203	216	209	201	216	201	220
50	212	202	209	206	224	212	204	220	203	225
55	216	205	212	209	231	216	207	227	207	229
60	225	207	216	212	233	221	211	232	210	233
65	230	210	219	215	236	230	214	235	215	237
70	236	213	224	218	239	234	216	240	218	242
75	244	216	234	227	249	237	224	249	225	247
80	251	220	238	233	254	245	235	253	231	252
85	258	230	245	238	257	253	250	259	238	258
90	267	243	256	252	262	258	262	268	248	265
95	277	259	268	263	273	268	284	280	262	275
FBP	297	289	301	302	305	307	363	300	303	360

FIGURE 11.

GAS CHROMATOGRAM OF JP-5 BASE FUEL

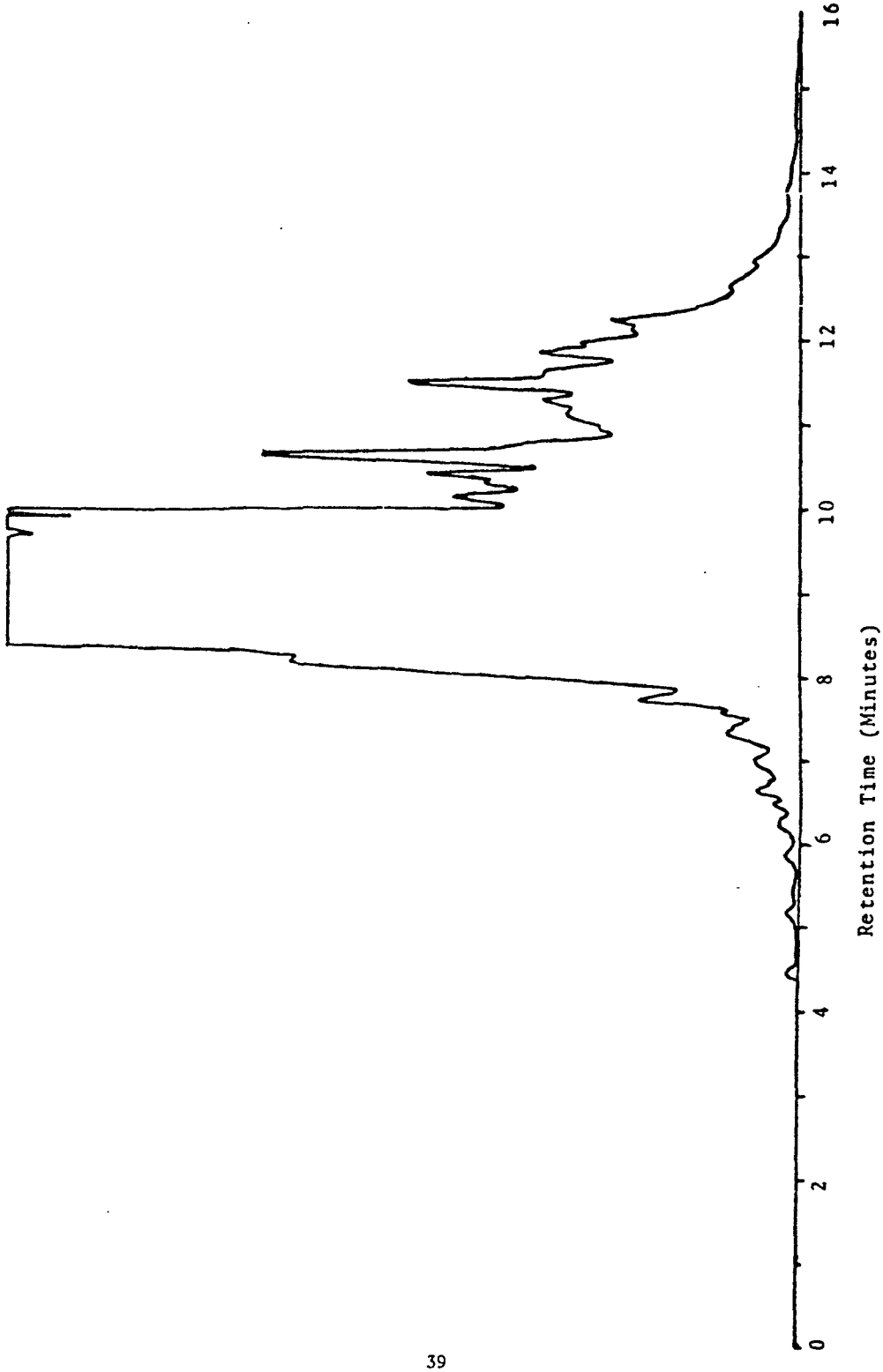

FIGURE 12.

GAS CHROMATOGRAM OF JP-5 BLEND No. 1

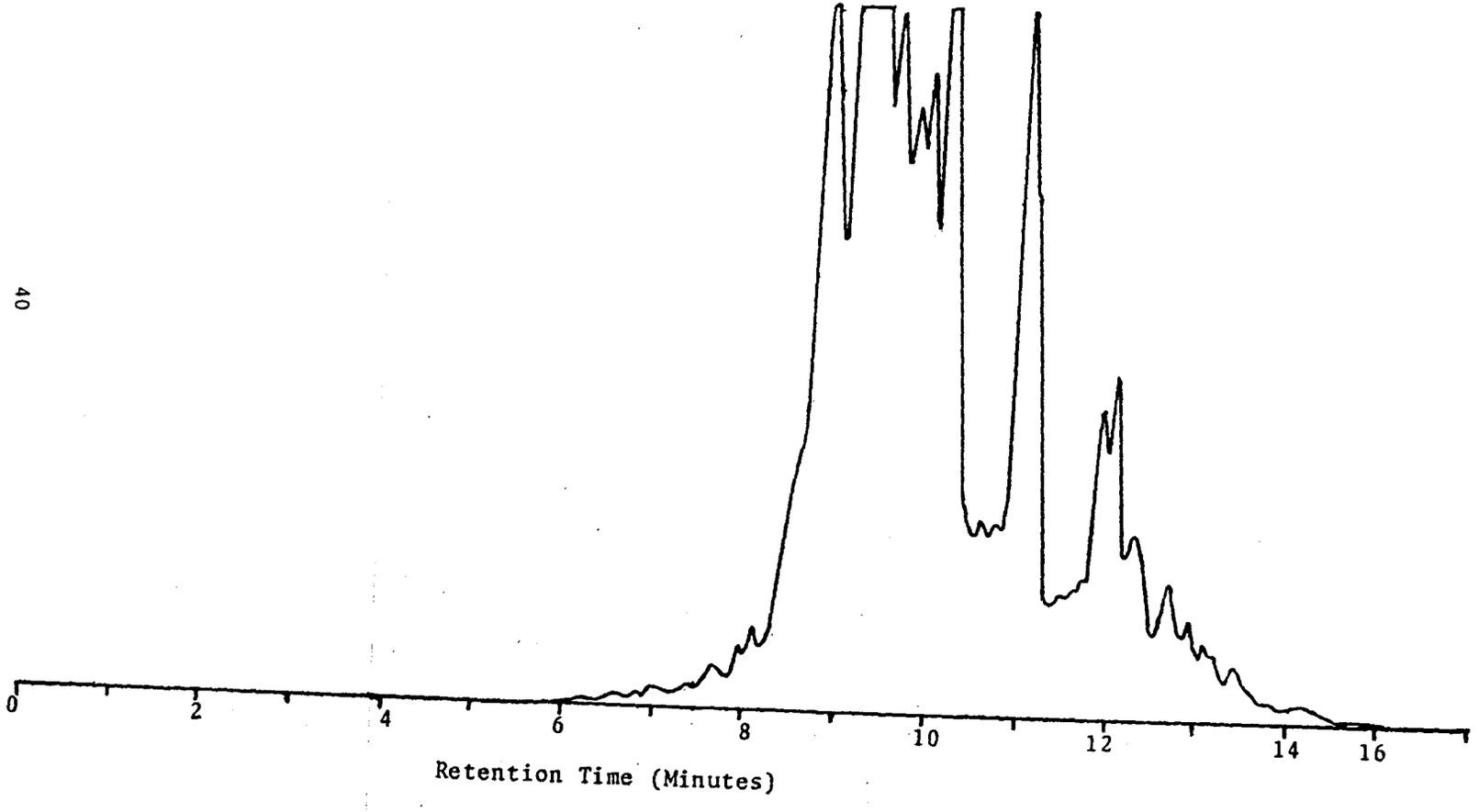

FIGURE 13.

GAS CHROMATOGRAM OF JP-5 BLEND No. 2

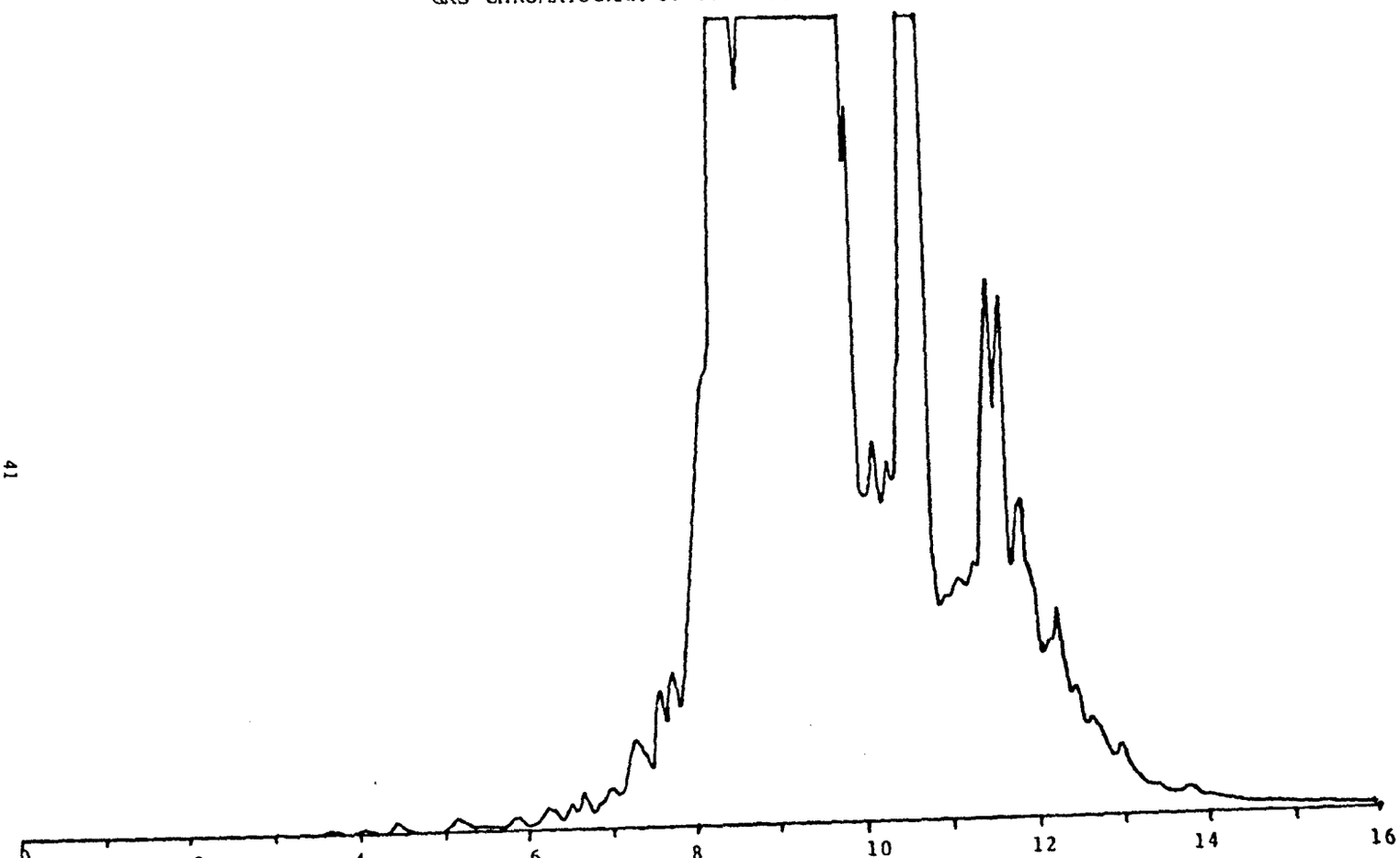

FIGURE 14.

GAS CHROMATOGRAM OF JP-5 BLEND No. 3

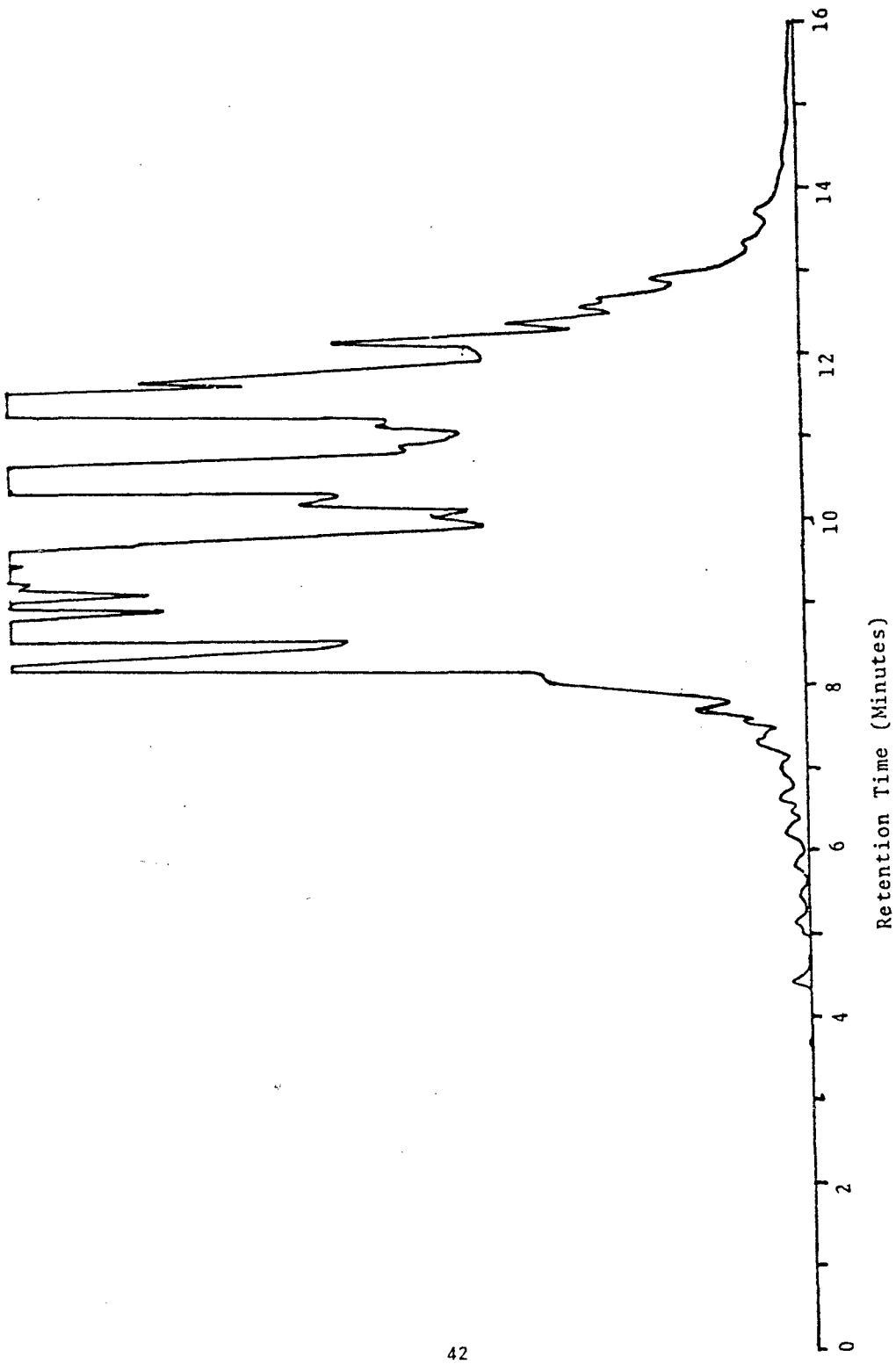

FIGURE 15.

GAS CHROMATOGRAM OF JP-5 BLEND No. 4

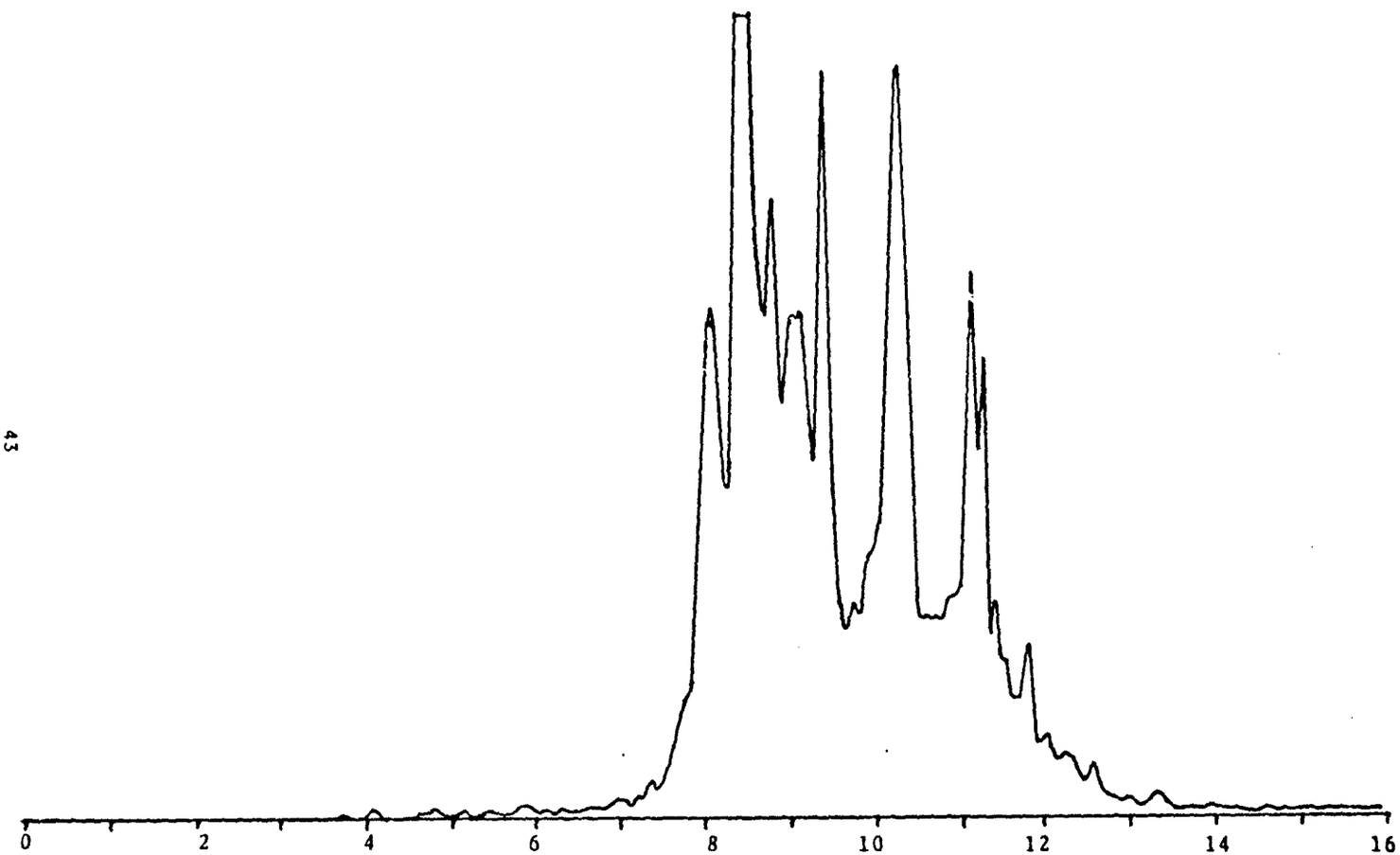

FIGURE 16.

GAS CHROMATOGRAM OF JP-5 BLEND No. 5

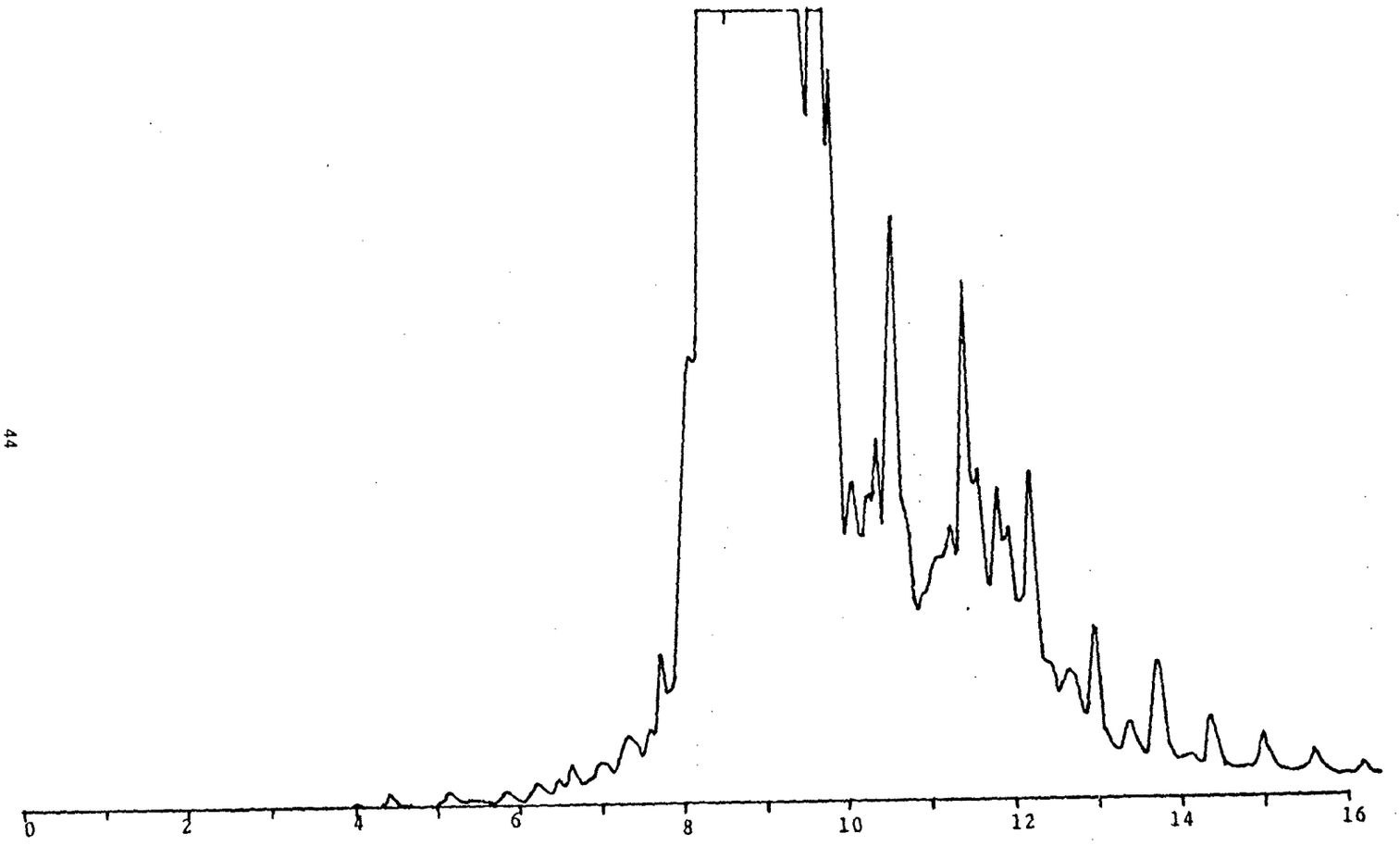

FIGURE 17.

GAS CHROMATOGRAM OF JP-5 FUEL No. 6 FROM OIL SHALE

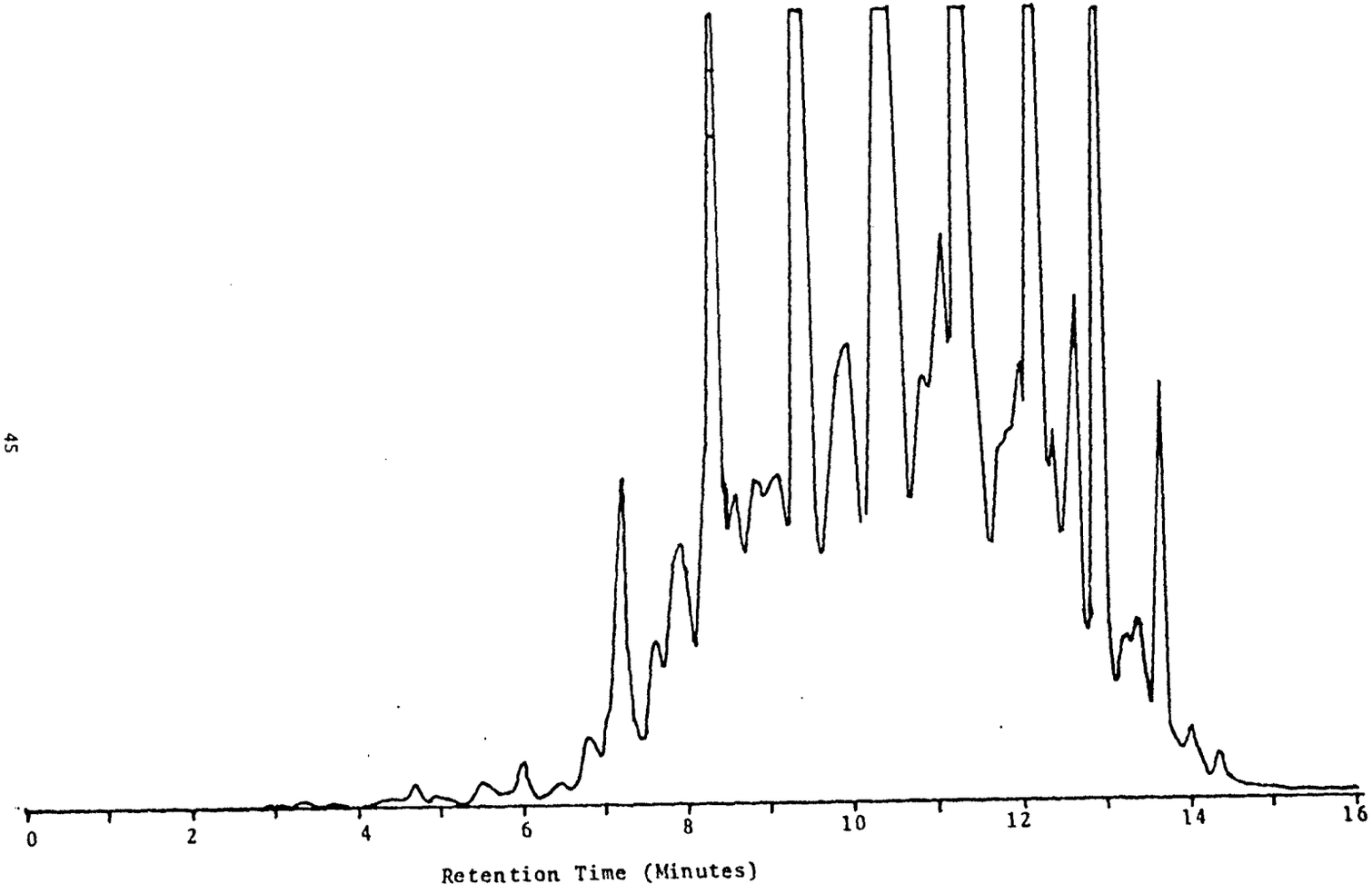

FIGURE 18.

GAS CHROMATOGRAM OF JP-5 FUEL No. 7 FROM COAL

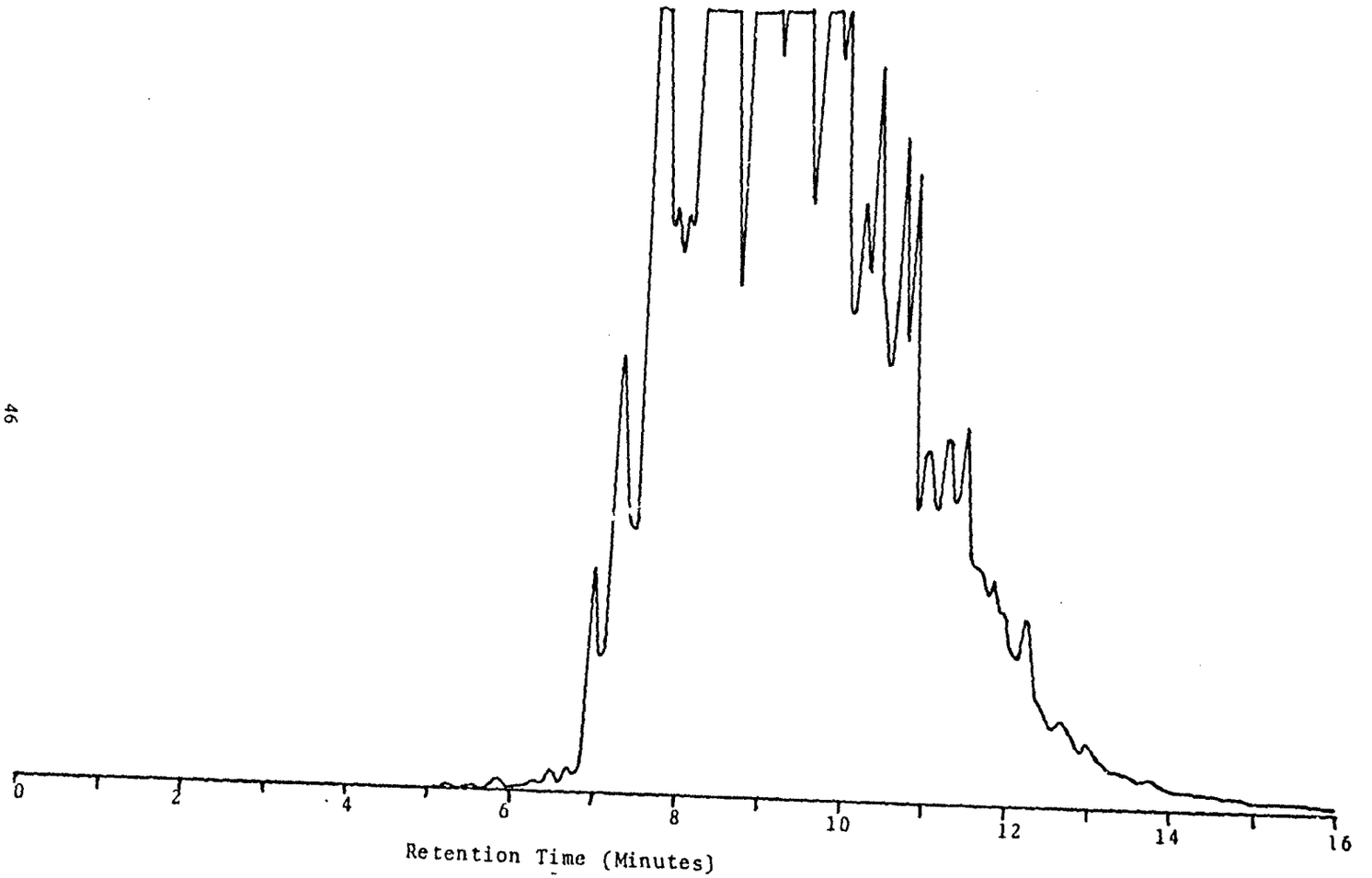

FIGURE 19.

GAS CHROMATOGRAM OF FUEL No. 8 FROM TAR SANDS

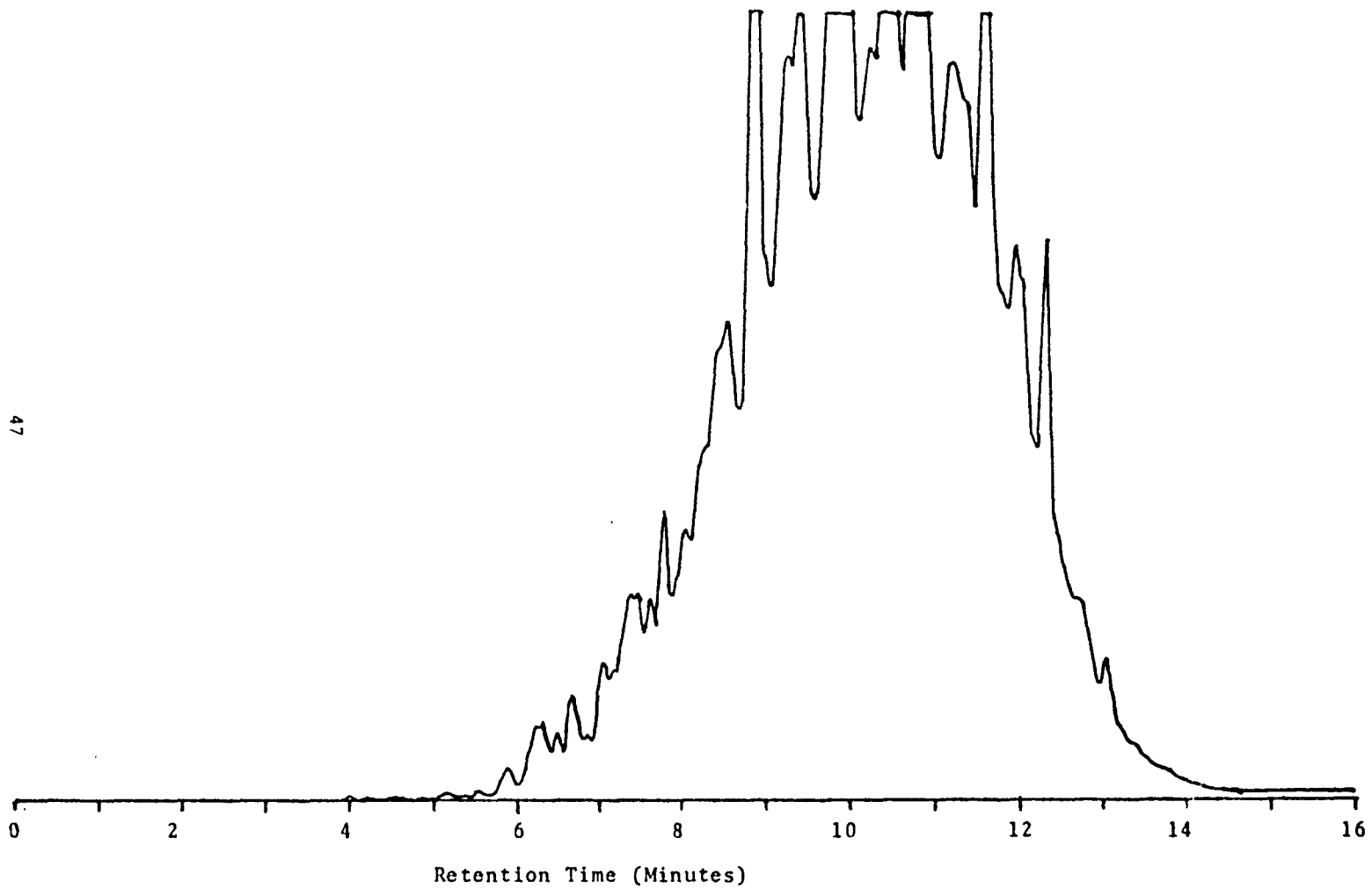

chromatographic spectra as determined by the SD/SE3 method; Figure 20 is a reference spectrum for normal saturates. The significance of these spectra is mainly to show that the blended test fuels appear to be typical kerosene-type fuels, undistorted by the blending agents. Aromatics and saturates were determined by high performance liquid chromatography (HPLC) and weight percent ring carbon, for single, double and triple ring aromatics, was analyzed by ultraviolet absorption spectroscopy. The hydrogen, carbon, nitrogen and oxygen analyses were done by Galbraith Laboratories, Inc. The net heat of combustion ΔHn was evaluated from

$$\Delta Hn = \Delta Hg - 91.23 \text{ (Percent Hydrogen)}$$

where ΔHg is the gross heat of combustion determined in a calorimetric bomb.

With only a few exceptions, the relatable fuel properties were found to show a strong correlation. As shown in Figure 21, the total aromatic content determined by HPLC gave a good correlation with the hydrogen content. It is expected that the JP-5 blends B and 1 through 5 would correlate well in that these fuels were prepared by adding blending stocks to the base fuel. The blending stocks have relatively low hydrogen content (10% or less) and thereby reduce the hydrogen content in the blended fuel by an amount directly proportional to the amount added. The syncrude fuels from coal (7) and tar sands (8) behave very much the same as the petroleum-base fuels B and 1 through 5 in the plot of HPLC aromatics versus hydrogen content, while the oil shale (6) derived JP-5 with a hydrogen content of 13.3 percent has an aromatic content that corresponds to a blended fuel with a hydrogen content of 12.9 percent. This deviation appears to be due to an unusually high concentration of normal saturates in the oil shale syncrude. Although the aromatic content of this fuel (6) is higher than fuels 7 and 8, its hydrogen content remains about the same because the high aromatics (low hydrogen) is balanced by the high normal saturates (high hydrogen). The syncrudes from coal and tar sands contain high concentrations of decalin and other cycloparaffins. These structures have an intermediate hydrogen content typical of olefins and probably similar to the non-aromatic fraction of the JP-5 base stock. The plot of ring carbon versus hydrogen shown in Figure 22 gives a good correlation for the blended fuels (B, 1 to 5), but the syncrude fuels tend to deviate from this behavior. The relatively low ring carbon values for the syncrudes from coal (7) and tar sands (8) suggests that the aromatic molecules in these fuels have a higher concentration of side chains attached to the rings as the cycloparaffins have a slightly higher than average hydrogen content than the normal JP-5 base stock. The deviation of fuel (6) can, as before, be attributed to unusually high normal saturates.

The smoke point was found to correlate with the hydrogen content as

$$\text{Smoke Point} = 86.7 - 17.0\ H + 0.9\ H^2$$

FIGURE 20.
CALIBRATION WITH STRAIGHT CHAIN ALIPHATICS

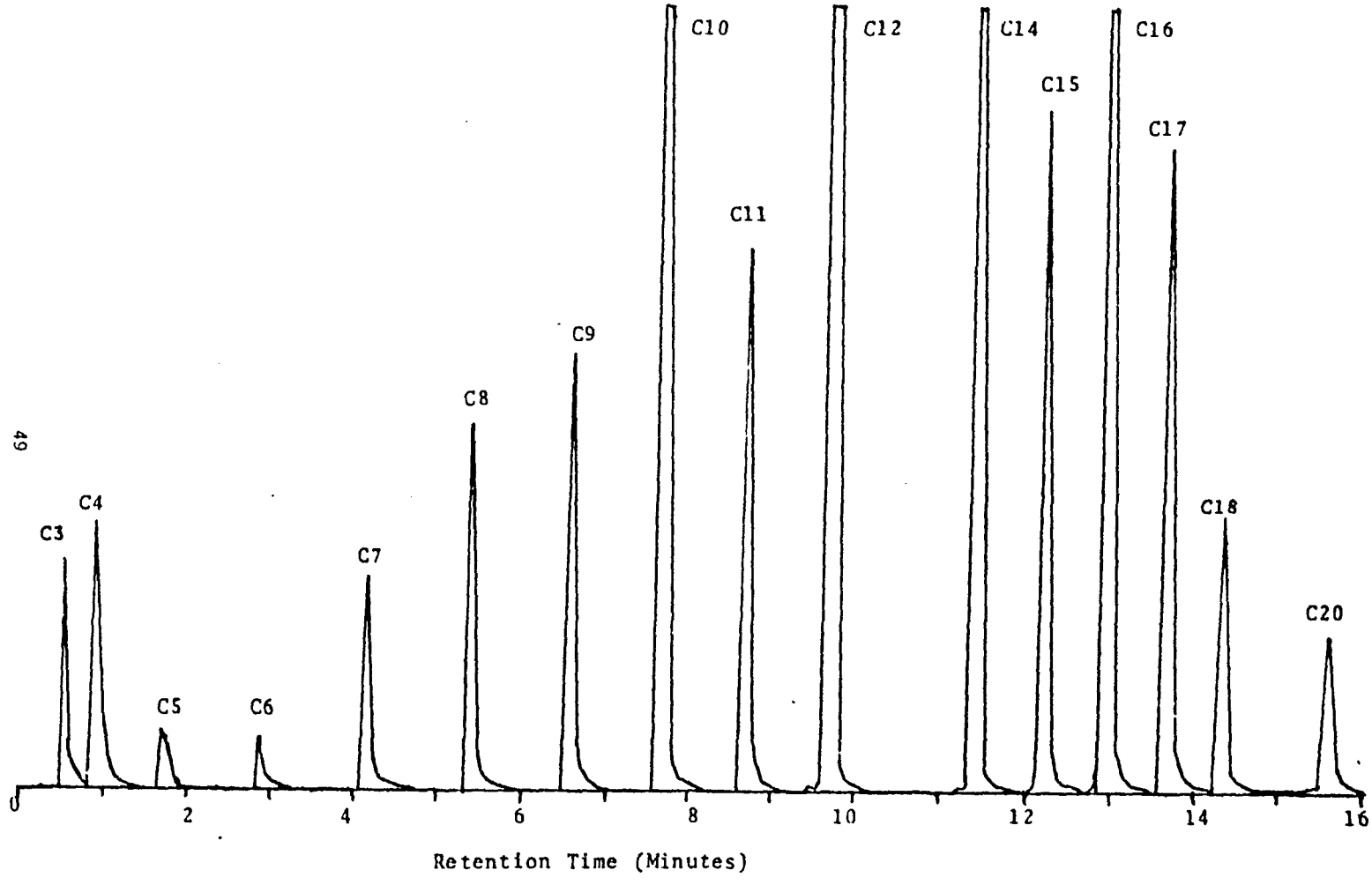

FIGURE 21. CORRELATION OF AROMATIC CONTENT WITH HYDROGEN CONTENT

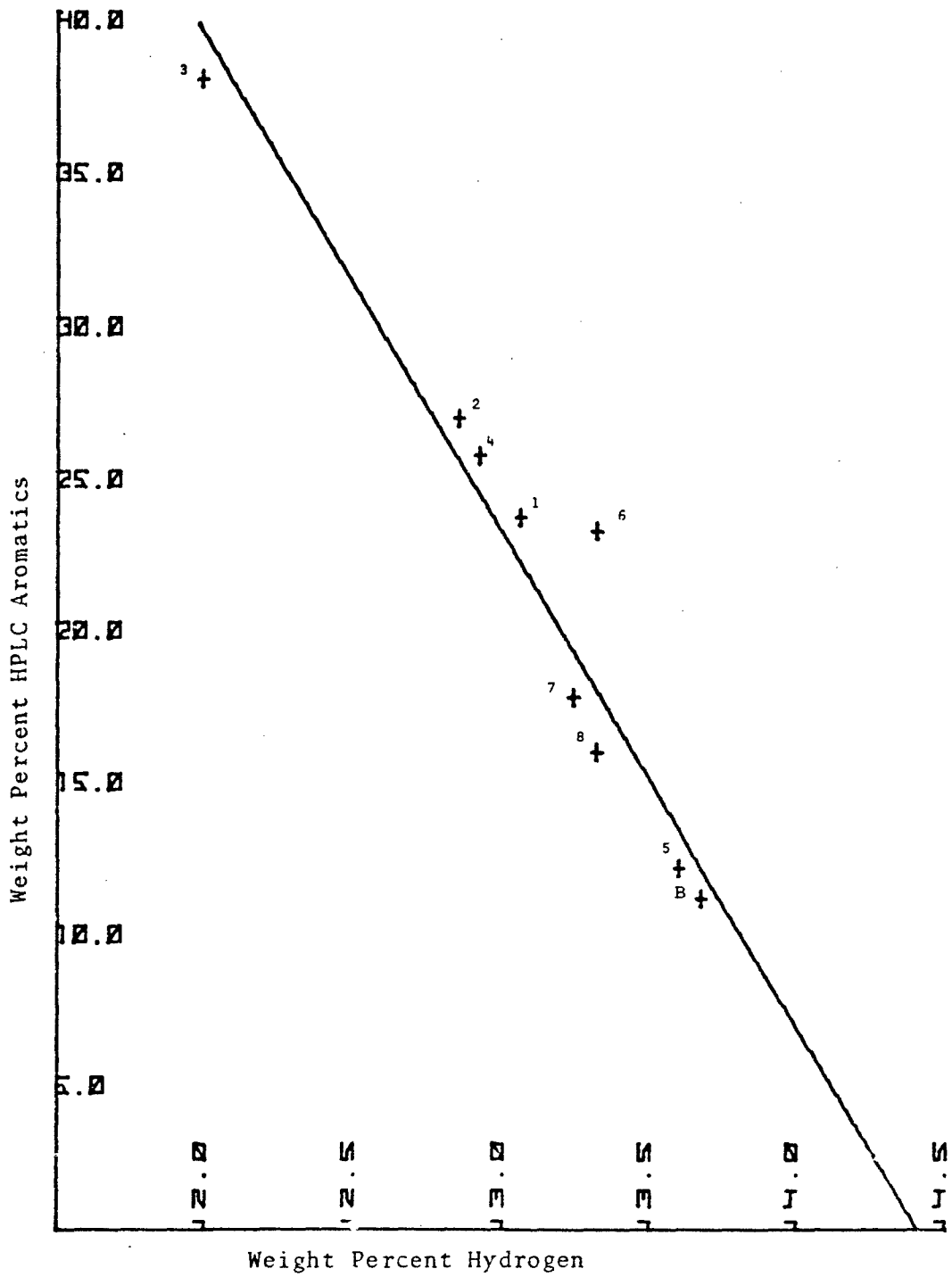

FIGURE 22. CORRELATION OF RING CARBON CONTENT WITH HYDROGEN CONTENT

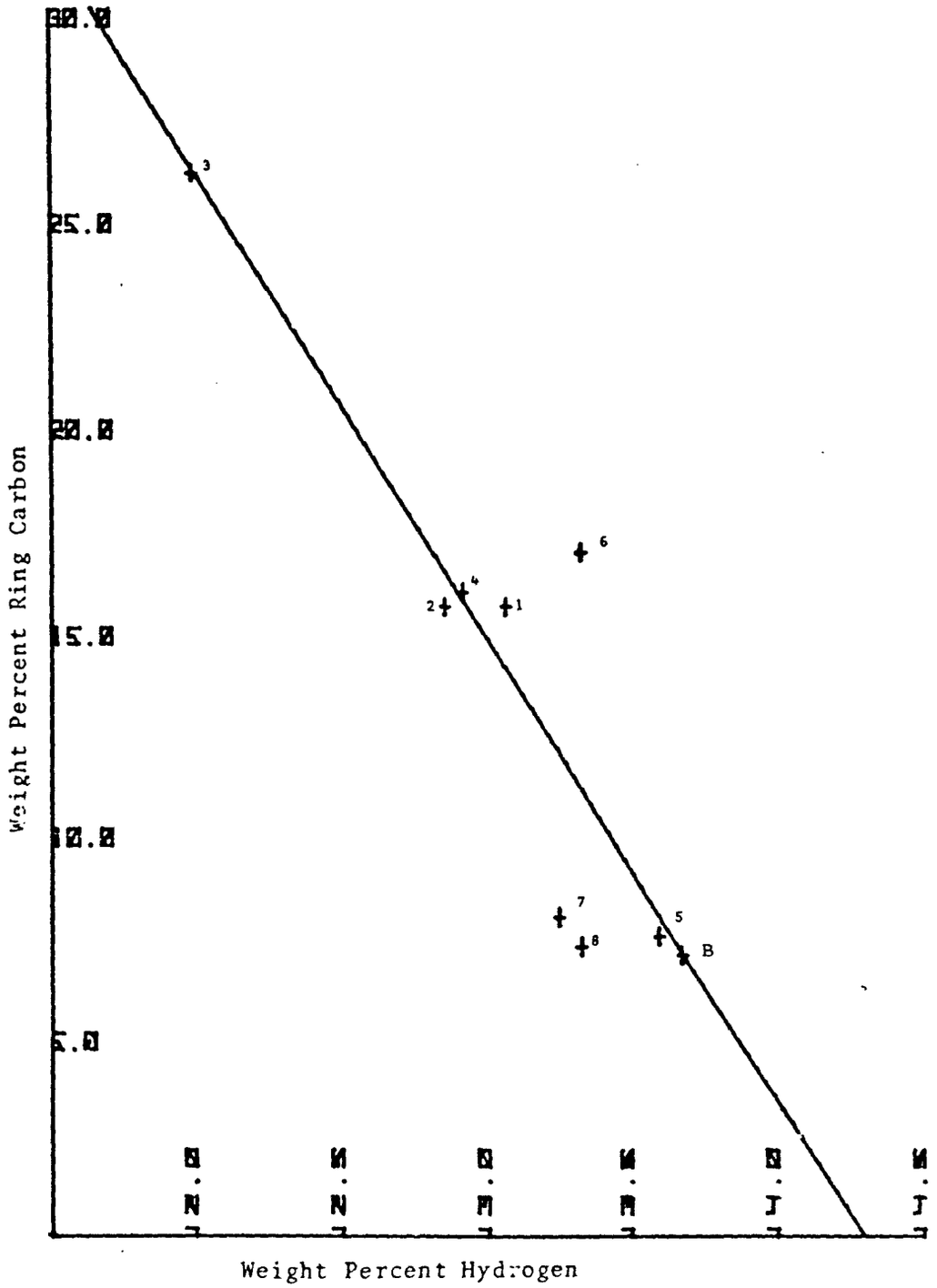

FIGURE 23. CORRELATION OF SMOKE POINT WITH HYDROGEN CONTENT

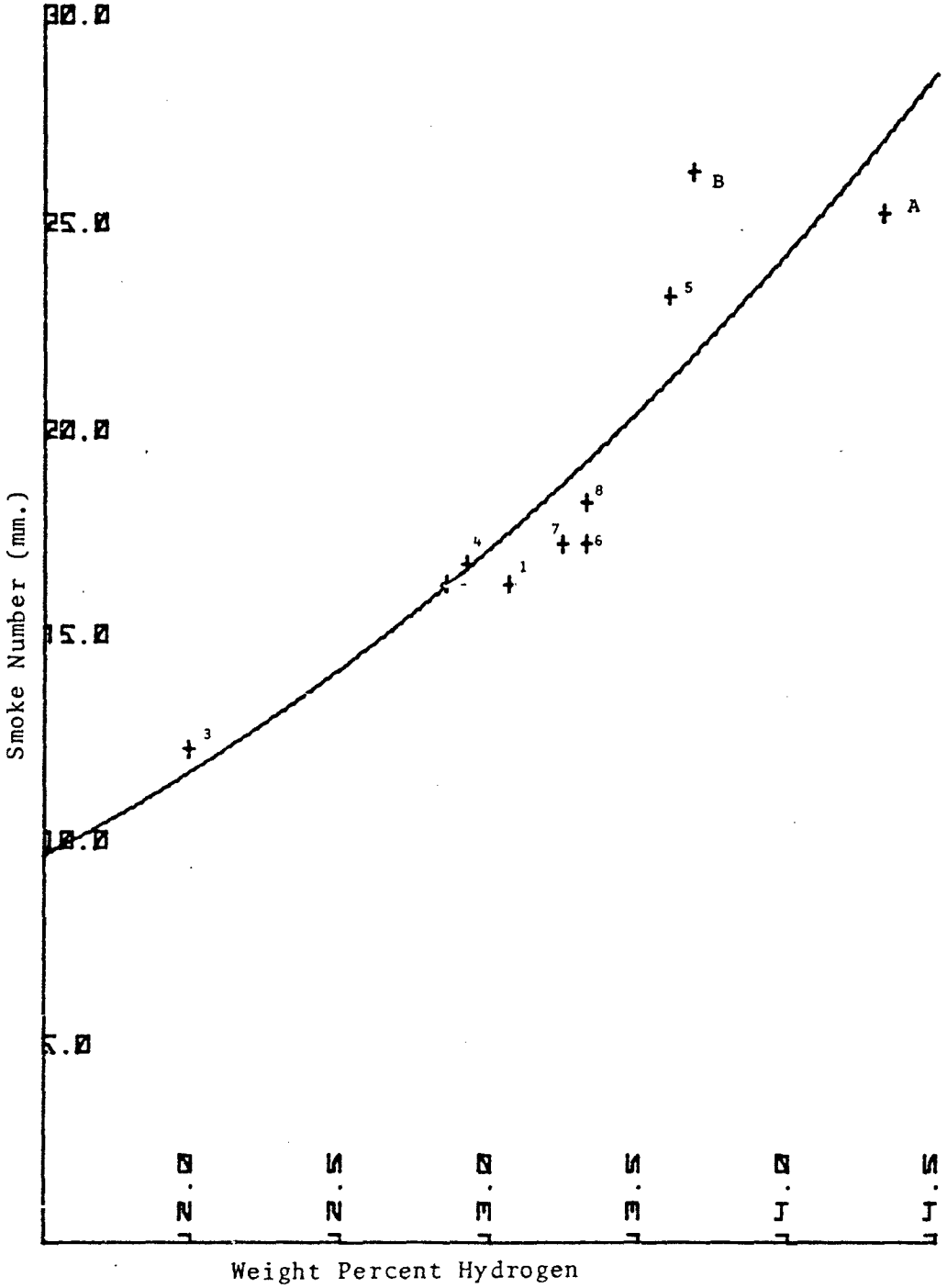

This relationship was developed as a least squares fit for the fuels in this program and is shown in Figure 23.

The correlation between end point and viscosity as shown in Figure 24 is weak; however, the trend is toward higher viscosities for the fuel with the highest end point.

The syncrude JP-5 derived from oil shale contained a significant amount of fuel bound nitrogen (0.10%). If all of this fuel bound nitrogen were to be converted into NO_x the contribution to the NO_x emissions index would be 3.29 grams of NO_2/kg of fuel.

TEST PROGRAM

Test Conditions

The test program for evaluating the fuels described above was designed by NAPTC to cover the combustion conditions for existing aircraft turbine engines. The conditions are basically defined by the pressure and temperature values as shown below.

Inlet Pressure BIP (atm)	Inlet Temperatures BIT (°F)
2	100, 500, 1000
5	500, 1000, 1500
10	500, 1000, 1500
15	1000, 1500

For each of these conditions of pressure and temperature, the reference velocities, 75, 150 and 225 ft/sec, and fuel/air ratios corresponding to heat inputs, 90, 180 and 360 BTU/pound of air were to be examined. (Heat input was used rather than fuel-air ratio to account for the different heats of combustion; this in essence holds the adiabatic flame temperature in the primary zone constant as the fuels are changed and any radiation changes are then due only to fuel properties.) This gave a total number of experiments equal to the 11 basic conditions above X 3 values of reference velocity X 3 values of BIH or 96 possible experiments, assuming no limitations. In practice, the operating characteristics of the combustor and excessive exhaust temperatures reduced the number elements of this matrix that could be obtained, e.g.,

(1) the flame could not be stabilized at burner inlet temperatures of 100°F, and

(2) fuel-line vapor lock precluded stable combustion at burner inlet temperatures of 1500°F and occasionally at 1000°F when the fuel flow rate was low.

FIGURE 24. CORRELATION OF END POINT WITH VISCOSITY

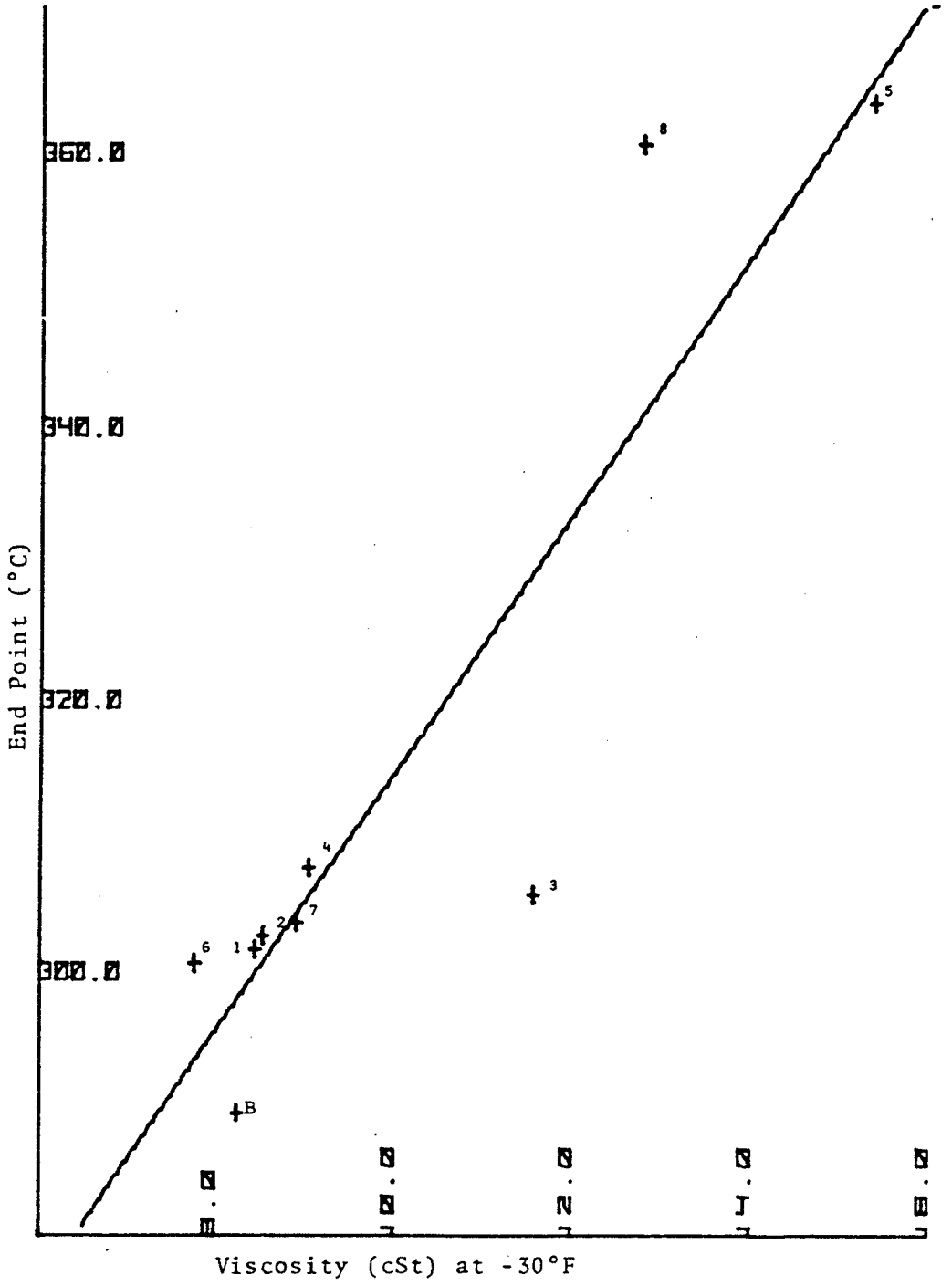

One severe problem that excluded several of the experiments was carbon deposition which brought about combustion instability and destruction of the combustor can. It appeared that this was related to vapor lock in the nozzle and a poor spray pattern.* It seemed that coking in the combustor can resulted from wall wetting by misguided fuel droplets.

The number of successful operating conditions was reduced to 37. It should be noted that the points which were unattainable were outside the envelope of operating conditions used by Shirmer at Phillips Petroleum over the many years that he used this combustor design suggesting that the original matrix for this study was perhaps somewhat ambitious.

Test Procedure

Because the Phillips 2" combustor does not have an ignitor, it was necessary to first establish air flow conditions suitable for autoignition of the fuel spray before establishing the desired weight of conditions for the test point. The combustor inlet conditions used to establish ignition were P = 10 atm, T = 800°F, V = 75 ft/sec and relatively high heat input of about 300 BTU/pound of air. High temperature and pressure are favorable for ignition and a low reference velocity suppresses the possibility of torching throughout the exhaust system. Jet-A fuel, which was in ample supply, was used initially in each run to obtain ignition and set the particular run conditions to conserve the test fuels. The fuel delivery system was designed to shut off the Jet-A fuel and simultaneously turn on the next test fuel in line, i.e., fuel number 1, etc. The adjustment time in switching from one fuel to the next is less than five minutes and the combustion performance measurements on a fuel are complete in about fifteen minutes. After the combustion conditions are stabilized, the smoke number and gaseous emissions (NO, NO_x, CO and UBH) are determined. Normally, the smoke number is determined by making five smoke readings. The radiation is monitored as a continuous readout on a chart recorder. The emissivity measurement is determined by blocking off the mirror opposing the radiation detector on the opposite side of the combustor housing (see Figure 2). This is described in the experimental section of the report.

The flow conditions in the combustor were very stable with standard deviations of about one percent in the parameters. Thus, it was possible to maintain parameters relatively constant for each of the fuels tested for a given test condition.

*Recently, after all the experiments had been completed, it was found that fuel number 1 (containing polycyclic aromatics) had been blended improperly. To rationalize this oversight, the experiments on fuel number 1 were repeated using fuel number 2 as a reference. However, the combustor had been changed slightly in that a water-cooled fuel line was installed. Time did not allow for an extensive test program, but nevertheless, it was found that the carbon deposition was significantly reduced and it was possible to operate at higher temperatures (1500°F).

Test Results

The test results are printed by the data acquisition system on test report sheets such as the one shown in Table 2. The test report sheets are not included in this report as there is one sheet for each fuel at each test condition for a total of close to 400 test reports. A summary of the test conditions and the combustion performance results including radiation, smoke number, COEI and NO_xEI, is presented in Tables 6 to 10. The combustion efficiency and the emissions of unburned hydrocarbons were neglected in the tabulations because there wasn't any significant variation in these parameters. Combustion efficiency was almost always 99 percent and the hydrocarbons emission index seldom exceeded 0.2 grams/kilogram of fuel consumed. Note, the results for fuel number 1 (i.e., smoke point of 16 mm by addition of polycyclic aromatics) is excluded from Tables 6 to 9, because this fuel was blended improperly in the original experiment. The test results for fuel number 1 and fuel number 2 as a reference are shown in Table 10. In these particular experiments, the differential fuel nozzle pressure was included in the tabulation of the test conditions. In the original set of experiments it was not realized that fuel pressure would change substantially from one set of conditions to another, so the fuel pressure was recorded in only a fraction of the experiments. In planning the test conditions, the fuel nozzles were selected such that the pressure drops would be in a narrow range, e.g., 200 to 250 psi. It was discovered later in the actual experiments that the nozzle pressures varied considerably depending on the inlet conditions. This was largely due to the high temperatures of the fuel line and nozzle. Thus, the flow characteristics of the nozzles in the combustor were significantly different than those observed when they were calibrated (mass flow rate versus pressure) outside the combustor at room temperature.

In the tests exclusively for fuels 1 and 2 it was found that the differential fuel pressure was an important variable at some of the conditions (e.g., low pressure), but as a whole it did not have a strong effect on the combustion performance results. This will be discussed in more detail later (see page63).

RESULTS AND CONCLUSIONS

Flame Radiation

As a whole, the flame radiation showed good stability and followed anticipated trends. This is illustrated in Figure 25 where radiation and exhaust smoke are correlated with combustor inlet conditions; the latter are defined in the symbol legend. Bearing in mind that radiation depends on particulates formed in the primary zone and exhaust smoke is simply what remains after oxidative consumption of particulates in the secondary and quench zones, the basic trends become apparent: radiation is increased by increasing temperature, pressure, heat input

TABLE 6. SUMMARY OF FLAME RADIATION MEASUREMENTS

Units: Pressure, P (atmospheres)
Temperature, T (°K)
Reference Velocity, V (meters/sec)
Heat Input, H (J/Kg at air)

					RADIATION (KW/M^2)								
Run	P	T	V	H	Jet A	JP-5 Base	Mod 2	Mod 3	Mod 4	Mod 5	Oil Shale	Coal	Tar Sands
1	2	533	46	840	8.19	8.19	7.79	10.91	7.79	55.2	55.2	55.2	55.2
2	2	812	69	770	28.14	31.43	44.80	------	------	------	------	------	------
3	2	533	69	837	6.57	6.57	6.57	8.98	52.2	6.57	6.57	6.57	6.57
4	2	533	69	418	13.53	14.27	21.37	------	------	15.72	14.27	17.87	17.87
5	5	533	46	209	35.33	32.74	48.51	68.83	49.73	38.52	36.61	44.80	46.66
6	5	533	46	419	26.81	56.40	77.20	95.58	61.18	26.81	42.93	33.39	30.13
7	5	533	46	697	33.39	38.52	------	------	------	------	------	------	------
8	5	533	69	209	19.98	19.98	22.06	25.[illegible]	22.06	20.68	20.68	21.37	21.37
9	5	533	69	419	35.33	34.68	59.39	93.35	62.36	44.18	50.95	62.95	53.99
10	5	811	46	209	50.34	46.04	53.38	------	44.80	41.68	42.93	------	------
11	5	811	46	419	109.4	115.3	136.2	154.5	138.8	120.2	124.5	136.2	127.2
12	5	811	69	419	61.18	67.07	103.8	138.84	95.58	67.07	78.65	95.58	78.65
13	5	811	69	698	65.31	68.24	106.0	------	------	------	------	------	------
14	5	811	69	837	------	------	------	------	------	------	------	------	------
15	5	811	69	720	------	73.48	83.21	------	------	68.83	82.65	98.36	85.48
16	10	811	69	209	36.61	35.33	35.33	38.52	36.61	35.33	36.61	36.61	36.61
17	10	811	69	419	55.2	59.39	86.05	126.63	87.18	64.72	69.41	83.21	74.05
18	10	811	69	660	62.36	70.58	105.5	145.15	106.07	79.23	83.78	101.12	84.92
19	10	811	46	209	39.79	33.39	36.6	------	34.04	35.33	37.89	39.79	41.05
20	10	811	46	419	164.87	170.00	180.6	185.27	------	------	------	------	------
21	10	815	46	660	101.12	109.36	139.89	168.98	144.10	123.96	130.90	137.79	128.24
22	10	533	69	209	35.33	34.68	38.52	51.56	38.52	33.39	36.61	49.12	41.05
23	10	533	69	419	81.51	88.87	51.64	75.78	51.56	37.89	43.56	52.17	48.51
24	10	533	46	209	47.27	46.66	59.39	82.08	59.39	50.34	52.78	61.18	60.58
25	10	533	46	419	64.13	65.90	75.78	------	------	136.20	149.33	154.54	146.72
26	10	533	46	510	------	115.88	------	------	------	------	------	------	------
27	10	533	23	209	112.08	109.36	129.83	149.33	127.17	106.62	118.58	133.55	129.83
28	10	533	23	435	117.50	128.24	144.10	190.31	170.00	159.71	154.54	144.10	128.24
29	10	533	23	435	47.72	41.14	39.85	------	------	------	------	------	------
30	15	810	23	209	78.65	69.99	------	------	------	------	------	------	------
31	15	812	23	419	136.2	175.11	185.27	180.20	144.10	149.33	151.94	162.29	154.54
32	15	812	23	660	156.61	158.16	167.95	180.20	170.00	159.71	163.33	167.44	163.33
33	15	812	46	209	52.17	49.12	46.04	49.12	46.04	46.04	46.04	49.12	42.93
34	15	812	46	419	94.47	98.36	127.17	155.57	125.56	104.98	111.54	128.24	114.80
35	15	811	46	610	122.88	128.24	155.57	182.73	158.16	135.14	147.24	164.87	150.37
36	15	811	69	209	33.39	36.61	35.33	46.04	37.89	33.39	31.44	38 52	36.61
37	15	811	69	419	83.21	91.67	121.81	147.76	113.17	84.35	103.33	115.34	104.98

TABLE 7. SUMMARY OF EXHAUST SMOKE MEASUREMENTS

Units: Pressure, P (atmospheres)
Temperature, T (°K)
Velocity, V (meters/sec)
Heat Input H, (KJ/Kg of air)

					SMOKE NUMBER									
Run	P	T	V	H	Jet A	JP-5 Base	Mod 2	Mod 3	Mod 4	Mod 5	Oil Shale	Coal	Tar Sands	Nozzle GPH
1	2	533	46	837	2.09	0.7	1.73	2.7	1.01	0.98	0.48	2.4	1.05	1.5
2	2	812	69	770	2.2	0.86	4.1	9.7	11.5	3.85	4.5	6.6	15.0	1.5
3	2	533	69	837	1.8	1.27	5.9	16.1	11.6	8.65	5.5	4.4	5.2	2.5
4	2	533	69	419	3.3	1.64	3.2	6.95	3.7	1.45	1.8	1.5	1.1	1.5
5	5	533	46	209	9.4	5.4	6.4	13.4	8.4	10.2	4.7	6.0	7.8	1.5
6	5	533	46	419	24.1	29.9	43.9	46.7	52.2	19.0	11.8	9.7	6.7	2.5
7	5	533	46	697	32.8	35.6								
8	5	533	69	209	2.0	1.9	1.9	3.0	2.3	1.5	1.0	1.9	2.1	1.5
9	5	533	69	419	12.4	19.0	28.7	41.8	20.6	15.3	22.9	28.9	18.8	2.5
10	5	812	46	209	3.1	2.7	3.3	2.7	3.99	2.5	2.7	3.6	5.2	1.5
11	5	813	46	419	50.4	60.0	50.8	32.9	30.8	48.9	53.9	63.7	65.7	1.5
12	5	812	69	419	3.4	3.7	6.5	7.9	3.7	6.4	6.9	5.5	4.8	2.5
13	5	812	69	698	6.7	12.4	49.9	64.5						
14	5	812	69	837	29.3	27.5	42.6	65.1	66.2	55.3	61.3	69.7		
15	5	812	69	720	5.9	21.4	27.7	45.7	62.97	11.7	11.7	15.0	9.1	
16	10	810	69	209	4.8	27.7	23.9	32.0	19.4	31.5	14.3	15.2	13.96	2.5
17	10	812	69	425	1.9	1.8	1.65	2.5	2.1	2.13	2.0	2.0	1.8	4.0
18	10	812	69	660	2.4	3.1	7.4	12.1	7.4	3.5	4.5	5.4	4.3	4.0
19	10	812	46	209	4.0	3.4	2.5	1.6	1.7	1.6	3.3	3.1	1.9	1.5
20	10	811	46	419	5.8	6.8	5.7	9.61						2.5
21	10	816	46	837(660)	6.6	6.6	12.5	17.7	14.6	10.3	10.8	12.3	15.3	4.0
22	10	533	69	209	57.9	31.6	34.5	26.1	21.1	14.6	34.1	18.1	15.6	4.0
23	10	533	69	419	24.9	36.6	34.4	43.3	30.4	18.7	21.8	28.2	27.1	4.0
24	10	533	46	209	14.9	7.0	8.4	10.5	7.5	5.5	4.6	8.0	5.5	2.5
25	10	533	46	419	38.5	55.8	65.0	69.2	59.0	57.8	53.5	66.0	73.7	4.0
26	10	533	46	837(500)	52.6	70.9	72.9	81.9	78.6	76.6	79.7	81.7	88.7	4.0
27	10	533	23	209	14.5	12.8	19.2	26.4	15.97	12.1	13.8	18.1	17.7	1.5
28	10	533	23	435	89.5	87.7	90.9	87.0	88.4	91.3	94.0	92.8	94.3	2.5
29	10	533	23	435	46.1	49.2	66.3							4.0
30	15	810	23	209	2.8	1.9	2.3	2.7	3.0	2.9	1.9	2.0		1.5
31	15	812	23	419	24.0	24.4	9.8	7.5	46.7	23.8	16.6	7.5	8.8	2.5
32	15	810	23	837(600)	15.4	17.3	17.4	19.8	16.4	16.8	16.4	19.2	19.0	4.0
33	15	812	46	209	12.9	13.7	9.4	9.1	10.1	13.1	11.5	10.5	4.2	2.5
34	15	812	46	419	9.5	17.4	10.1	8.5	6.7	6.7	4.8	4.6	6.4	4.0
35	15	812	46	837(600)	10.0	9.8	12.9	18.8	13.7	9.7	12.3	15.9	14.2	4.0
36	15	812	69	209	12.9	8.9	6.3	5.8	5.7	8.4	3.7	6.3	3.4	4.0
37	15	812	69	419	1.6	2.5	3.5	3.5	2.3	2.2	2.9	3.1	2.7	4.0

TABLE 8. SUMMARY OF CO EMISSIONS INDEX MEASUREMENTS

Units: Pressure, P (atmospheres)
Temperature, T (°K)
Velocity, V (meters/sec)
Heat Input H (KJ/Kg of air)

COEI (g/Kg of Fuel)

Run	P	T	V	H	Jet A	JP-5 Base	Mod 2	Mod 3	Mod 4	Mod 5	Oil Shale	Coal	Tar Sands
1	2	533	46	840	30.18	28.38	24.38	25.83	27.21	27.01	24.27	25.97	23.23
2	2	812	69	770	5.72	5.04	5.14	5.65	6.13	6.10	6.19	6.33	6.00
3	2	533	69	837	38.21	36.50	32.89	33.20	35.21	33.04	32.44	32.43	31.32
4	2	533	69	418	39.26	38.61	40.73	42.16	41.90	40.85	38.87	40.38	40.25
5	5	533	46	209	4.85	4.41	5.68	6.04	5.50	4.98	5.35	5.39	5.19
6	5	533	46	419	8.05	9.10	7.49	8.35	11.87	34.24	35.49	32.08	32.55
7	5	533	46	697	13.45	13.30	-----	-----	-----	-----	-----	-----	-----
8	5	533	69	209	12.25	12.17	14.08	15.28	13.64	12.00	11.93	11.34	13.52
9	5	533	69	419	11.24	11.77	12.80	13.66	13.59	12.47	11.87	12.70	12.76
10	5	811	46	209	2.09	1.74	4.48	5.39	5.36	5.65	5.00	5.11	4.63
11	5	811	46	419	2.06	2.01	1.99	2.36	1.99	2.02	1.97	1.96	1.93
12	5	811	69	419	2.54	3.03	2.96	2.39	3.01	3.01	3.05	7.89	2.95
13	5	811	69	698	2.17	2.05	2.68	2.63	-----	-----	-----	-----	-----
14	5	811	69	837	2.75	1.78	2.91	3.13	3.53	3.54	3.53	3.69	-----
15	5	811	69	720	1.82	1.75	1.97	3.10	3.25	1.73	1.85	2.07	1.94
16	10	811	69	209	4.00	4.11	4.08	3.87	4.40	5.15	4.99	4.90	4.91
17	10	811	69	419	1.50	1.50	1.77	1.94	1.99	1.99	1.99	1.96	2.00
18	10	811	69	660	1.32	1.60	1.26	1.23	1.25	1.28	1.28	1.27	1.27
19	10	811	46	209	3.30	3.53	3.74	2.83	3.02	3.08	3.10	2.99	3.87
20	10	815	46	419	1.43	1.20	0.99	0.88	1.50	-----	-----	-----	-----
21	10	533	46	660	0.98	0.94	0.95	0.94	0.96	0.63	0.96	0.94	0.94
22	10	533	69	209	3.95	3.90	3.94	4.19	4.00	4.03	3.95	3.96	3.88
23	10	533	69	419	5.53	4.96	12.11	11.53	0.99	11.92	9.91	11.71	11.20
24	10	533	46	209	4.04	4.32	2.92	2.83	2.37	3.05	3.00	3.31	2.89
25	10	533	46	419	4.07	4.00	4.90	5.37	4.54	4.01	4.54	5.46	4.97
26	10	533	46	510	6.33	4.91	5.41	6.50	5.03	5.08	4.87	5.28	4.89
27	10	533	23	209	3.05	2.04	1.99	2.79	2.95	3.16	3.11	1.83	2.85
28	10	533	23	435	2.88	2.95	2.95	3.73	3.45	2.88	2.94	2.83	3.81
29	10	533	23	435	3.82	2.82	4.19	-----	-----	-----	-----	-----	-----
30	15	810	23	209	3.02	1.60	2.13	1.87	2.03	2.08	3.16	3.33	-----
31	15	812	23	419	2.10	0.98	0.75	0.95	2.51	1.99	1.98	1.72	1.76
32	15	812	23	600	0.73	0.68	0.71	1.05	1.08	1.09	1.06	1.27	1.07
33	15	812	46	209	4.13	3.84	3.94	3.82	4.44	4.19	3.88	3.34	3.39
34	15	812	46	419	1.52	1.49	1.30	1.44	1.31	1.31	1.32	1.46	1.51
35	15	811	46	610	1.06	1.03	1.24	1.33	1.22	1.25	1.04	1.21	1.21
36	15	811	69	209	4.00	2.91	4.24	4.27	4.28	4.36	44.25	3.91	3.93
37	15	811	69	419	1.54	1.97	2.17	1.96	1.97	2.03	2.03	1.95	1.98

TABLE 9. SUMMARY OF NO_x EMISSIONS INDEX MEASUREMENTS

Units: Pressure, P (atmospheres)
Temperature, T (°K)
Velocity, V (meters/sec)
Heat Input, H (KJ/Kg of Air)

					NO_x EI (g/Kg Fuel)										
Run	P	T	V	H	Jet A	JP-5 Base	Mod 2	Mod 3	Mod 4	Mod 5	Oil Shale	Coal	Tar Sands	NO_x from Oil Shale Fuel Nitrogen	Nc, FBN %
1	2	533	46	840	2.8	2.9	3.1	3.2	3.1	3.2	5.5	3.3	3.2	2.39	72
2	2	812	69	770	8.3	8.5	8.5	8.2	8.1	8.0	9.5	8.5	8.5	1.12	34
3	2	533	69	837	2.3	2.4	2.6	2.7	2.7	2.8	4.9	3.0	2.9	2.23	68
4	2	533	69	418	4.1	3.8	3.9	3.9	4.0	3.9	5.8	3.4	3.3	2.00	61
5	5	533	46	209	7.9	8.8	8.2	8.0	8.4	8.3	10.6	8.2	7.5	2.47	75
6	5	533	46	419	5.5	5.4	5.4	5.3	5.2	3.1	4.6	3.9	3.6	---	--
7	5	533	46	697	4.8	4.7	----	----	----	----	----	----	----	---	--
8	5	533	69	209	6.5	6.3	6.8	6.5	6.6	6.4	8.1	6.7	6.3	1.58	48
9	5	533	69	419	4.4	4.3	4.7	4.8	4.8	4.7	6.6	4.9	4.8	1.94	59
10	5	811	46	209	31.3	33.6	33.4	28.9	35.2	36.7	39.0	44.0	37.7	3.83	--
11	5	811	46	419	18.5	17.0	16.4	16.6	16.7	17.1	18.0	17.7	17.4	0.82	25
12	5	811	69	419	14.0	13.9	14.2	14.9	13.8	13.8	15.5	14.3	14.2	1.44	44
13	5	811	69	698	13.0	13.5	12.9	11.3	----	----	----	----	----	------	--
14	5	811	69	837	10.7	10.9	12.1	11.2	11.5	10.7	15.1	10.2	----	4.1	--
15	5	811	69	720	13.5	12.6	13.6	11.8	12.5	13.0	15.1	14.3	13.9	2.06	63
16	10	811	69	209	35.8	37.1	37.9	39.4	39.1	37.2	39.4	38.7	39.4	1.53	47
17	10	811	69	419	17.9	17.8	18.6	19.6	18.8	18.1	19.6	19.7	19.7	0.8	24
18	10	811	69	660	17.1	17.3	17.9	18.5	18.0	17.9	18.8	18.4	17.7	0.94	28
19	10	811	46	209	45.3	52.2	47.5	48.6	51.9	49.3	51.6	50.1	47.1	2.72	82
20	10	811	46	419	20.6	19.6	19.5	20.6	20.9	----	----	----	----	------	--
21	10	815	46	660	22.3	21.9	22.7	23.2	23.2	23.0	24.0	22.2	22.1	1.43	43
22	10	533	69	209	7.8	7.5	7.6	8.3	7.8	7.5	9.2	7.6	7.5	1.49	45
23	10	533	69	419	5.1	5.1	5.5	5.8	5.6	5.5	7.5	5.7	5.8	2.00	61
24	10	533	46	209	10.8	10.8	11.7	11.6	11.4	11.1	13.0	11.7	10.9	1.71	52
25	10	533	46	419	6.1	6.1	6.3	6.3	6.2	6.3	7.5	6.4	6.7	1.2	36
26	10	533	46	510	5.7	5.4	5.9	5.7	5.6	5.7	7.3	6.3	6.0	1.5	45
27	10	533	23	209	8.2	7.4	7.7	8.1	7.4	8.2	9.4	8.2	7.8	1.58	48
28	10	533	23	435	9.2	8.5	8.2	8.6	8.1	8.0	9.1	8.0	8.4	0.71	22
29	10	533	23	435	7.9	8.5	8.6							------	--
30	15	810	23	209	55.6	56.5	54.9	53.9	62.0	64.1	70.3	71.8	----	0.90	27
31	15	812	23	419	41.0	42.3	41.5	43.9	46.2	47.5	48.5	46.7	45.4	4.22	--
32	15	812	23	600	40.3	38.0	40.0	41.9	40.9	40.5	39.9	41.4	42.0	-0.68	--
33	15	812	46	209	66.1	66.2	64.0	67.8	70.3	69.5	70.4	69.3	59.3	4.4	--
34	15	812	46	419	26.1	25.8	27.2	28.1	26.9	26.9	27.8	27.8	26.9	0.84	25
35	15	811	46	610	24.3	24.2	25.9	26.4	25.8	25.9	26.5	26.2	25.1	1.07	33
36	15	811	69	209	22.2	22.1	20.4	23.1	21.1	20.5	21.1	22.9	22.5	-0.789	--
37	15	811	69	419	20.5	20.9	21.4	21.2	19.9	20.0	21.5	21.2	21.0	0.70	21

TABLE 10. SUMMARY OF COMBUSTION PERFORMANCE RESULTS FOR FUEL BLENDS 1 AND 2

Units: Pressure, P (atmospheres)
Temperature, T (°K)
Velocity, V (meters/sec)
Heat Input, H (KJ/Kg of air)

Run	P	T	V	H	ΔP	Radiation (kw/m^2)		Smoke Number		COEI (g/Kg)		NO_x EI (g/Kg)	
						Fuel 1	Fuel 2	Fuel 1	Fuel 2	Fuel 1	Fuel 2	Fuel 1	Fuel 2
1	2	533	45.9	842	530	6.16	5.32	1.5	0.8	35.0	32.2	2.3	2.4
2	2	534	67.8	264	131	17.9	18.4	6.0	5	33.1	~0	4.1	4.3
3	2	534	69.9	429	351	12.5	12.5	5.0	7.5	40.9	41.1	2.7	2.8
4	2	534	68.8	838	281	7.5	7.2	2.0	3.5	33.7	32.3	1.7	1.8
5	2	535	69.6	687.3	771	------	6.8	-----	3.0	-----	48.9	----	1.8
6	2	812	67.7	753	521	26.8	26.8	24.0	17.32	6.7	6.78	6.8	6.6
7	5	534	46.0	215	262	44.1	40.4	6.0	20.0	7.72	5.84	6.8	6.7
8	5	532	45.3	421.9	217	91.	84.3	48.2	52.1	7.91	8.78	4.7	4.7
9	5	532	46.2	849	797	37.2	40.1	28.8	40.0	8.93	8.74	4.4	4.5
10	5	535	68.4	297	507	22.7	22.1	2.4	2.0	12.1	12.2	5.9	5.9
11	5	534	68.2	426.5	457	50.9	48.5	20.4	40.1	12.2	12.86	3.7	3.7
12	5	812	45.7	212	147	36.6	38.2	0.5	0.5	1.96	1.94	27.5	27.1
13	5	811	46.6	403	427	109.4	112.1	32.6	46.0	2.07	2.05	13.0	13.2
14	5	813	67.6	213.0	282	22.7	23.4	8	5	3.9	4.09	22.1	23.1
15	5	813	68.4	422.6	217	101.1	96.7	41.6	51.95	2.47	2.48	11.1	10.9
16	5	1034	67.8	230	202	37.9	37.9	3.5	2.0	2.71	2.91	55.9	64.8
17	10	534	22.7	206	243	94.5	93.3	14.1	13.5	3.02	2.05	6.8	7.2
18	10	534	21.8	431.7	203	125.6	128.2	82.2	76.4	1.74	2.93	7.4	8.0
19	10	533	46.0	223.5	243	53.1	51.3	19.9	16.6	3.72	3.44	8.9	9.3
20	10	532	45.6	426.4	263	114.3	115.3	70.9	58.4	4.4	4.34	5.2	5.4
21	10	533	45.8	702	703	80.9	77.5	61.2	62.3	5.38	5.4	5.7	5.7
22	10	534	68.4	212	153	26.8	27.14	31.3	16.0	5.3	5.3	8.1	8.0
23	10	534	67.9	421	553	89.9	88.3	45.2	46.14	6.44	6.24	4.8	4.8
24	10	811	44.9	211	413	31.4	30.8	1.5	1.8	2.95	2.02	41.0	41.8
25	10	814	44.0	435	363	149.9	151.9	42.7	37.9	1.73	1.44	19.2	20.0
26	10	812	44.9	709.0	303	122.9	128.0	39.4	33.4	0.89	0.89	17.6	19.9
27	10	813	66.8	123.3	223	31.4	31.1	12.0	8.0	2.92	2.91	33.9	32.5
28	10	812	66.8	422	253	130.9	129.8	20.4	18.3	1.48	1.49	15.0	15.0
29	10.1	811	68.5	706.8	723	125.6	128.2	25.9	31.6	1.07	1.07	15.9	16.0
30	10.1	1033	68.3	430.1	173	136.2	129.3	55.6	50.8	0.78	0.78	42.5	43.0
31	15	532	22.6	856.6	580	106.6	106.6	78.9	82.4	2.95	3.52	7.4	7.6
32	15	813	23.9	202.1	260	53.4	55.8	2	1.8	3.08	3.71	57.3	44.6
33	15	812	22.3	426.7	210	151.9	151.9	43.1	36.7	0.98	-----	32.4	32.2
34	15.1	810	23.7	651.8	180	135	135	47.2	50.72	0.32	0.32	29.8	32.8
35	15.1	812	45.3	211.8	230	32.1	32.1	45.27	21.1	1.96	2.9	48.9	48.3
36	15.1	812	44.2	429.1	260	168.5	167.4	12.12	18.12	1.46	1.29	22.0	20.8
37	14.8	811	46.1	673.9	620	122.9	122.0	37.8	45.3	0.62	0.63	23.0	23.1
38	15.1	809	67.4	209.6	140	28.8	29.8	15.6	7.7	1.98	1.97	39.6	39.7
39	15.1	811	67.8	429.3	560	161.8	160.7	16.2	12.3	1.46	1.46	17.9	17.9
40	14.9	1035	67.5	429.1	360	164.9	157.1	52.0	43.1	0.49	0.5	48.7	51.1

FIGURE 25.

EFFECTS OF COMBUSTOR OPERATING CONDITIONS ON FLAME RADIATION AND EXHAUST SMOKE

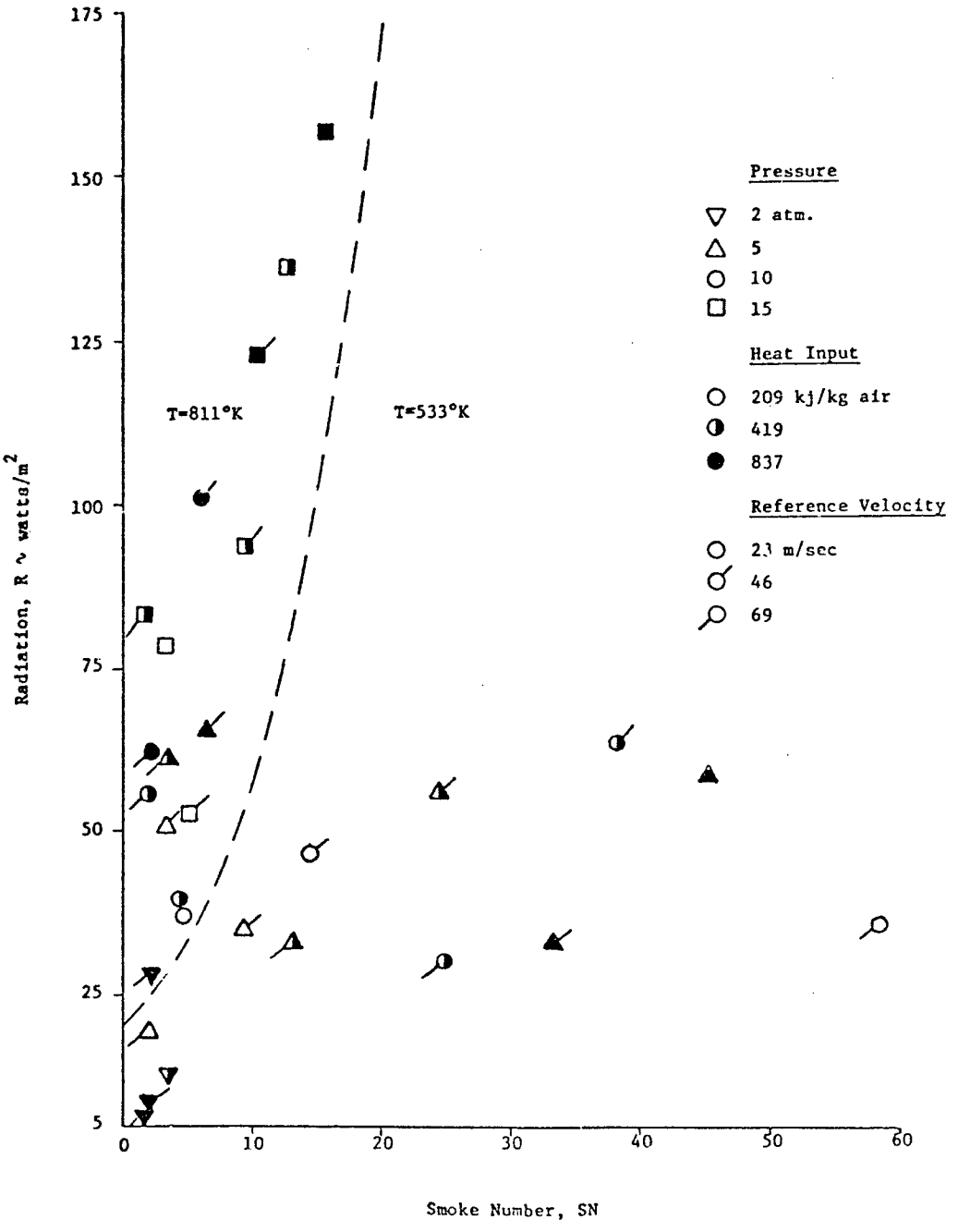

(fuel/air ratio) and decreasing velocity; smoke is increased by increasing pressure, heat input and decreasing temperature and velocity.

Although the radiation measurements followed anticipated trends, the results were considered to be semi-quantitative due to the limited viewing angle of the radiometer and the variation of flame length with inlet conditions. It was apparent that the most intense regions of the flame were not always visible. This was particularly evident at the highest inlet temperature (812°K) and pressure (15 atm) where the flame receded closer to the fuel nozzle, out of the viewing cone of the radiometer. For example, the radiation for the conditions (P = 15 atm, T = 812°K, V = 23 m/sec and H = 202 KJ/kg) was 53.4 Kw/m^2 as compared with a value of 94.5 for the conditions (P = 10, T = 533, V = 22.7 and H = 206). Clearly, an increase of pressure and temperature from 10 to 15 atm and 533 to 812°K respectively is expected to substantially increase flame luminosity. Fortunately, this was only an occasional occurrence and, for the most part, the flame radiation was predictable on the basis of inlet conditions. This problem manifests itself when comparing the radiation at one set of combustor conditions with that of another. It is expected that at a given operating condition the flame position would remain constant as the fuels are changed and thus the fuel sensitivity is unaffected.

A second problem that was realized later, when a separate project was initiated to test the newly blended fuel number 1 and the reference fuel number 2, was that the fuel nozzle differential pressure (ΔP) was found to be a significant inlet parameter. This is illustrated in Figure 26 where the radiation is plotted versus the $(\Delta P)^{-0.354}$. The exponent (-0.354) was chosen because this is the dependence sauter mean diameter has on ΔP for a typical nozzle. The experimental conditions for the three points shown in Figure 26 are P = 2 atm, T = 534°K, V = 69.6 with H = 264, 429 and 687 KJ/Kg of air. The heat input values were obtained by applying varying amounts of pressure to a 1.5 gph nozzle. Contrary to what might be expected, the increased fuel/air ratios gave reductions in the radiation. This suggested strongly that atomization can play an important role in the combustion process. However, this rather exclusive effect of atomization (i.e., ΔP) was found to be unimportant at higher pressures (>2 atm) where fuel vaporization is enhanced by higher droplet temperatures and greater convective heat transfer.

A simple exponential model with assumed stoichastic independence of variables was used in an attempt to correlate the radiation with inlet conditions. The model is expressed as

$$\text{Flame radiation (FR)} = KP^{a}T^{b}V^{c}H^{d}(\Delta P)^{e}$$

where the constant K and the exponents are derived by a regression analysis of the data. The results of this analysis were typically

$$FR \approx 0.03\ P^{0.9}T^{0.7}V^{-0.3}H^{0.4}$$

FIGURE 26. CORRELATION OF FLAME RADIATION AND DIFFERENTIAL NOZZLE PRESSURE

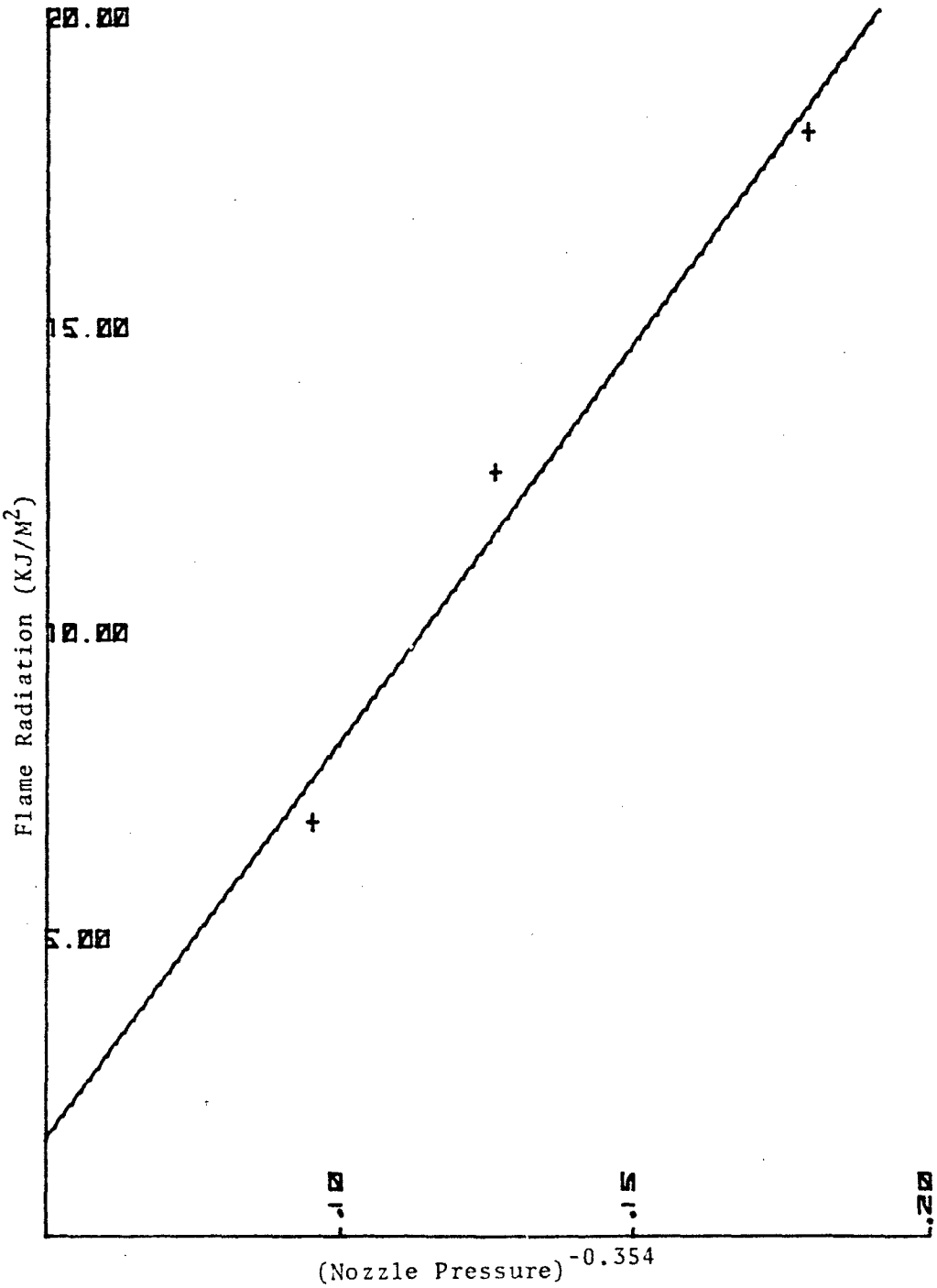

with essentially zero dependence on ΔP. Since only a small fraction of the experiments were done at low pressure, the effect of ΔP was insignificant in the model. This model fits the data with a correlation coefficient (R^2) of about 0.6, indicating that either the model was inadequate or there was considerable scatter in the data. If it is assumed that the model is adequate, the radiation data must be only qualitatively accurate. This is not an unreasonable conclusion since there was no assurance that the radiometer was directed at the most intense regions of the flame at all of the conditions examined. Although the model was not derived on the basis of physical concepts, it was chosen because of its ability to empirically describe a dependent variable that is monotonically dependent on the independent variable. The literature on combustion performance in turbine combustors indicates that the combustion performance parameters are monotonically dependent on the inlet conditions. For example, radiation increases continuously as pressure is raised; it does not suddenly began to decrease.

The results of the regression analysis indicated by the above equation for FR are basically in good agreement with previous studies. In the work of Schirmer and Quigg[2], the flame radiation was increased by increases in inlet pressure, temperature and heat input and reduced by increasing the reference velocity. The above empiricisim for flame radiation shows a direct dependence on P, T and H, and an inverse dependence on V; in general agreement with Schirmer and Quigg and other investigators[6,15].

The effect of operating conditions on flame radiation is shown graphically in Figures 27 to 32 where the radiation from each of the fuels is plotted versus hydrogen content.* The graphical representation is in general agreement with the empirical model and previous work.

Flame Radiation vs. Fuel Properties

Previous studies[1,2] on the effects of fuel properties on flame radiation have consistently shown a strong correlation with hydrogen content. Shirmer and Quigg[2] measured flame radiation from twenty-five fuels, including normal, iso- and cycloparaffins, cyclic olefins, subhstituted monocyclic aromatics, decalins and several JP-5 blends, with hydrogen contents ranging from 7.7 to 16.4 weight percent. Their results show an almost linear relationship between flame radiation and hydrogen content.

In the present investigation, the flame radiation from the petroleum-based fuels (i.e., B and 1 thru 5) correlated equally well with the following fuel properties:

1. hydrogen content (percent wt)
2. aromatic content (percent wt)
3. ring carbon (percent wt)

*See key to operating conditions for graphs in Table 11 (page 66).

TABLE 11

KEY TO OPERATING CONDITIONS FOR GRAPHS
CODE IS PTVH

	Pressure atm	Temperature °K	Ref. Velocity m/sec	Heat Input Rate kj/kg air
1 =	2	533	23	209
2 =	5	811	46	419
3 =	10		69	837
4 =	15			

Example:

2132 translates to P = 5 atm

T = 533°K

V_{ref} = 69 m/sec

H = 419 kj/kgm air

FIGURE 27. EFFECT OF FLOW VELOCITY ON FLAME RADIATION

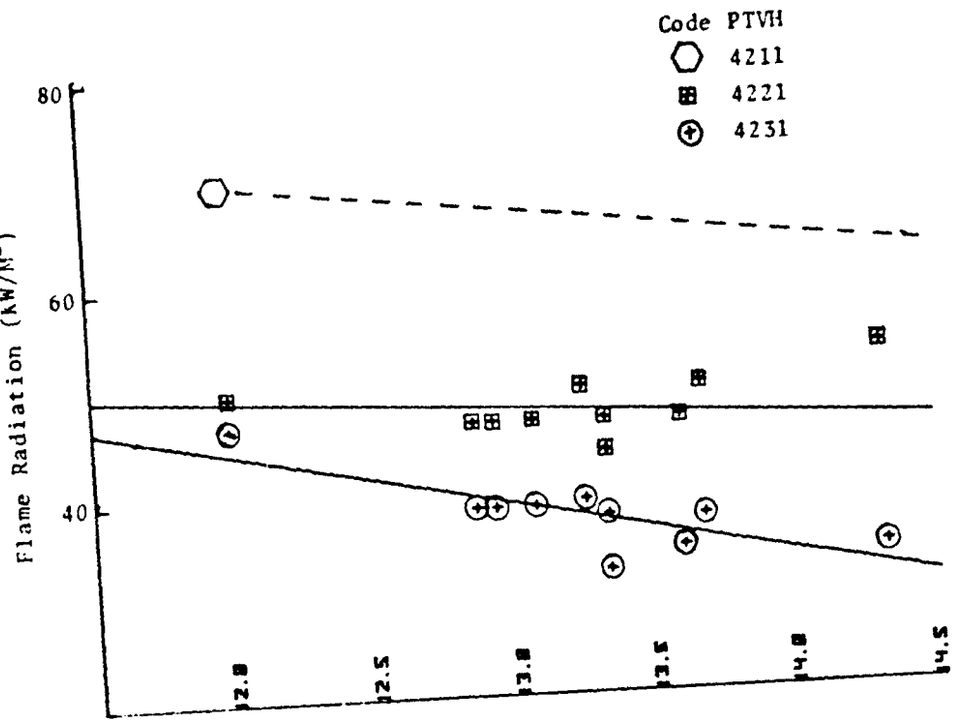

EFFECT OF PRESSURE ON FLAME RADIATION

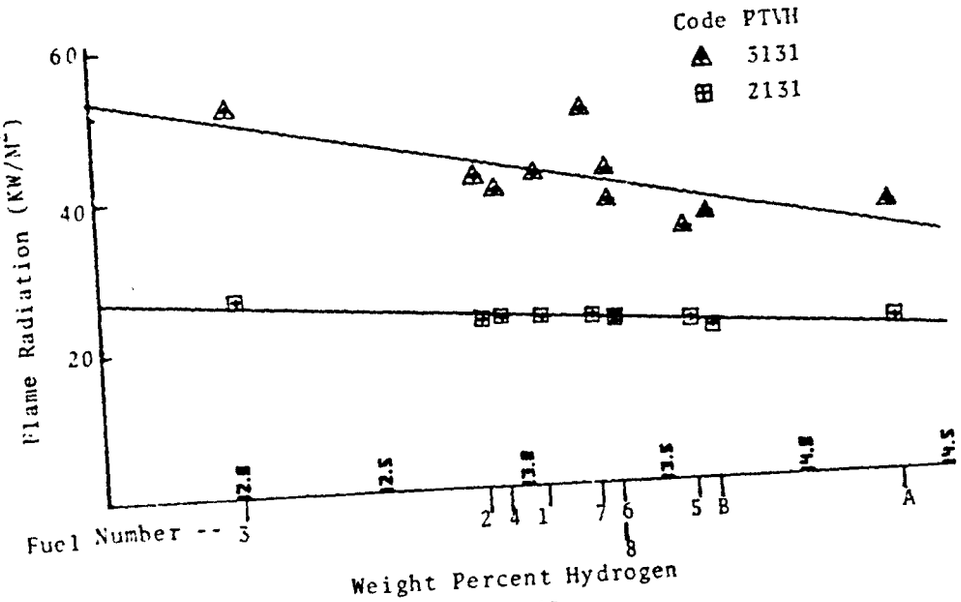

FIGURE 28. EFFECT OF FUEL/AIR RATIO ON FLAME RADIATION

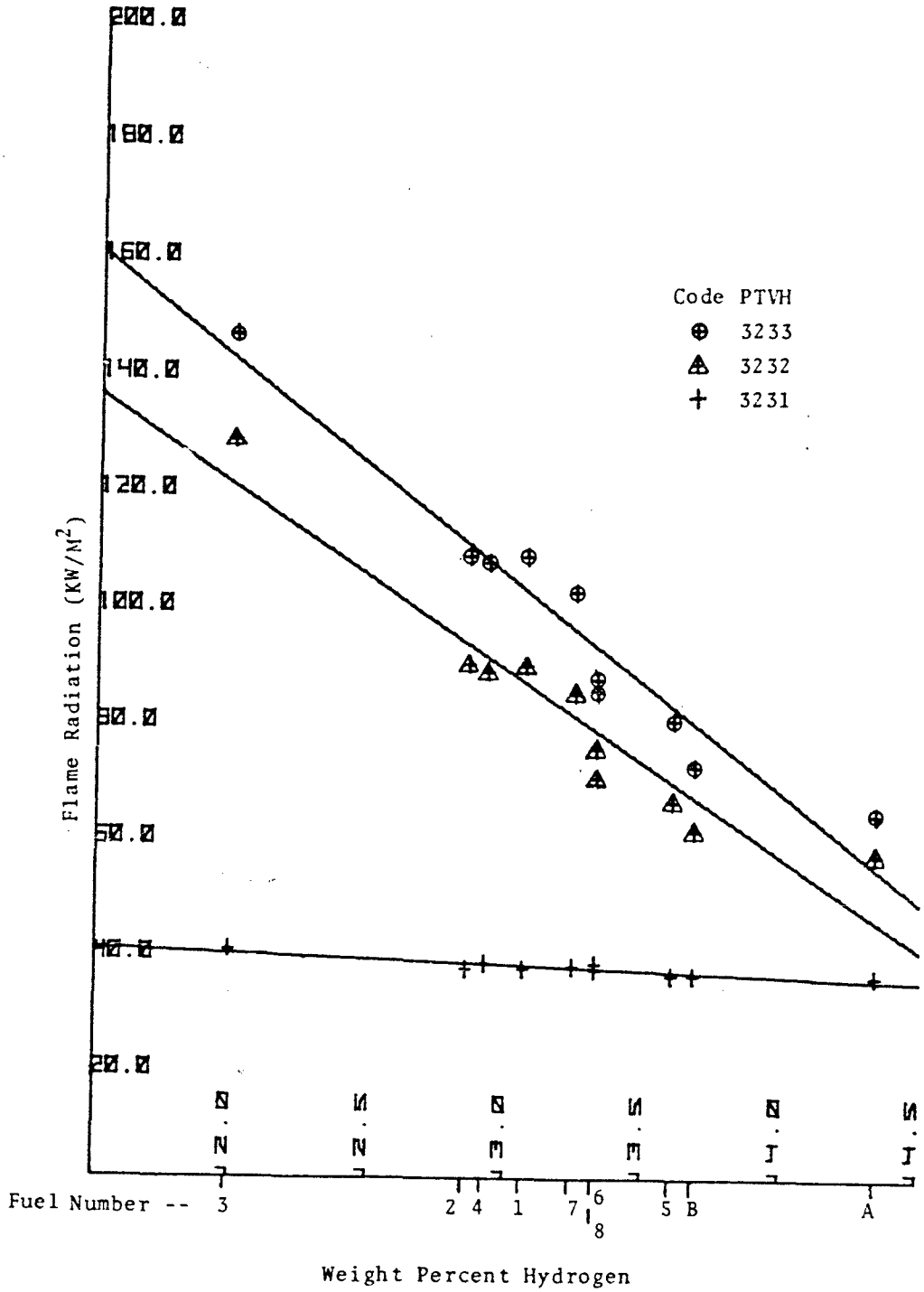

FIGURE 29. EFFECT OF PRESSURE ON FLAME RADIATION

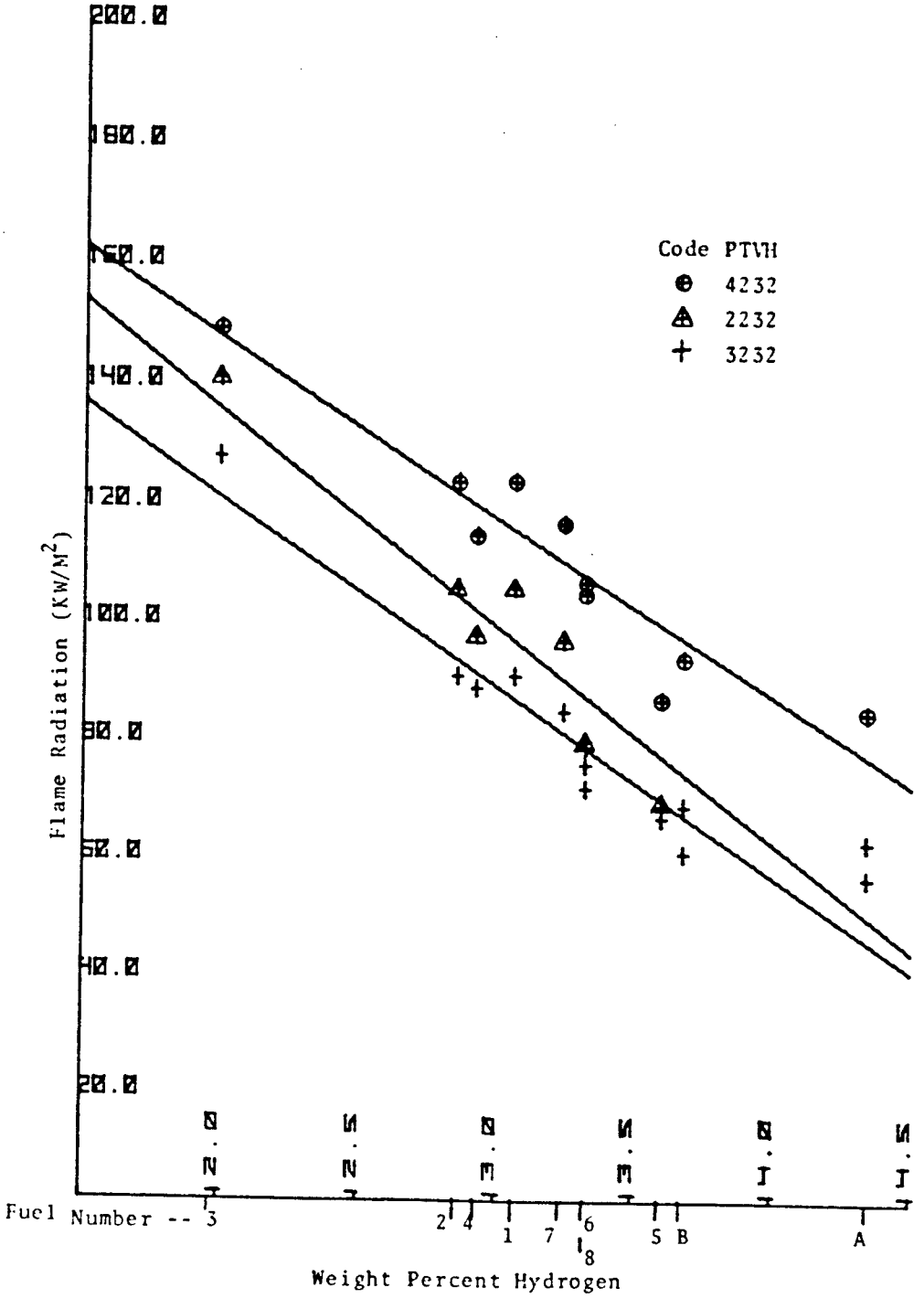

FIGURE 30. EFFECT OF PRESSURE ON FLAME RADIATION

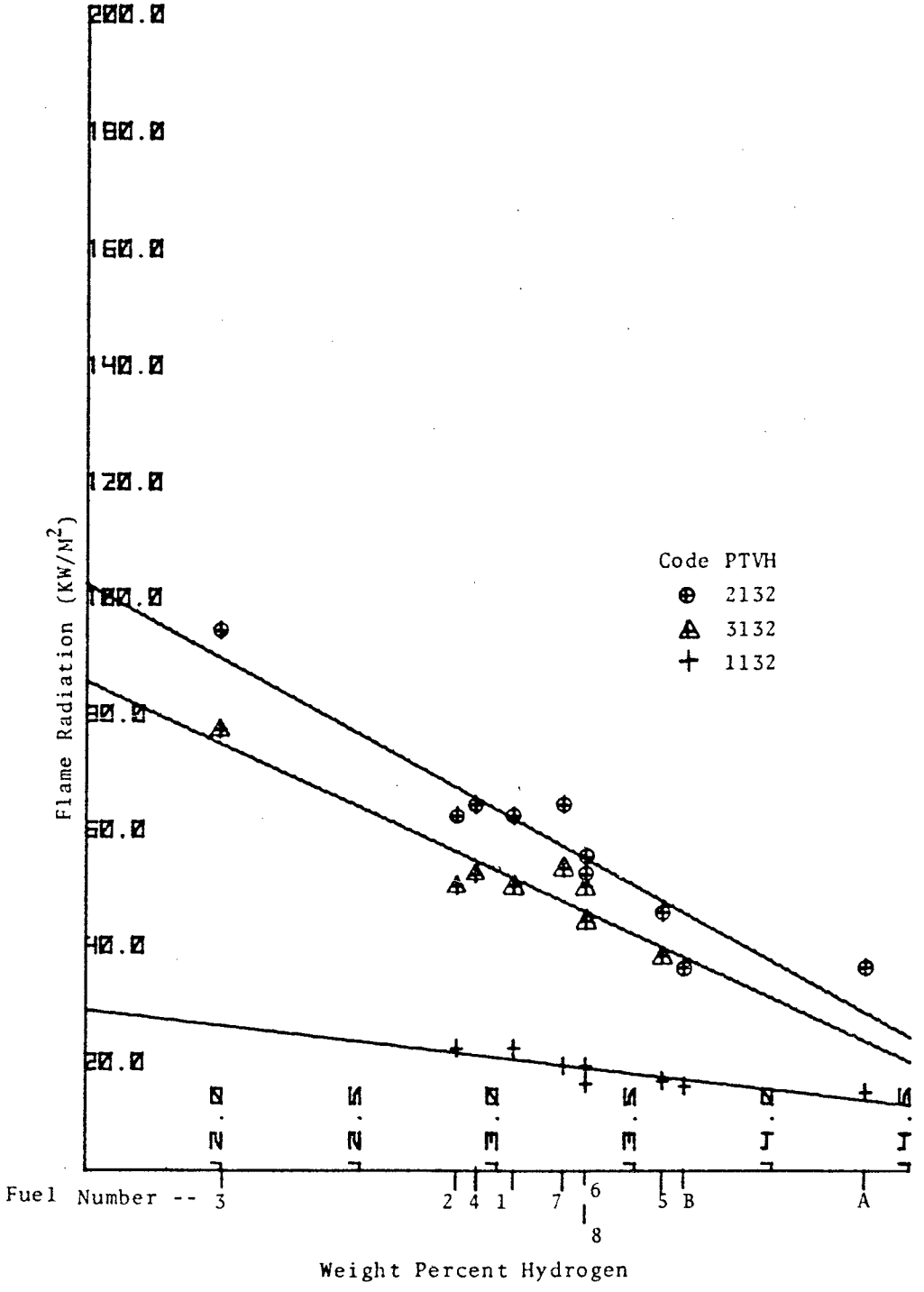

FIGURE 31. EFFECT OF FLOW VELOCITY ON FLAME RADIATION

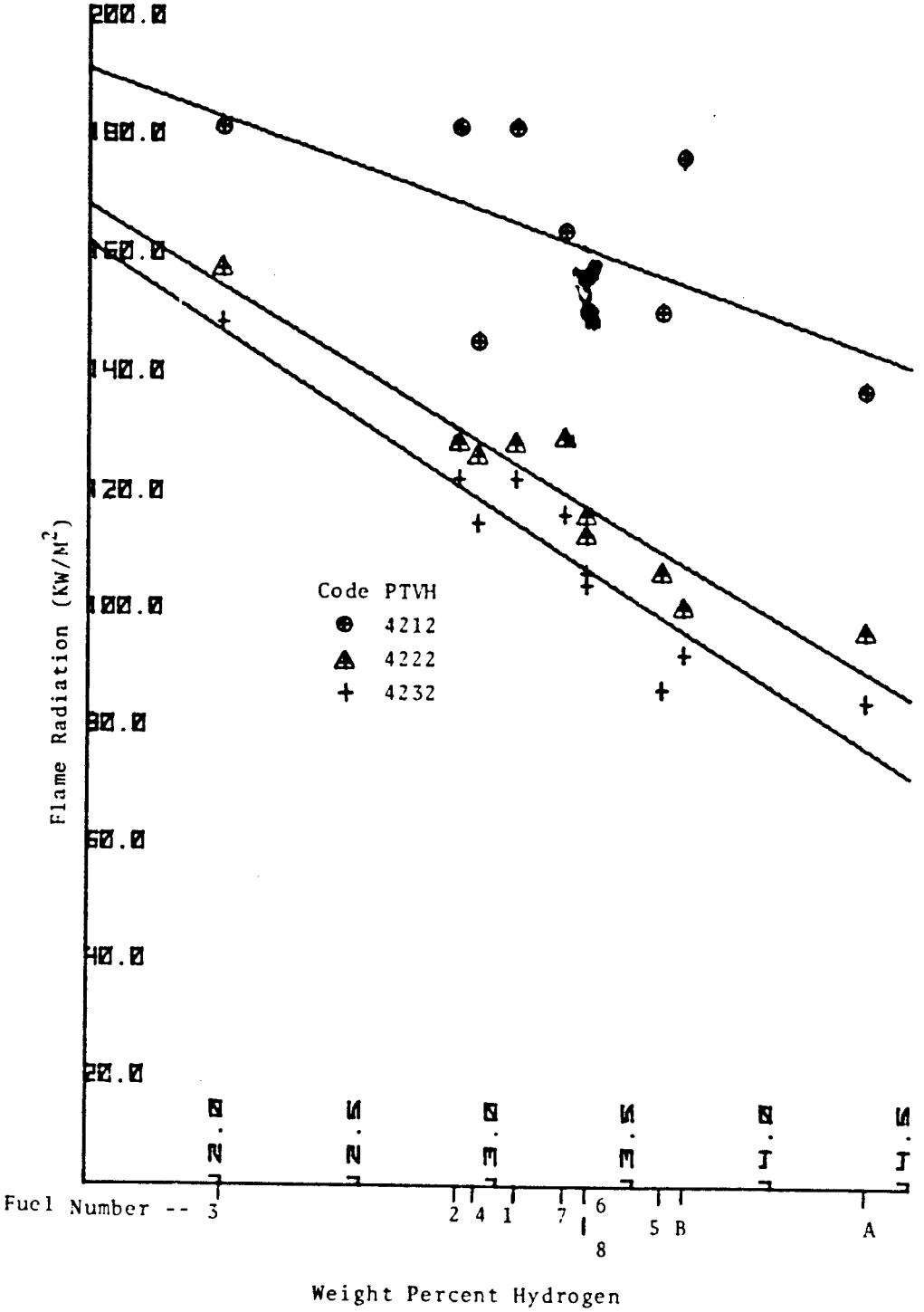

FIGURE 32. EFFECT OF PRESSURE ON FLAME RADIATION

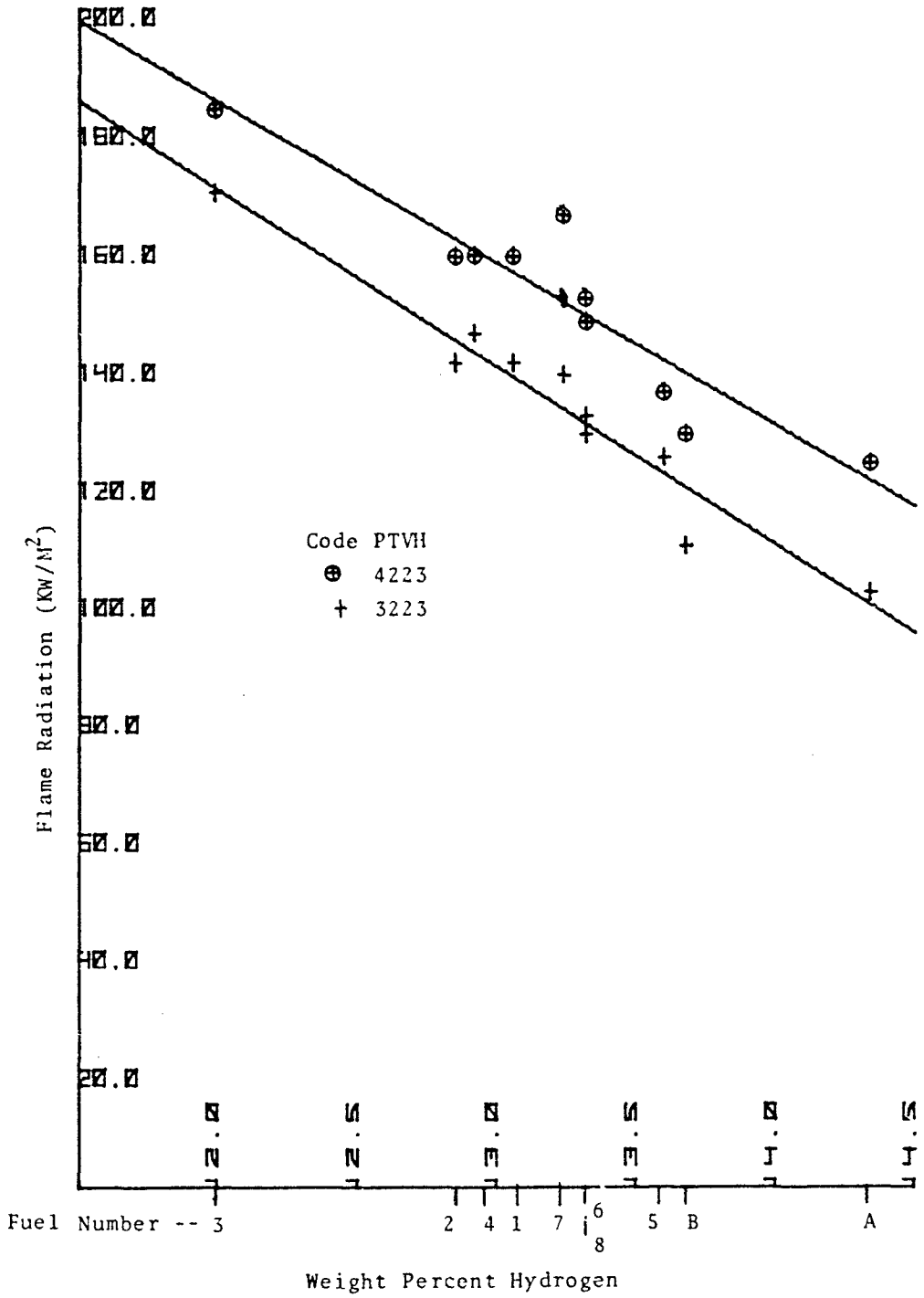

This is predicted for these fuels since a linear correlation exists between the hydrogen contents of the JP-5 blends and HPLC aromatic content and the ring carbon (refer to Figures 21 and 22).

Base fuels number 1 and 2 gave almost identical radiation at all conditions tested. Fuel number 1 contained the higher concentration of polycyclic aromatics with a hydrogen content of 13.06 percent and fuel number 2 was high in monocyclic aromatics with a hydrogen content of 12.85 percent. The total aromatic content of fuel number 1 (23.6%) was less than that for fuel number 2 (26.7%), but the weight percent ring carbon and smoke points of both fuels were the same. Although the data are limited in that only one comparison of monocyclic versus dicyclic aromatics is examined, it appears that percent ring carbon may be a sensitive indicator of radiation from fuels containing mono and polycyclic aromatic structures. Otherwise, hydrogen content gives a good correlation.

Of the JP-5 fuels, fuel number 3 with 37.8 percent aromatics consistently gave the highest radiation while the base fuel and fuel number 5 gave the lowest radiation. There was no detectable effect of the higher end point of fuel number 5. Fuel number 4 had an aromatic content and a corresponding radiation intensity similar to fuels number 1 and 2.

In comparing the plots shown in Figures 33-35 of radiation versus ring carbon, total aromatics and hydrogen content, it is found that the syncrude fuels (numbers 6, 7 and 8) correlated best with hydrogen content in spite of the relatively high aromatic content of the oil shale (6) fuel. The flame radiation from the fuels processed from oil shale (number 6) and tar sands (number 8) correlated with hydrogen content in the same manner as the petroleum base fuels; however, as shown over a broad range of conditions in Figures 27-32, the radiation from the coal-derived fuel (number 7) averaged about 8 percent higher for its hydrogen content than the other fuels. This may be related to the types of cycloparaffins present in fuel (7) as compared with fuel 8. Depending on the structure of the cycloparaffin, the combustion process (abstraction of hydrogen atoms from the ring) could lead to intermediate aromatic structures, which may result in higher particulate formation.

Similarly, this effect could explain the correlation with aromatics or ring carbon (see Figures 33 and 34). The coal (number 7) and tar sand-derived fuels (number 8) produced higher radiation than the petroleum fuels, while the shale oil-derived fuel (number 6) high in normal saturates, produced lower radiation. These differences relate to the correlations of hydrogen content with aromatics and ring carbon for the fuels. See discussion of fuel properties under Test Fuels.

A characteristic fuel sensitivity factor defined as $-dR/dH$, where R is radiation intensity and H is hydrogen content, may be derived from plots similar to those shown in Figures 27 to

FIGURE 33. EXAMPLE OF THE EFFECT OF RING CARBON ON FLAME RADIATION

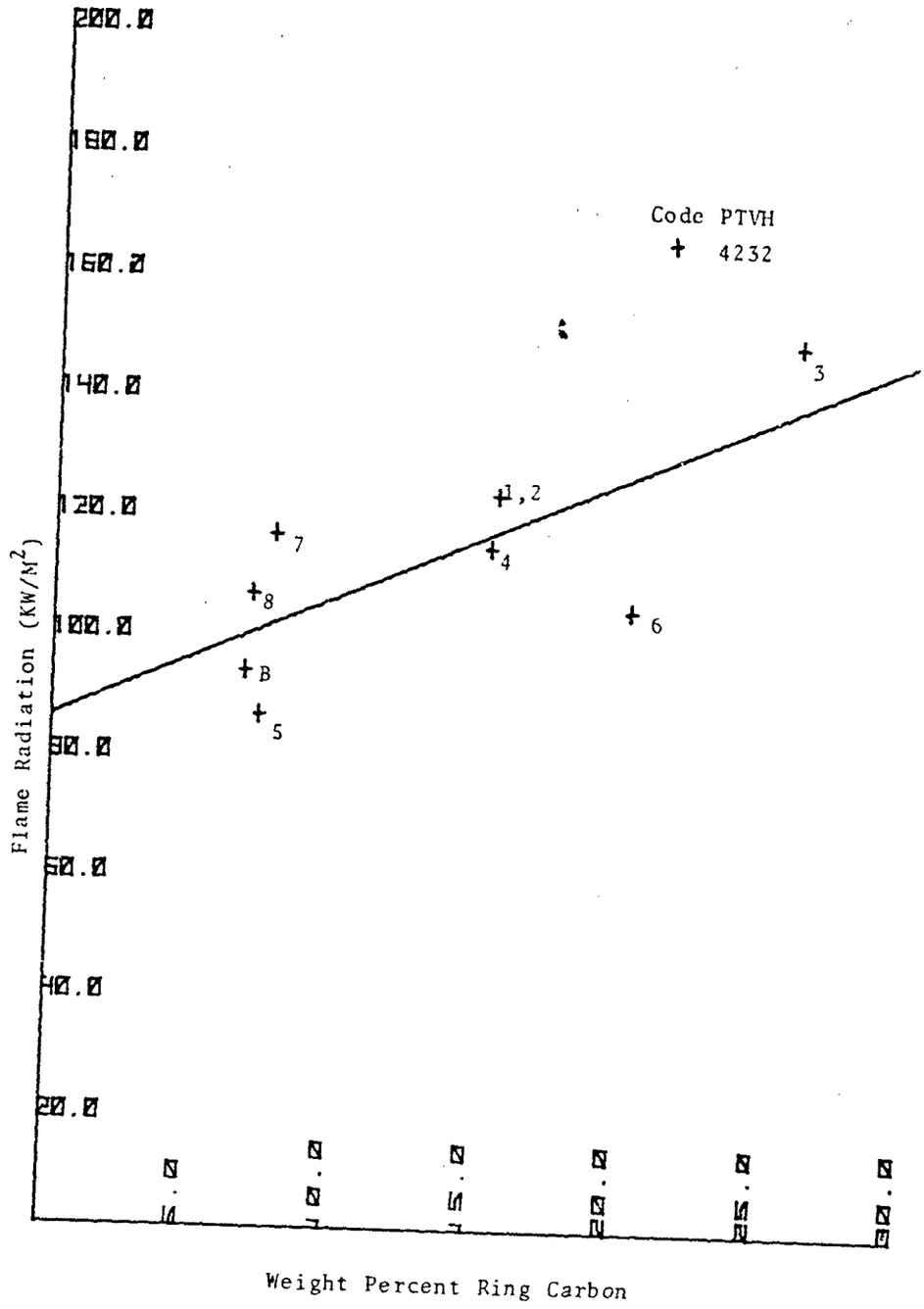

FIGURE 34. EXAMPLE OF THE EFFECT OF AROMATIC CONTENT ON FLAME RADIATION

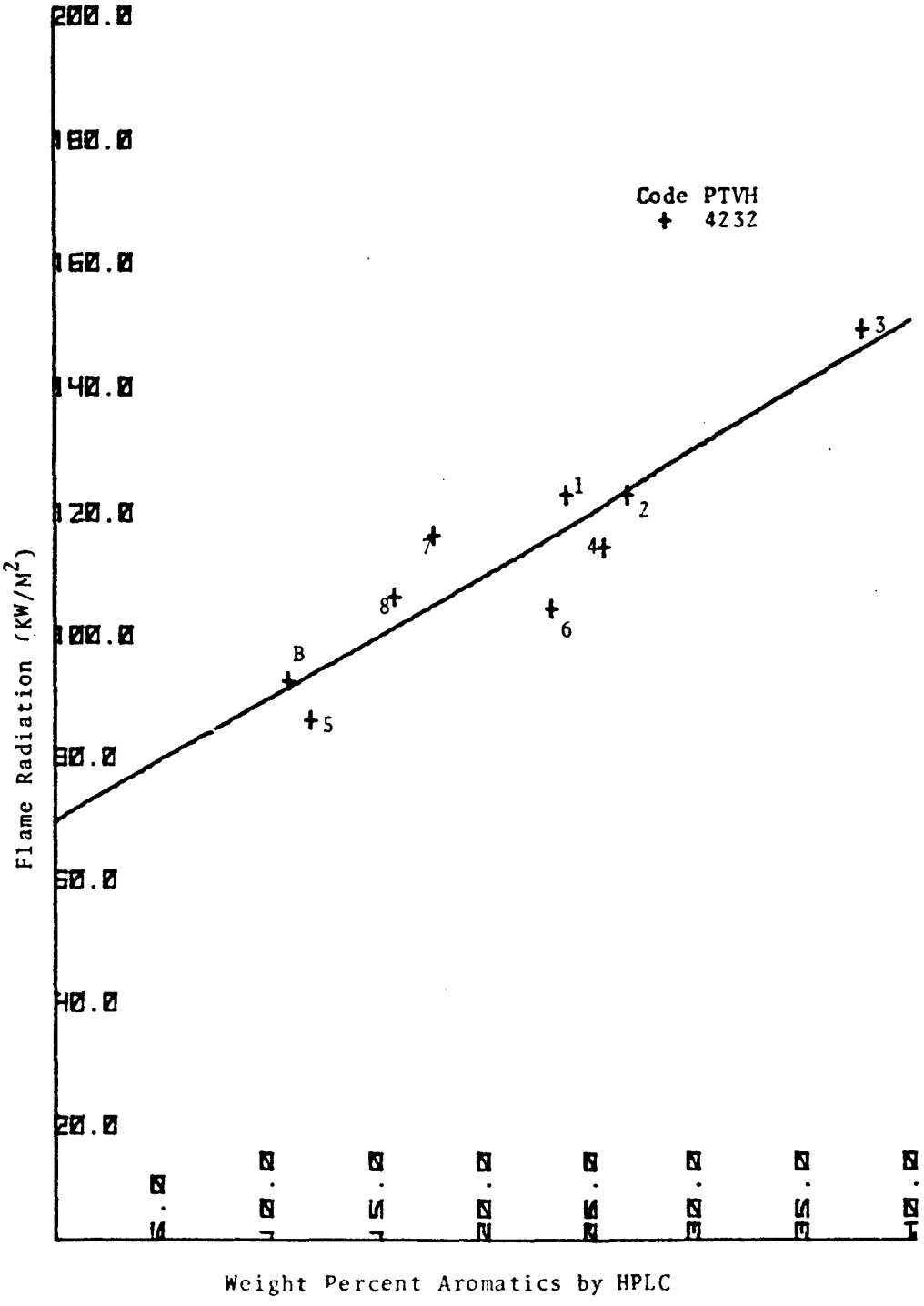

FIGURE 35. EXAMPLE OF THE EFFECT OF HYDROGEN CONTENT ON FLAME RADIATION

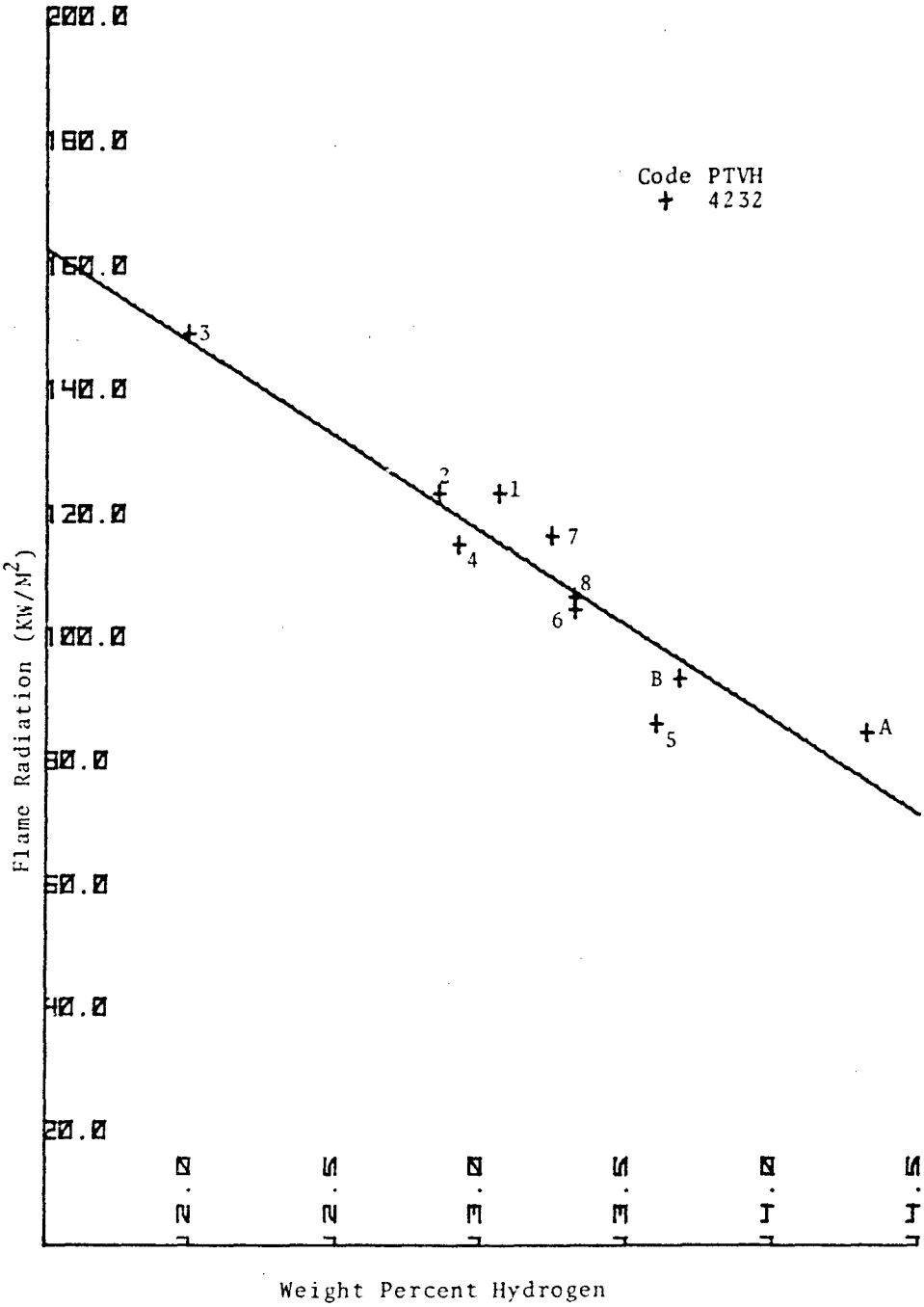

32. A plot of the fuel sensitivity versus the flame radiation, which is characteristic of a fuel blend containing 13 percent hydrogen, is shown in Figure 36. At conditions of low-flame radiation (generally less than 40 KW/M^2), the radiation intensity is relatively independent of fuel properties. However, as the radiation level increases, the fuel sensitivity initially increases to a maximum value and then falls as the flame emissivity approaches unity. As shown in Figures 27-32, the radiation intensity versus hydrogen curves were relatively linear (no significant downward curvature at the lower hydrogen content was evident) even at conditions of high pressure and heat input where the flame emissivity is expected to approach unity. If, in fact, conditions were to be achieved where the emissivity was unity, radiation intensity would be independent of fuel properties. Although, a unit emissivity was anticipated at some of the more drastic inlet conditions, it appears from the results that it was never actually achieved.

The absence of an appreciable dependence of radiation on fuel properties under low-flame radiation conditions, suggests that engines with combustors of low luminosity (clean combustors) may not be as strongly affected by changes in aromatics as those which have inherently high flame radiation.

Smoke

The smoke measurements had more scatter than the radiation measurements. The reason for this is not understood, since the combustor air and fuel flow parameters were quite stable and consistent from fuel to fuel at a prescribed combustor operating condition. Inasmuch as the smoke number and radiation are both dependent on soot concentration and that the radiation measurement was only somewhat better than semi-quantitative, the scatter in the smoke measurements should have been more favorable. The smoke measurements were carried out by the method described earlier in the experimental test equipment section. The scatter in the low smoke readings was greater than that of the readings made for medium to high smoke concentrations because of the difficulty in making an accurate reflectance measurement. The reflectivity of the standard filter paper was slightly uneven and these fluctuations were comparable with the opacity of the soot stain at light-smoke conditions.

Smoke vs. Operating Conditions (Previous Work)

Bagnetto and Shirmer[3] concluded that smoke emissions from gas turbine engines could be reduced if (a) combustors were operated at minimum inlet-air pressure and temperature, with maximum exhaust-gas temperature; and (b) fuels were selected for maximum hydrogen content. Similar to, but not identical with, the method used in the present work, they obtained exhaust-smoke samples with a Von Brand continuous filtering recorder and evaluated them with a Welch Densichron meter in terms of optical density. These results were relatively free of scatter and showed that smoke density increased nearly linearly over the

FIGURE 36. FUEL SENSITIVITY OF FLAME RADIATION

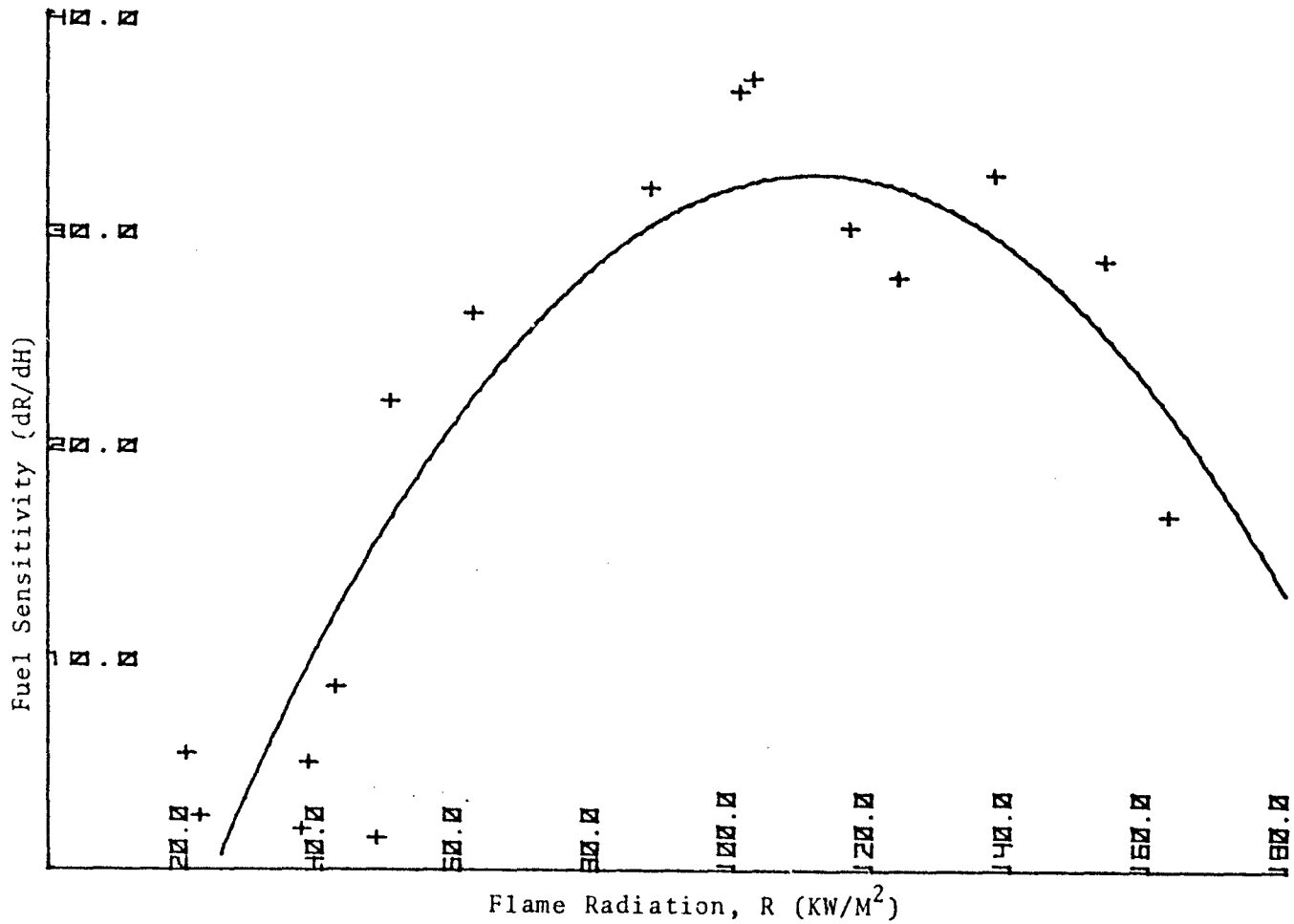

pressure range, 5 to 15 atmospheres. Increases in inlet temperature decreased smoke, increases in fuel/air ratio raised the smoke level, and reference velocity had a peaking effect, i.e., the maximum smoke density appeared for all fuels at an intermediate gas velocity. The fuel property that correlated best with smoke density was hydrogen content. The low (3.4%) aromatic JP-5 fuel examined by Bagnetto and Shirmer produced less smoke than either the normal production JP-5 (13.67% aromatics) or the high (24.51%) aromatic JP-5 fuel; but no difference was found between the normal production and high aromatic JP-5 fuels with essentially equal hydrogen contents.

Smoke vs. Operating Conditions (This Work)

Exhaust smoke was particularly sensitive to parameters such as inlet temperature which have a significant effect on exhaust gas temperature (see Figures 37-42). The relationship between radiation and smoke in Figure 24 shows that most of the high smoke readings were obtained at the lower inlet temperature of 533°K. This is in agreement with the understanding that a higher inlet air temperature means higher temperatures in the secondary and quench zones, thus increasing the oxidation rate of free carbon formed in the primary zone. Dodds et al[5] used a sample probe to extract soot at several positions axially along the center line of a disc stabilized combustor and observed an exponential decay in the concentration of particulate matter. In essence then, the disappearance rate of carbon -dc/dt after its formation in the primary zone, may be expressed as

$$-dc/dt = Kc$$

where K is a pseudo first order rate constant for the heterogeneous oxidation of carbon particles. The high temperature dependence of the rate constant K, given by A exp E/RT where A is a pre-exponential factor, E is an activation energy and T is the absolute temperature, illucidates the observed sensitivity of smoke emissions to exhaust gas temperature.

As shown in Figures 37-42, increases in inlet pressure and heat input (fuel/air ratio) increased the smoke levels as is typical of real combustors. Reference velocity can have two effects on smoke; one, in terms of the turbulent mixing in the primary zone which reduces the production of soot and, two, the residence time in the secondary and quench zones for the oxidation of the free carbon. Figures 40-42 show that smoke is reduced by increasing velocity, indicating that mixing in the primary zone is the dominant process.

Various attempts were made to mathematically correlate the smoke measurements with the inlet conditions. In the first trial, the model

$$\text{Smoke Number (SN)} = K\, P^a\, T^b\, V^c\, H^d$$

similar to that used for radiation was employed. For all the fuels tested, the typical values of the constants derived by

FIGURE 37. EFFECT OF PRESSURE AND TEMPERATURE ON EXHAUST SMOKE

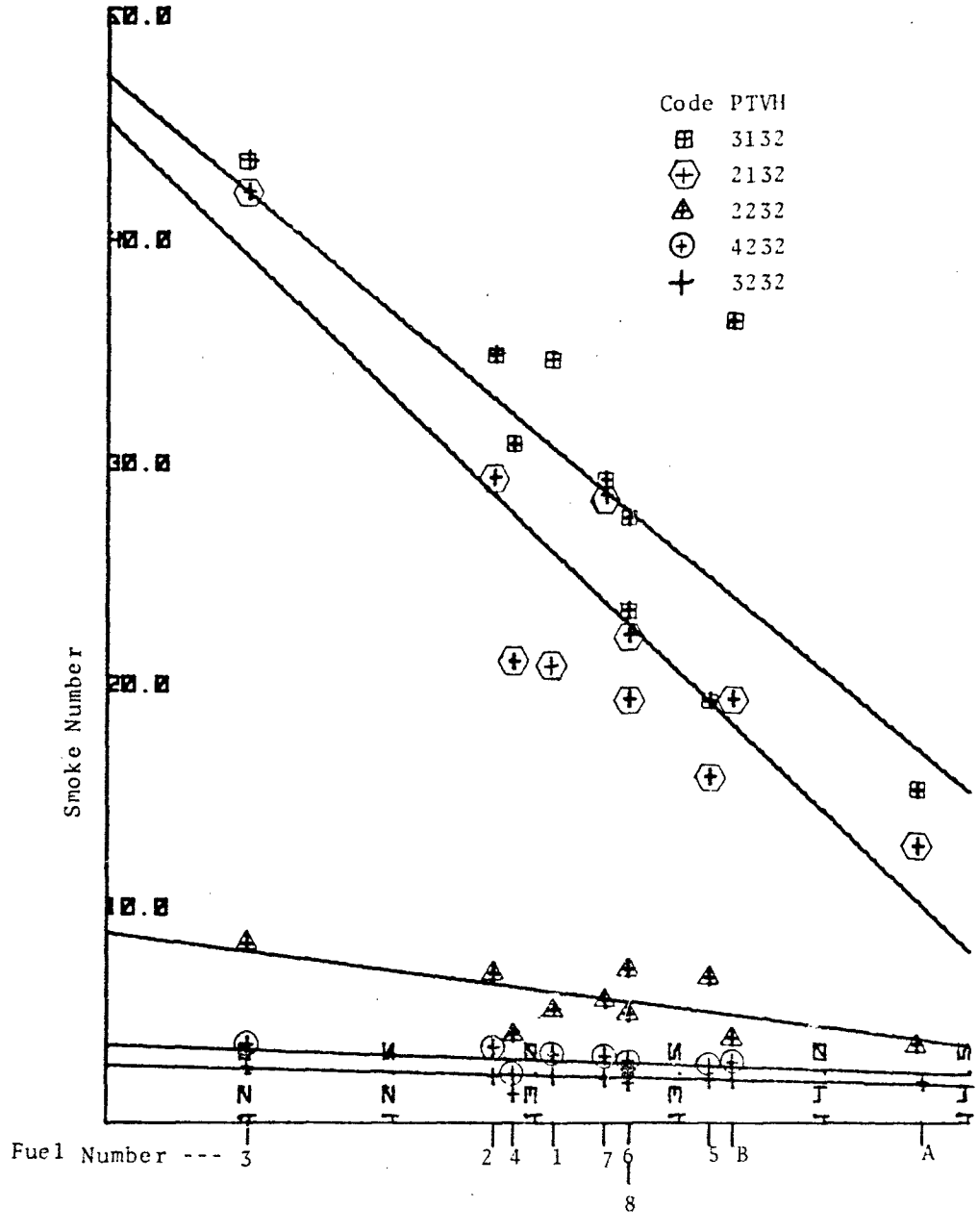

FIGURE 38. EFFECT OF FUEL/AIR RATIO ON EXHAUST SMOKE

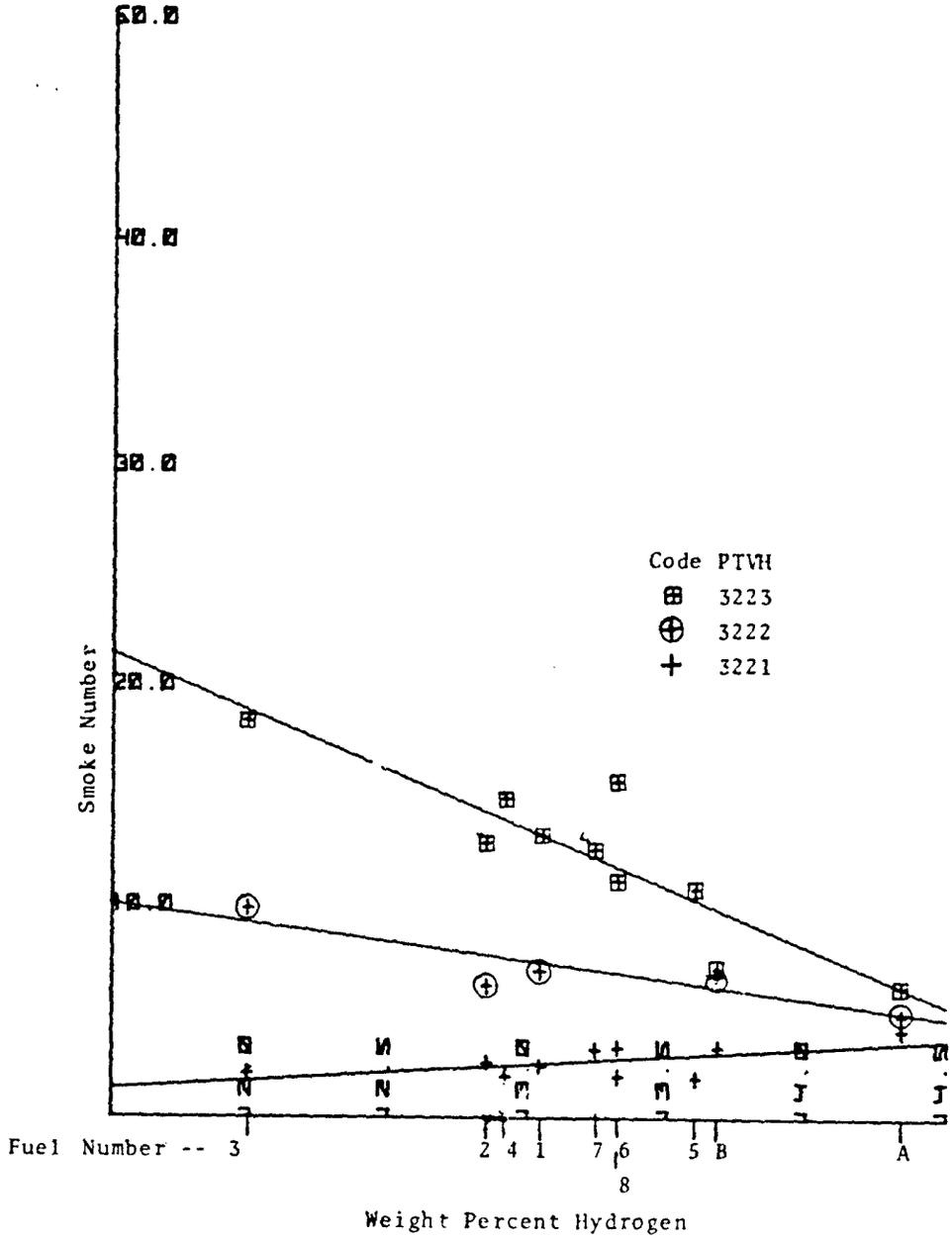

FIGURE 39. EFFECT OF FUEL/AIR RATIO ON EXHAUST SMOKE

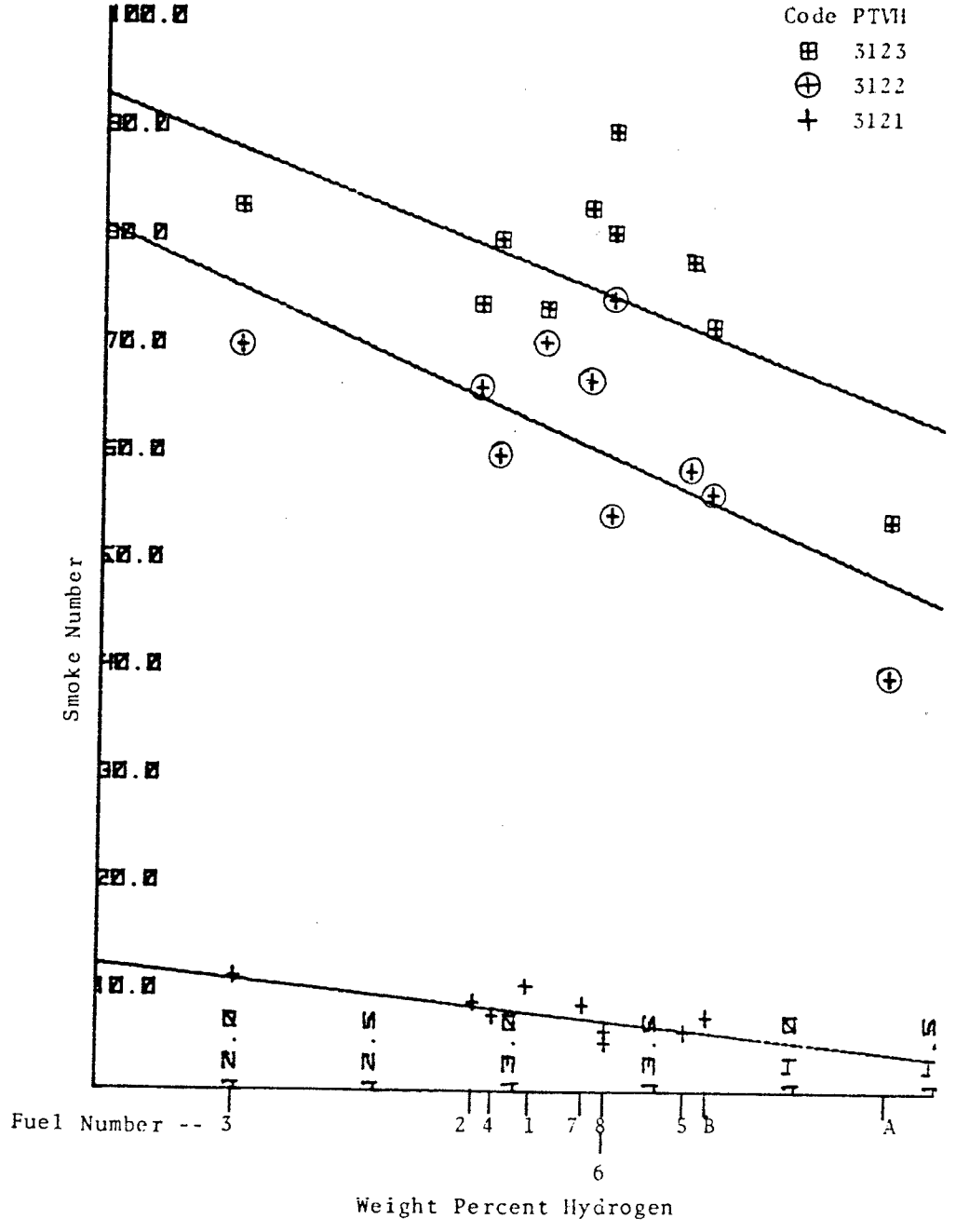

FIGURE 40. EFFECT OF FLOW VELOCITY ON EXHAUST SMOKE

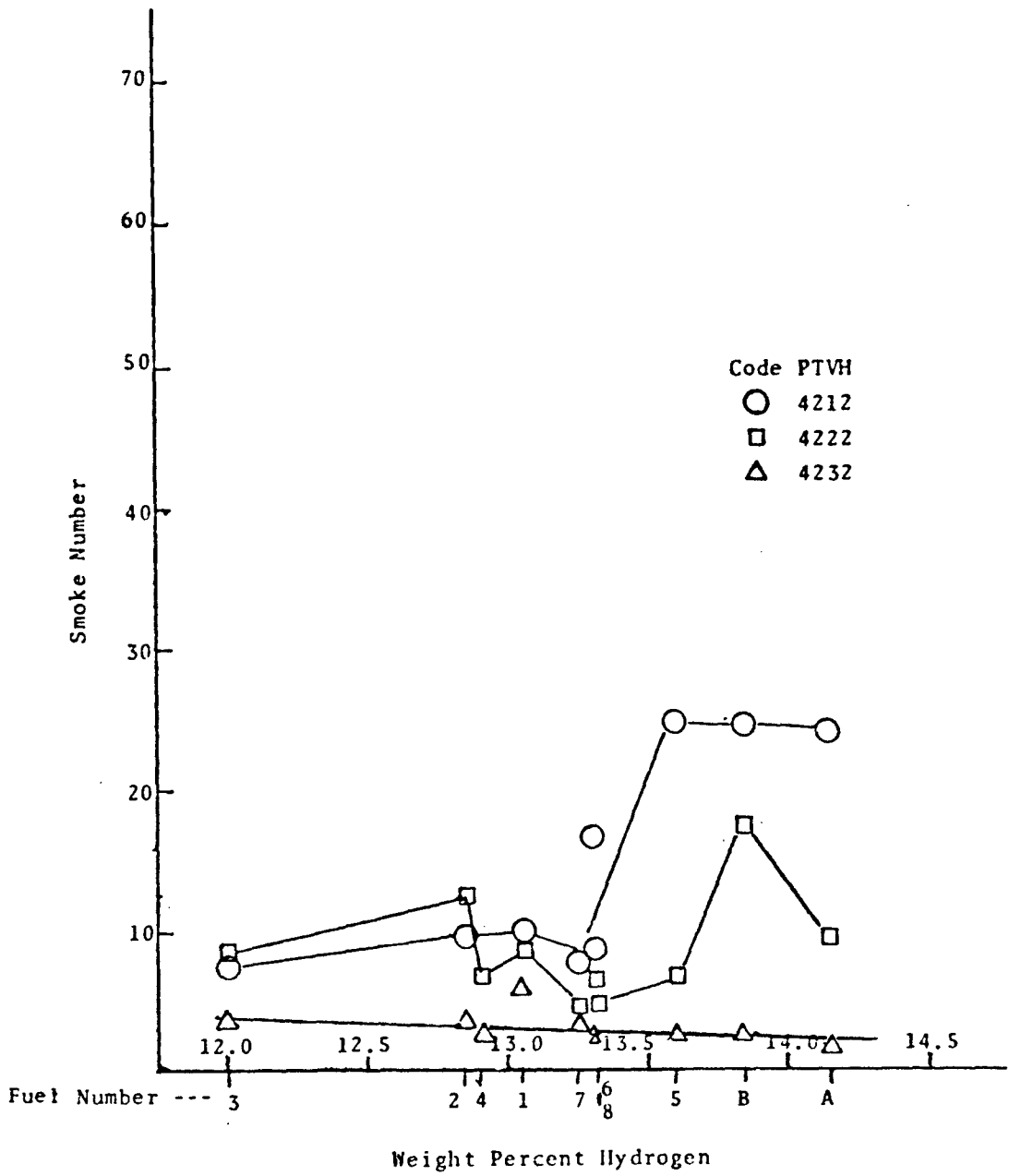

FIGURE 41. EFFECT OF FLOW VELOCITY ON EXHAUST SMOKE

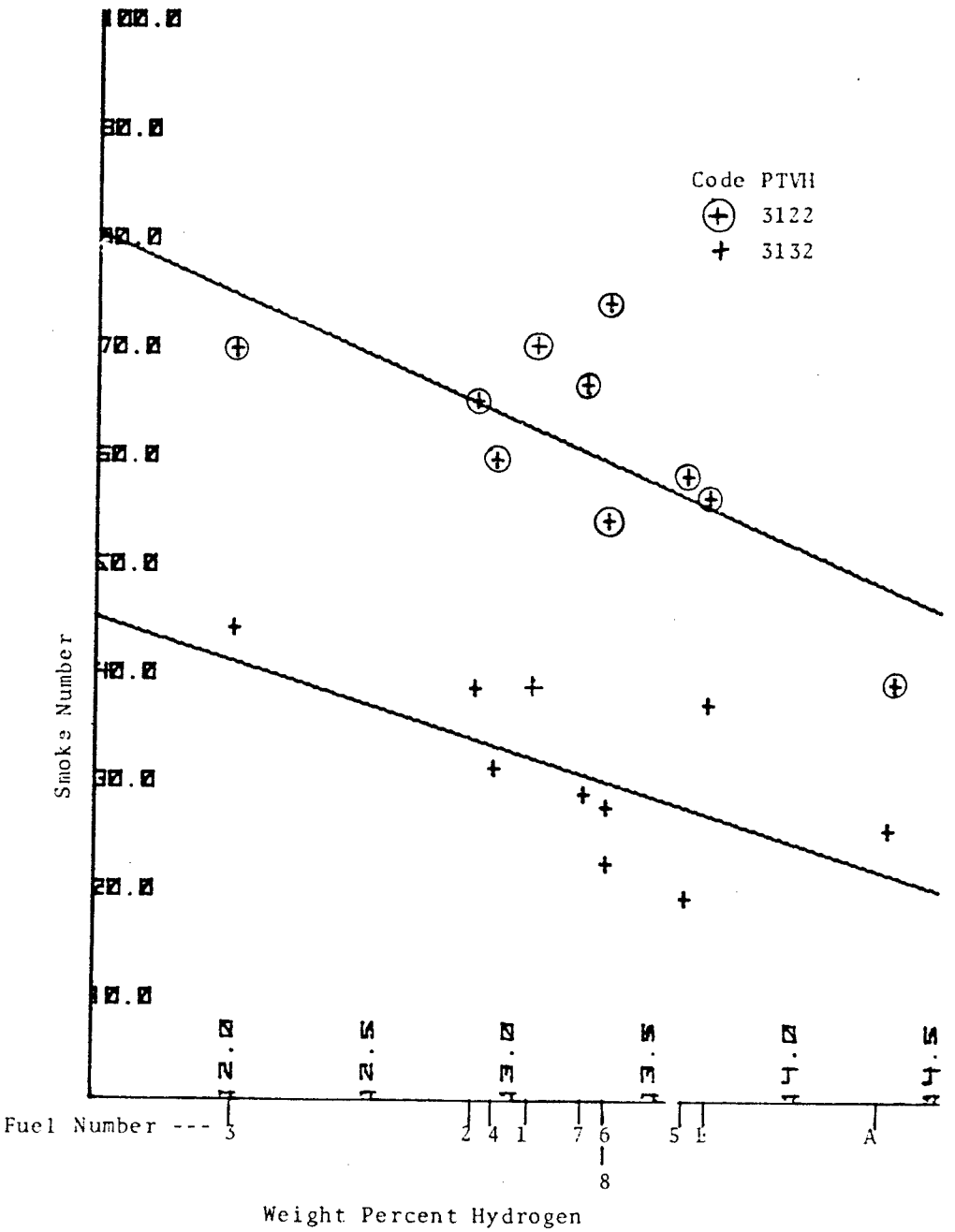

FIGURE 42. EFFECT OF FLOW VELOCITY ON EXHAUST SMOKE

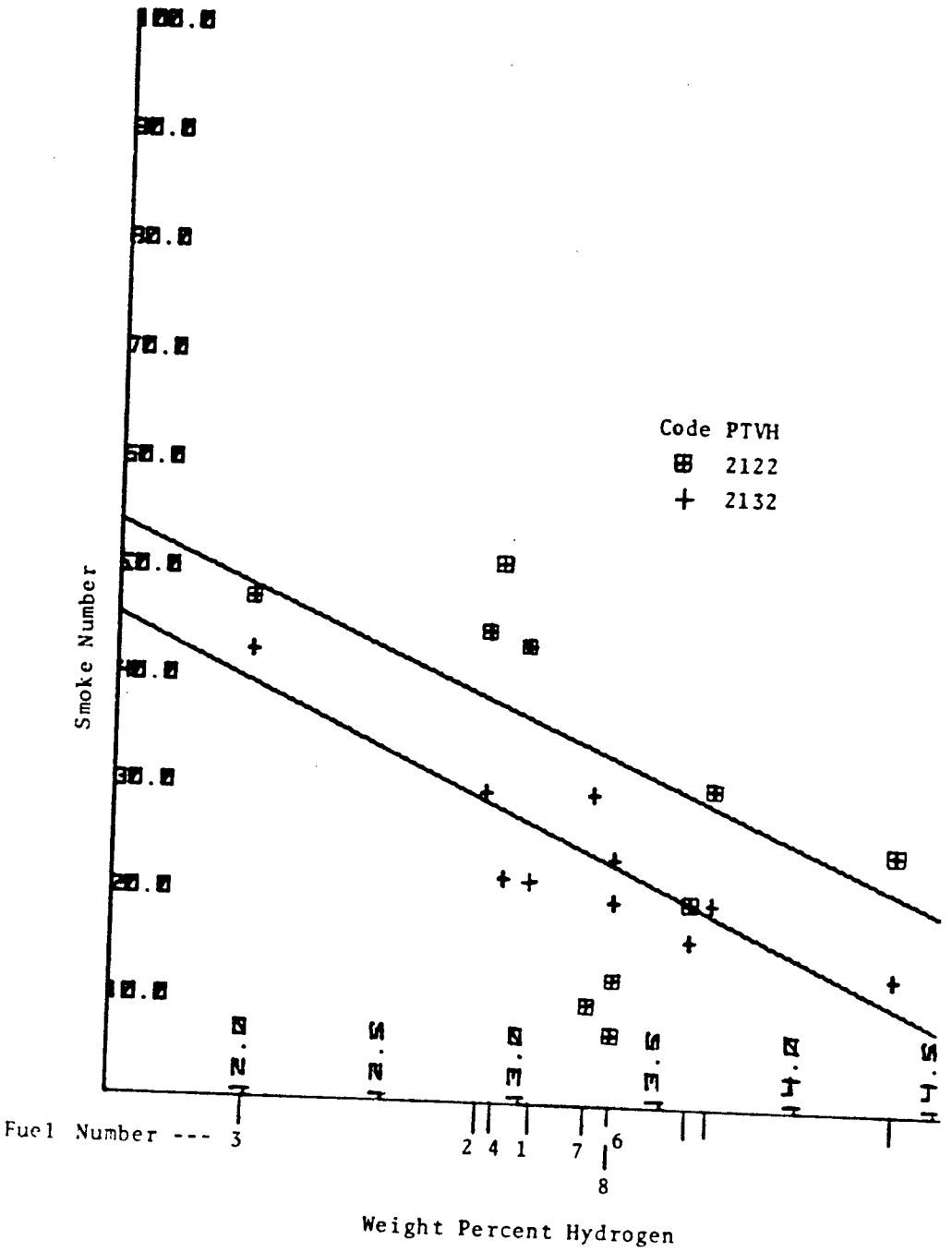

a regression analysis were $K = 4 \times 10^4$, $a = 0.8$, $b = -2$, $c = -0.3$ and $d = 0.8$. Because the correlation coefficient R^2 for this analysis was so low (ca. 0.3), the most that could be concluded was that the exponents a, b, c and d were consistent with the anticipated trends and theory.

When fuels numbered 1 and 2 were examined in a separate test program, an additional inlet parameter, i.e., differential nozzle pressure, ΔP, was recorded and a regression analysis of the data was performed using the model

$$(SN) = K\ P^a\ T^b\ V^c\ H^d\ \Delta P^e.$$

In this case, the values of the constants were $K = 1.3$, $a = 1.4$, $b = -1.4$, $c = 0,6$, $d = 1.6$ and $e = -0.5$, and the correlation coefficient $R^2 = 0.48$. This model gives a strong dependence on pressure and temperature similar to the first model. The dependence on heat input is particularly high and there is a direct dependence on the velocity rather than the inverse behavior of that shown by the first model. The dependence of SN on nozzle pressure, i.e., $\Delta P^{-0.5}$, is interesting in that the sauter mean diameter of the spray is proportional to $\Delta P^{-0.35}$, and because the droplet vaporization depends on the square of the droplet diameter, the rate of vaporization should be proportional to $\Delta P^{-0.7}$. The positive exponent for the velocity dependence in this model suggest that droplet size dominates the effect of velocity on the vaporization and mixing process in the primary zone. Thus the main effect of velocity is that of residence time in the secondary and quench zones.

A third model was proposed in which special emphasis was placed on exhaust gas temperature. The exhaust gas temperature was expressed as $(T + 1.156\ H)$ where the constant 1.156 is simply a conversion of H to temperature assuming an average heat capacity of 6 cal/mole deg. The model is expressed as

$$SN = K\ P^a\ (T + 1.156\ H)^b\ V^c\ S^d\ \Delta P^e$$

where the new variable S is the nozzle size in terms of gph at a specified pressure and viscosity. Approximate values of the constants as determined by the regression analysis are $K \approx 1.5 \times 10^3$, $a = -0.4$, $b = -0.7$, $c = -1.2$, $d = 2.7$ and $dP = 0.6$ and the correlation coefficient for this model was somewhat better at $R^2 = 0.52$. The inverse dependence on the effective exhaust gas temperature was anticipated. The small inverse dependence on pressure seems to be compensated by the terms $S^{2.7}\ dP^{0.6}$ expressing the mass flow rate of fuel. Increased pressure reduces the rate of simple diffusion of fuel vapor in the primary zone and increases the partial pressure of oxygen in the secondary and quench zones, thereby increasing the rate of oxidation of free carbon. The model suggests that simple diffusion is unimportant relative to eddy diffusivity, since the inverse dependence on velocity (i.e., turbulent mixing/convective vaporization of fuel droplets) is quite strong. The

dependence on nozzle pressure ($dP^{.6}$) suggests at first glance that it is proportional to the fuel input rate. Obviously, the higher the fuel input rate, the greater the concentration gradients (fuel rich zones) in the primary zone where the fuel pyrolysis and nucleation of carbon occurs.

Smoke vs. Fuel Properties

The following general conclusions can be drawn from the illustrations shown in Figures 43-45. As with radiation, the smoke number from the petroleum based fuels correlated equally well with hydrogen content, aromatics and ring carbon. The syncrude fuels again correlated best with hydrogen content. On the average, the shale oil-derived fuel produced less smoke relative to its aromatic content or ring carbon than the correlation for the other fuels.

The plot of fuel sensitivity (-dS/dH) versus smoke number (smoke number of a fuel blend containing 13 percent hydrogen) shown in Figure 46 indicates that the fuel sensitivity, while initially low, increases and asymptotically approaches a maximum value as the smoke emissions increase. The curve in Figure 46 represents a fit of the data to a parabolla, which explains the slight downward curvature of the line at high smoke number. These results suggest that combustors that yield low smoke emissions are relatively insensitive to fuel properties.

Also shown in Figures 37-45 is the comparison of fuels 1 and 2. Similar to radiation, the smoke number, on the average, was about the same for both fuels. As noted earlier these fuels each have almost identical smoke point, % ring carbon and hydrogen content. The significant difference in these fuels is that of monocyclic versus polycyclic aromatic content; the experimental results (see Table 10), in addition to mathematical analysis of the data using models 1, 2 and 3 mentioned above, do not show any obvious differences in smoke or radiation between the two fuels. This observation may be in correspondence with possible theories for smoke formation. The origin of smoke is believed to be due to the formation of acetylenic species by the oxidative pyrolysis of the fuel. The acetylenes polymerized forming high molecular weight molecules rich in carbon that eventually form soot particles via nucleation. There appears to be two possible major C_2 products in the pyrolysis of hydrocarbon fuels. The species are either acetylene or ethylene depending on the original hydrogen content of the fuel. The heavier hydrocarbon molecules generally break down into C_2H_x units and if the hydrogen content is low, the result is mostly C_2H_2. If then, the monocyclic and polycyclic aromatics in the fuels each break down into acetylenic species before soot formation begins, it is expected that they should both yield equivalent amounts of smoke.

Smoke In Other Combustors

As was the case for radiation, it appears that clean burning engines may have less sensitivity to fuel aromatics than engines which produce more smoke.

FIGURE 43. EXAMPLE OF THE EFFECT OF HYDROGEN CONTENT ON EXHAUST SMOKE

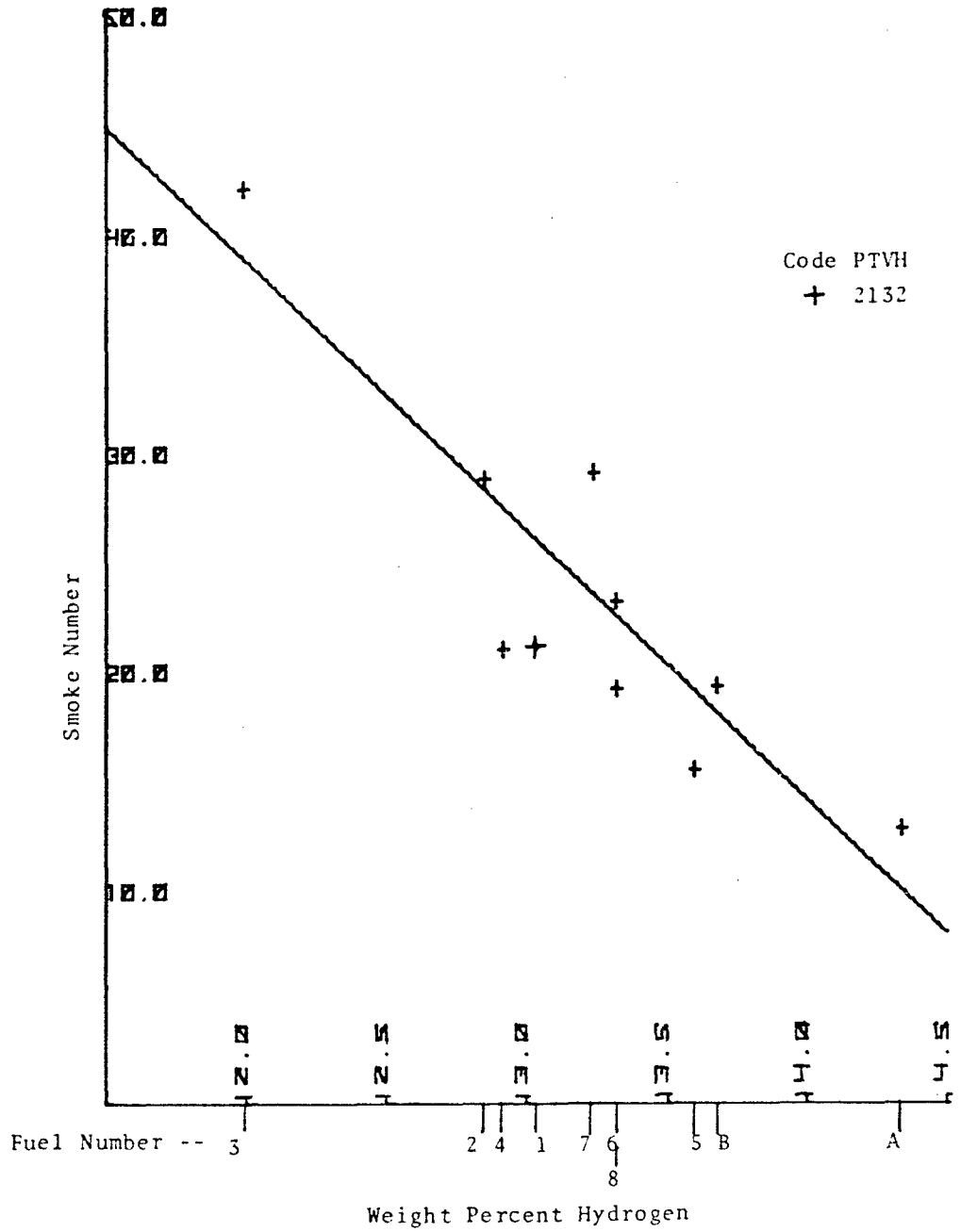

FIGURE 44. EXAMPLE OF THE EFFECT OF AROMATIC CONTENT ON EXHAUST SMOKE

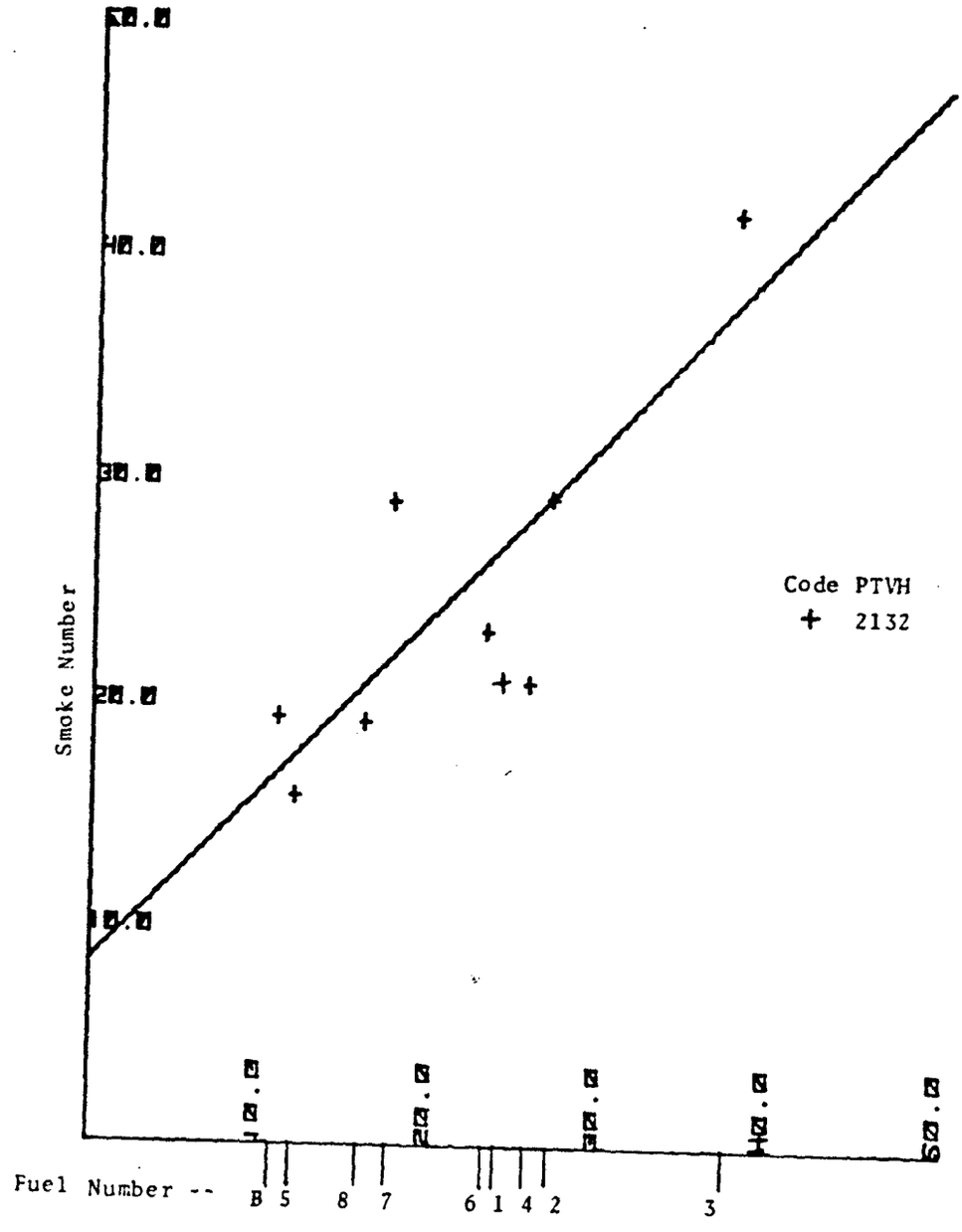

FIGURE 45. EXAMPLE OF THE EFFECT OF RING CARBON ON EXHAUST SMOKE

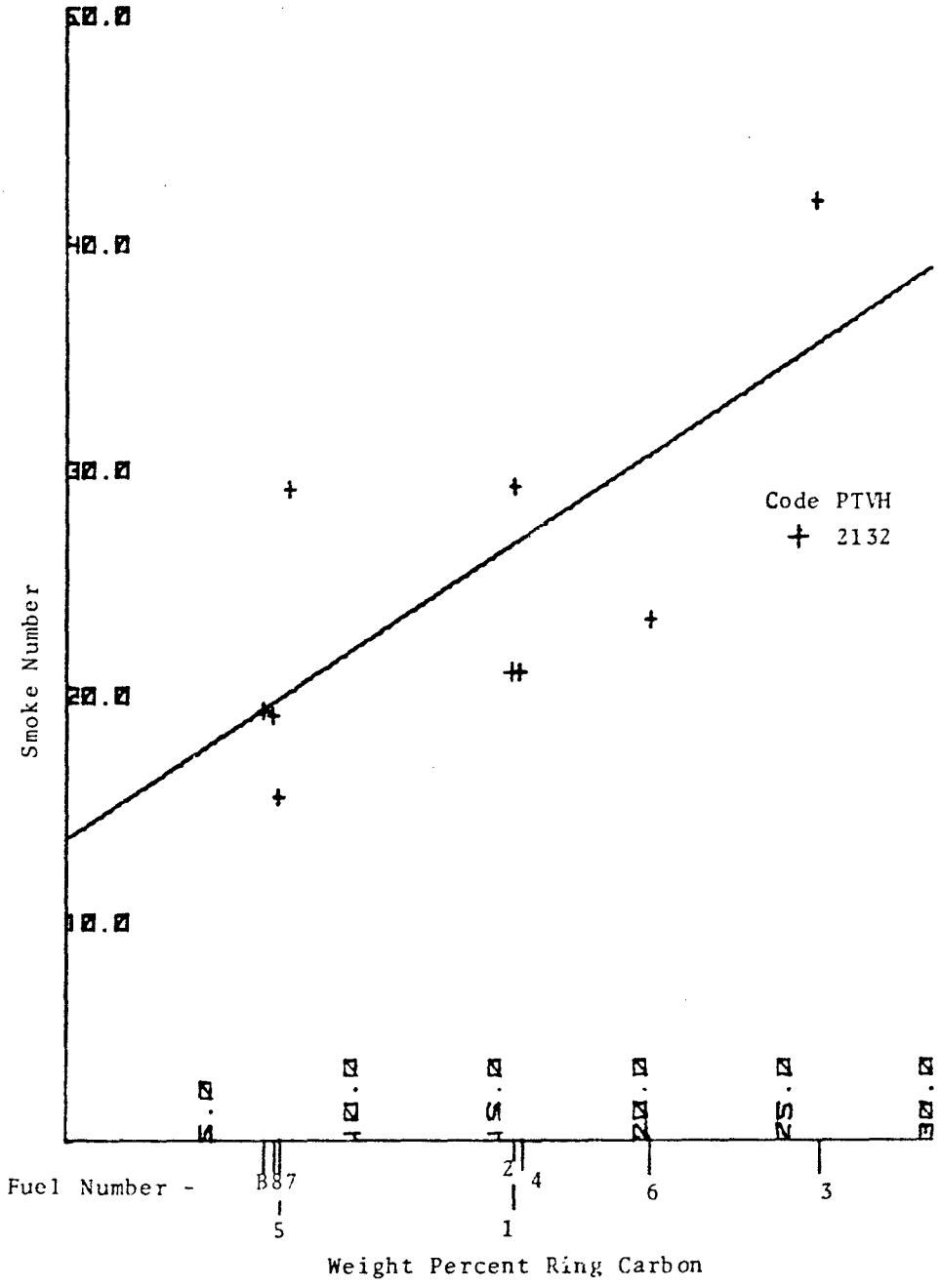

FIGURE 46. FUEL SENSITIVITY OF EXHAUST SMOKE

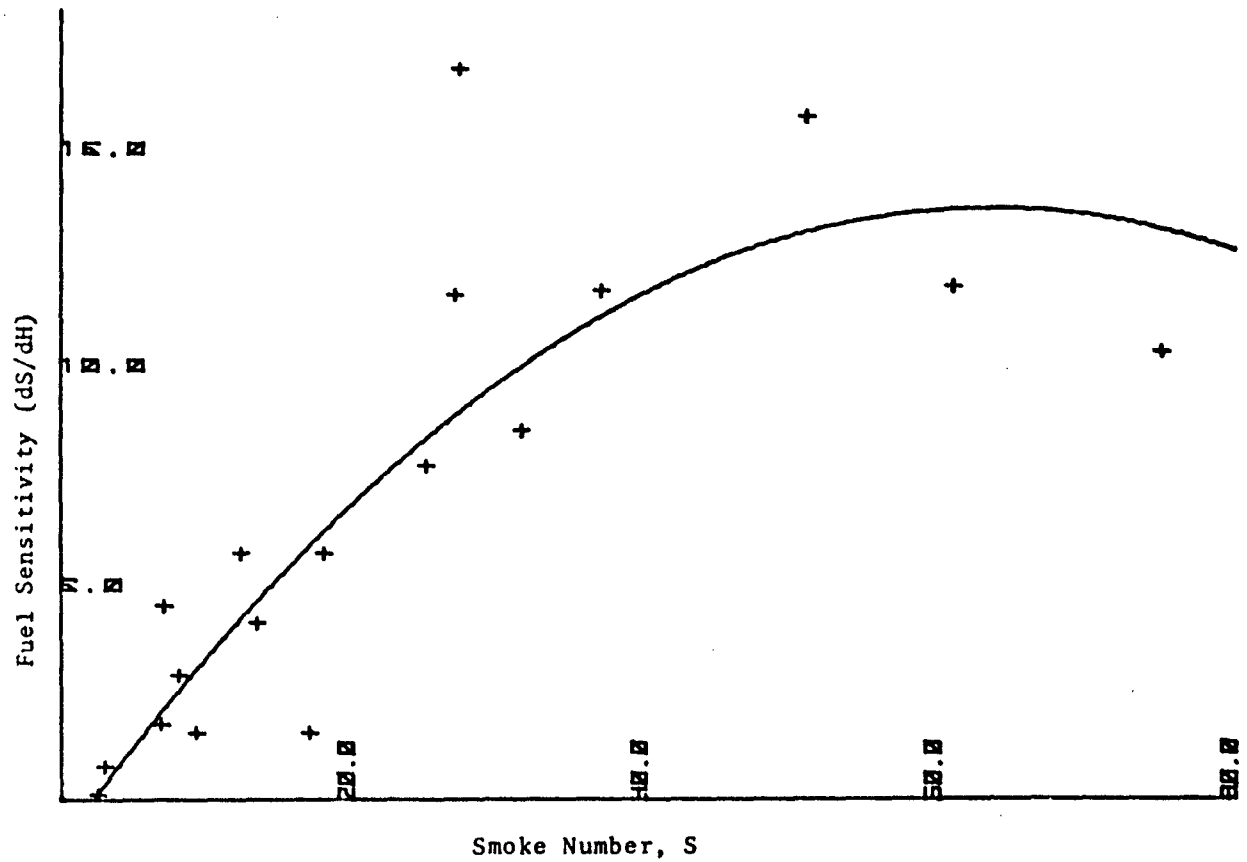

The smoke and radiation readings on the Phillips 2" combustor were comparable with similar measurements made by Shirmer and Quigg[1] and Bagnetto and Shirmer[2]. As compared with conventional combustors, the smoke and radiation from the Phillips 2" combustor appeared to be somewhat higher, but not abnormal. Compared with the T-63 combustor, the 2" combustor gave typically about twice as much smoke; radiation data for the T-63 was not available. Note, the comparison which is based on data obtained from the combustion of jet-A fuel, is only approximate and may not necessarily correlate similarly when the fuel properties are changed.

Gaseous Emissions

The emissions of CO, NO_x and unburned hydrocarbons were measured at all test conditions. Due to high combustion efficiency (99%), the unburned hydrocarbon emissions were very low (approximately 1 ppm) and the variation with inlet conditions was not significant. Thus, this discussion will be restricted to the effect of test conditions on the emissions of CO and NO_x. NO_x is discussed rather than both NO and NO_2 separately since the emissions index is based on NO_x (i.e., the oxides of nitrogen, NO_2 equivalent). The experimental results on the emissions of CO and NO_x are listed in Tables 8, 9 and 10.

Gaseous Emission vs. Operating Conditions

The measured values of CO and NO_x followed expected trends with the air and fuel flow parameters. Temperature, of course, is the greatest factor in the production of NO_x, which is formed very rapidly in the primary zone and remains essentially frozen in the rest of the combustor.

The NO_x emissions index (i.e., grams NO_2/kg fuel) was found by a regression analysis to correlate very well ($R^2 = 0.96$) with the empirical model:

$$E.I.\ (NO_x) = 6.6 \times 10^{-7}\ P^{0.4}\ T^{3.15}\ V^{-0.34}\ H^{-0.54}$$

where P, T, V and H are the inlet pressure, temperature, reference velocity and heat input (fuel/air ratio) respectively. The greatest dependence is on the inlet temperature while P, V, and H have relatively small effects that appear to be indirectly related to temperature. Increased pressure inhibits mixing by depressing simple diffusion while increased velocity intensifies turbulence and improves mixing. Poor mixing can cause local zones that burn closer to stoichiometric and, therefore, at higher temperatures. This explains the direct dependence of NO_x formation on pressure and the inverse dependence on velocity. The inverse dependence on H is at first suprising in that higher heat inputs should create higher temperatures in the primary zone. The difficulty is caused by the normalization with fuel flow rate to get Emissions

Index. If the concentrations of NO_x are considered, then NO_x is roughly proportional to $H^{0.5}$. Quigg[1] also found an inverse relationship between E.I. (NO_x) and H.

It appears that NO_x formation is not strongly related to droplet size and vaporization in this study since the regression analysis gave absolutely no dependence on the differential nozzle pressure (ΔP). This suggests that the characteristic time for fuel droplet evaporation may be less than that for mixing in the Phillips 2" combustor. In the case of radiation, the dependence on ΔP was weak except at low pressures while the importance of droplet evaporation to smoke formation was uncertain in that it depended on the model.

The CO emissions index was found to correlate very well (R^2 = 0.88) with the following empirical model.

$$\text{E.I. (CO)} \propto P^{-1.02}\ T^{-2.7}\ V^{0.4}\ H^{-0.4}\ \Delta P^{0.25}$$

The emission of CO is dependent on the parameters that control its combustion to CO_2. There is no concern about the formation of CO because every fuel carbon atom becomes CO before it is converted to CO_2 in the secondary zone. As demonstrated by the model above, higher inlet pressures and particularly higher temperatures reduce the emissions of CO. Both increased temperature and pressure reduce flame length by increasing the rates of chemical reactions; also, higher air temperatures mean higher temperatures in the secondary zone to increase the oxidation rates. The moderate increase in the CO emissions index due to increased velocity can be attributed to shorter residence times in the combustor overshadowing the better mixing. It appeared that higher heat input reduced the CO emissions index by increasing the exhaust gas temperature. CO emissions were weakly dependent on nozzle pressure (ΔP), indicating that greater droplet penetration could possibly increase flame length. The $dP^{0.25}$ dependence does not seem to be related to droplet size and evaporation.

Gaseous Emissions vs. Fuel Properties

As a whole, the NO_x and CO emission indexes were not highly sensitive to fuel properties. There was only one fuel that showed any significant differences in the NO_x levels: the shale oil derived fuel contained 0.10 percent fuel bound nitrogen as compared with the 0.01 percent for all the other fuels. The fuels with higher end points, fuel number 8 from tar sands and fuel number 5 blended for high end point, produced somewhat lower NO_x emissions, but the emissions indices were essentially the same as the other fuels after normalizing for fuel flow rate.

If all the fuel bound nitrogen in fuel number 6 derived from oil shale was converted to NO_x, the emissions index would be

increased by 3.29 grams/Kg of fuel. The NO_x contribution from the fuel bound nitrogen was calculated at each test condition as the difference between the NO_x from the oil shale fuel and the average NO_x from all other fuels.

The NO_x contribution from fuel bound nitrogen as shown in Table 9 contains a considerable amount of scatter. The average value for the conversion of fuel bound nitrogen to NO_x was about 46 percent based on a maximum yield of 3.29 grams NO_2/kg of fuel.

An attempt was made to correlate the NO_x from fuel bound nitrogen with the test parameters using the model

$$E.I.\ (NO_x)_{F.b.} = K\ P^a\ T^b\ V^c\ H^d$$

and performing a regression analysis on the data. The regression analysis gave the following correlation,

$$E.I.\ (NO_x)_{F.b.} \approx 172\ (P^{-0.28}\ T^{-0.54}\ V^{0.17}\ H^{-0.24})$$

but the correlation ($R^2 = 0.40$) was weak. In agreement with the work of Blazowski[16], this correlation suggests that the conversion of fuel bound nitrogen to NO_x is reduced as inlet temperature is raised. Blazowski observed a decrease in the percent conversion as inlet temperature was increased and also found that conversion was inversely proportional to the concentration of nitrogen in the fuel.

It appears reasonable to conclude that temperature should be an important variable in the formation of NO_x from fuel bound nitrogen. It has been proposed that NO from fuel bound nitrogen is formed by the oxidation of HCN, which in turn is formed from the pyrolysis of the fuel nitrogen compounds. Axworthy and Schuman[9] found that heterocyclic-N aromatic compounds yield HCN on thermodecomposition.

It has also been found by deSoete[8] that lean and stoichiometric flames give a much higher conversion of fuel nitrogen to NO than fuel rich flames. This may relate to the inverse dependence of NO_x from fuel bound nitrogen on H, i.e., fuel/air ratio. Higher pressures and higher heat input increase the lifetime of fuel rich eddies by reducing simple diffusion and enriching the mixture. Hence, more fuel rich combustion would tend to reduce conversion and support an inverse dependence of pressure and heat input. Increased velocity should tend to lean the fuel rich eddies by enhanced mixing, and thus increase formation of NO from fuel bound nitrogen.

It is clearly evident from the data in Table 8 that the CO emissions index was independent of fuel characteristics. The slight variations that did occur from fuel to fuel at a particular test condition are within the scatter of the measurements and show no consistent trends in comparing test

conditions. Two of the fuels were expected to show some difference in the CO emissions. The JP-5 from oil shale and JP-5 fuel number 5 both have higher viscosity and end point, which control droplet size and vaporization rate. However, the effects of viscosity and end point were not apparent because the CO emissions did not appear to be mixing and vaporization rate limited. Instead, the dependence of the CO emissions index on velocity (E.I. (CO) α $V^{0.4}$) suggests that the oxidation of CO is reaction rate limited. This is in accordance with the observed high combustion efficiency. To see a meaningful correlation, experiments should be conducted with a burner that can be operated at lower efficiencies typical of engines at low power or ground idle where CO production is appreciable.

Gaseous Emissions in Other Combustors

Relative to conventional combustors, the emissions in general from the Phillips 2" combustor were low for CO and hydrocarbons and about normal for NO_x. Compared with the T-63 combustor, the 2" combustor gave typically about 1/5 the CO, less than 1/10 the hydrocarbons and about twice as much NO_x.

Combustion Efficiency

The geometry of this combustor is such that if the flame can be stabilized in the primary zone, then combustion is very efficient, > 99 percent. This can be seen from the very low levels of CO and UBH. As a result, it is very difficult to draw significant conclusions about the effects of fuel properties on combustion efficiency. Even the two fuels with the highest end points and viscosities were not significantly different. As was suggested in the previous section, experiments should be conducted in a burner which can be operated at lower efficiencies, e.g., 90-95%, to obtain a meaningful correlation.

REFERENCE LIST

1. H.T. Quigg, "Reduction of Pollutants from Aircraft Turbine by Fuel Selection and Prevaporization", Philips Petroleum Company R&D Report No. 6607-73.

2. R.M. Shirmer and H.T. Quigg, "High Pressure Combustor Studies of Flame Radiation as Related to Hydrocarbon Structure", Philips Petroleum Company, Report No. 3952-65R.

3. L. Bagnetto and R.M. Shirmer, "Smoke Abatement in Gas Turbines, Part I: Survey of Operating Variables", Phillips Petroleum Company, Report No. 4884-67R.

4. J.H. Tuttle, M.B. Colket and A.M. Mellor, "Characteristic Time Correlation of Emissions from Conventional Aircraft Type Flames", Purdue University, Report No. PURDU-CL-76-05.

5. W.J. Dodds, M.B. Colket and A.M. Mellor, "Radiation and Smoke from Gas Turbine Flames, Part I: Carbon Particulate Measurements Within a Model Turbine Combustor", Purdue University, Report No. PURDU-CL-76-06.

6. M.B. Colket, J.M. Stefucza, J.E. Peters and A.M. Mellor, "Radiation and Smoke from Gas Turbine Flames, Part II: Fuel Effects on Performance", Purdue University, Report No. PURDU-CL-77-01.

7. R.F. Sawyer, N.J. Brown, R.D. Mathews, M.C. Branch and S.M. Banna, "The Formation of Nitrogen Oxides from Fuel Nitrogen", College of Engineering, University of California, Berkeley, Report No. EPRI-223-1, March 1976.

8. G.G. de Soete, "Overall Reaction Rates of NO and N_2 formation from Fuel Nitrogen", Fifteenth Symposium (International) on Combustion, Combustion Institute, Pittsburgh, 1093 (1974).

9. A.E. Axworthy and M. Shuman, "Investigation of the Mechanism and Chemistry of Fuel Nitrogen Conversion to Nitrogen Oxides in Combustion", Coal Combustion Symposium, Environmental Protection Agency, Research Triangle Park, North Carolina (1973).

10. A.H. Lefebvre, "Progress and Problems in Gas-Turbine Combustion", Tenth Symposium (International) on Combustion, University of Cambridge, England (1964).

11. R.L. Schalla and R.R. Hibbard, Basic Considerations in the Combustion of Hydrocarbon Fuels with Air, Chapter IX, Smoke and Coke Formation in the Combustion of Hydrocarbon-Air Mixtures, NACA Report 1300.

12. D.L. Champagne, "Standard Measurement of Aircraft Turbine Engine Exhaust Smoke", USAF, Air Force Aero Propulsion Laboratory, Wright Patterson Air Force Base, Ohio, 71-GT-88, ASME, New York (1971).

13. D.L. Troth, A.J. Verdouw and F.J. Verkamp, "Investigation of Aircraft Gas Turbine Combustor Having Low Mass Emissions", USAAMRDL Technical Report 73-G, Eustis Directorate, U.S. Army Air Mobility Research and Development Laboratory, Ft. Eustis, Virginia, April (1973).

14. M.C. Hardin, "Calculation of Combustion Efficiency and Fuel-Air Ratio from Exhaust Gas Analysis", Technical Data Report RN73-48, Detroit Diesel Allison Division, General Motor Corporation, Indianapolis, Indiana, 27 July (1973).

15. E.R. Norster and A.H. Lefebvre, "Influence of Fuel Preparation and Operating Conditions on Flame Radiation in a Gas Turbine Combustor", ASME Paper 72-WA/HT-26 (1974).

16. W.S. Blazowski, "Combustion Considerations for Future Jet Fuels", Sixteenth Symposium (International) on Combustion, p. 1631 (1976).